NASA CR-72748
MDC G0933

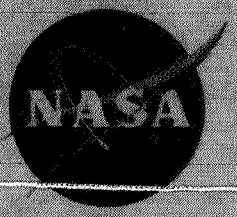

PRESSURE SENSING CONTROL DEVELOPMENT FOR PRESSURIZATION AND VENTING SYSTEMS

by

W. J. Wachtler and J. Tobolski

McDONNELL DOUGLAS ASTRONAUTICS COMPANY–WEST

prepared for

NATIONAL AERONAUTICS AND SPACE ADMINISTRATION

NASA Lewis Research Center
Contract NAS3-13310
R. E. Grey, Project Manager

NASA CR-72748
MDC G0933

FINAL REPORT

PRESSURE SENSING CONTROL DEVELOPMENT FOR PRESSURIZATION AND VENTING SYSTEMS

by

W. J. Wachtler and J. Tobloski

McDONNELL DOUGLAS ASTRONAUTICS COMPANY–WEST
5301 Bolsa Avenue
Huntington Beach, California 92647

prepared for

NATIONAL AERONAUTICS AND SPACE ADMINISTRATION

March 1971

CONTRACT NAS3-13310

NASA Lewis Research Center
Cleveland, Ohio
R. E. Grey, Project Manager
Liquid Rock Technology Branch

FOREWORD

This report was prepared by McDonnell-Douglas Astronautics Company-West, under Contract NAS 3-13310. The contract is administered by the National Aeronautics and Space Administration, Lewis Research Center, Liquid Rocket Technology Branch, Cleveland, Ohio. The NASA Project Manager for the contract is Mr. R.E. Grey. This is the Final Report on the contract, and it summarizes the technical effort from 2 July 1969 to 2 August 1970.

The major contributions of G.W. Burge, K. Oliver, I.A. Robins, D.C. Webster and R. Yeaman of McDonnell Douglas Astronautics Company-West, to the technical effort described in this report are gratefully acknowledged by the authors.

ABSTRACT

A technology program is discussed in which a hybrid (analog/digital) electronic controller is developed. The controller is designed to provide propellant tank pressurization control during engine operation and tank venting during standby for a cryogenic space propulsion system requiring multiburn operations and long coast times (1 to 3 years). The system also solves the problem of "true" net positive suction pressure (NPSP) control. The total program encompassed analysis, design, fabrication, and testing. The analysis includes the assessed benefits of "true" NPSP control and accuracy requirements. The developed system performed essentially as designed while under the environmental test conditions.

TABLE OF CONTENTS

TABLE OF CONTENTS (Con't)

LIST OF APPENDICES

LIST OF FIGURES

LIST OF FIGURES (Con't)

LIST OF FIGURES (Con't)

LIST OF TABLES

LIST OF TABLES (Con't)

SECTION 1

SUMMARY

A technology program was conducted to develop a long-life "flight type" (prototype) cryogenic tank pressure sensing and control system to provide tank venting during standby and "true" NPSP pressure control during engine operation. The program encompassed analysis, design, fabrication and testing of the sensors and the control logic system. The system senses the total and vapor pressure within a space vehicle propellant tank and provides these inputs to a digital logic system which in turn provides electrical signals to open and close vent and pressurant supply solenoid valves, based on certain preset pressure limits. The controller is designed to provide "true" net positive suction pressure (NPSP) control where the tank pressure is established by adding a preset NPSP to the propellant vapor pressure. Two units were fabricated and delivered to NASA LeRC. These systems were tailored for liquid fluorine and liquid hydrogen systems; however, they may be adapted to LO_2, FLOX, or CH_4 by providing the proper temperature probe and signal conditioning for the vapor pressure measurement. The system is also designed to be used with a pressurization system requiring: 1) helium for prepressurization and (autogeneous) vaporized propellant for expulsion pressurization, 2) helium for both prepressurization and expulsion pressurization, and 3) autogeneous propellants for both the prepressurization and expulsion. In addition to driving two vent valves and two pressurant valves, the controller also outputs a prepressurization complete signal.

A limited feed system analysis was conducted to assess the benefits of true NPSP control and to establish the accuracy requirements for the pressure sensors. A rather extensive effort was made to evaluate and select adequate total pressure sensors for the temperature extreme [-423°F (-253°C)] and the long term stability required in the control application. Techniques were also evaluated for measuring liquid propellant vapor pressure.

A platinum temperature sensor was selected for the vapor pressure measurement system and a variable impedance, flat diaphragm transducer was selected for measuring total pressure. The two controllers were tested in a hard vacuum less than 1×10^{-5} torr (1.33×10^{-3} pascals). They were also subjected to

vibration and shock tests and proved to be structurally sound. No performance degradation or failure resulted from the vacuum tests; however, one of the total pressure sensors failed when cycled from ambient temperature to -423°F (-253°C).

Functional tests were performed, and both systems performed in the manner for which they were designed. Pretest and posttest calibrations were made for the controllers and their sensing systems. The maximum static error for the controllers, independent of the transducer inputs, was 0.6% of full scale. The sensors output maximum static errors were:

Liquid Hydrogen		Liquid Fluorine	
Total Press.	Vapor Press.	Total Press.	Vapor Press.
0.6%	1.2%	0.6%	2.5%

Pressure switches are used on the Saturn S-IVB and other existing pressurization systems but they are generally designed for specific pressure limits. This controller, however, provides flexibility with respect to various pressure control levels and modes of operation. It also implements the "true" NPSP approach which minimizes pressurant gas consumption and maximizes the time that the feed system can be maintained in space until the tank vent pressure is reached. Other benefits associated with the use of the pressure sensing controller are:

a. Lower tank pressure levels
b. Minimized propellant tank weight
c. Increased payload
d. Minimized long term error

SECTION 2

INTRODUCTION

Cryogenic space propulsion systems involving multiburn operations, long coast times (1 to 3 years), and zero venting will require a pressure sensing and control system. The objectives of this NASA sponsored program were to design, fabricate and test a long-life "flight type" (prototype) controller that will sense conditions within a vehicle propellant tank and provide electrical signals for opening and closing both vent and pressurization valves while satisfying preset pressure limits. The venting requirement is to provide pressure relief in the event of over-pressure due to unexpected conditions. Pressurization valves are used to provide the pressurant for increasing the tank pressure, above the propellant saturation pressure for the net positive suction pressure (NPSP) required by the engine pumps. The system is designed to be adaptable to LH_2, LO_2, LF_2, FLOX, or CH_4 propellants, but the delivered hardware is designed specifically for LF_2 and LH_2 propellants. The pressurization system controller has a mode selection capability to perform the logic necessary to drive the appropriate valves that allow either helium or vaporized propellant for prepressurization, vaporized propellant for expulsion pressurization, or helium for both prepressurization and expulsion. Figure 1 illustrates the overall system, its input and output and the hardware covered under this procurement. During the analysis phase of this program, two basic tank pressure control approaches were evaluated and compared for engine firing periods: (1) fixed ΔP_T (differential total tank pressure) control, where the minimum total tank pressure during engine operation is determined by having the control system add the preset NPSP to the measured total tank pressure at the time of firing command signal and (2) "true" NPSP control where the minimum total tank pressure during engine operation is determined by having the control system add the preset NPSP to the actual propellant vapor partial pressure. The latter approach is termed "true" NPSP because the system is applying the real or true definition of NPSP, the pressure difference required above propellant vapor pressure. These two control approaches are illustrated in Figure 2.

Pressure sensors are an integral part of the controller. They are required to operate at -320°F (-196°C) or lower. As a part of the program, the merits of

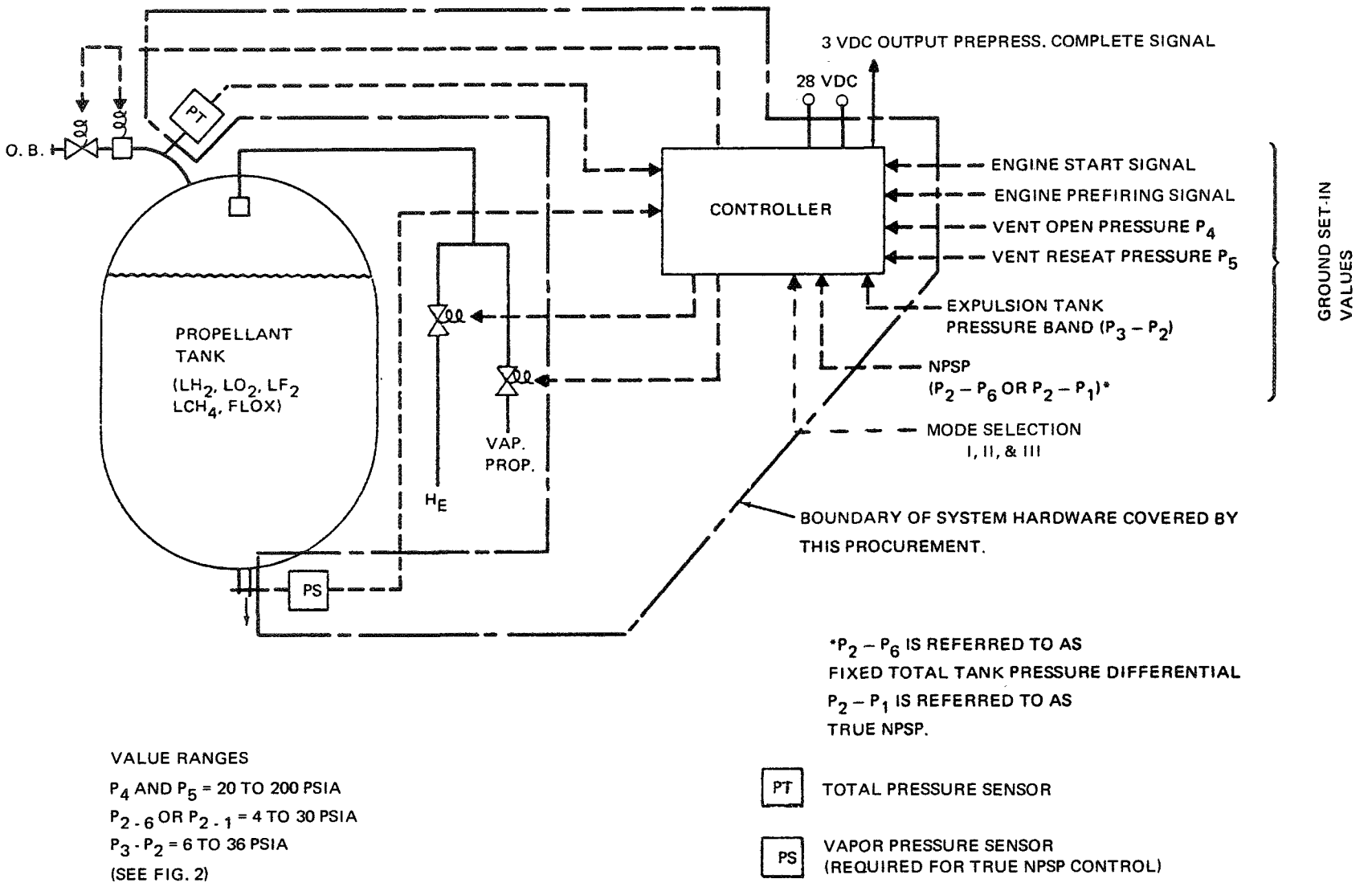

Figure 1. Overall Control System Schematic

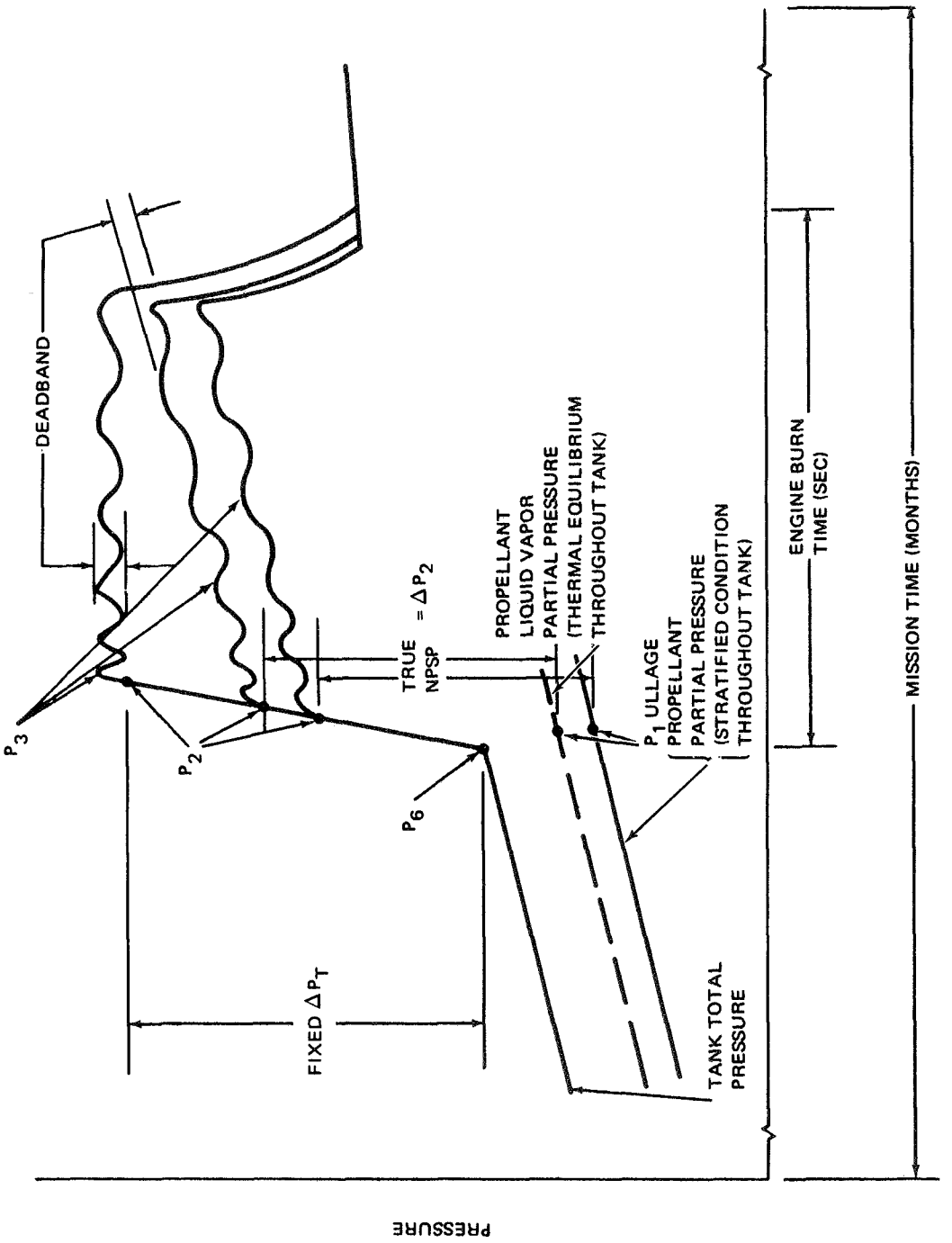

Figure 2. Comparison of True NPSP and Fixed ΔP_T Control

a number of pressure sensing devices were evaluated and sensor selections were made and incorporated into the design.

Because of the inherent long-term "drift" problems associated with analog logic, a digital logic system was implemented. The basic philosophy used in the design of the prototype controller was to use the latest technology and where possible employ off-the-shelf, flight qualified components and subsystems. The design objective was to develop a flight-type model which would represent, as nearly as possible, an actual flight model while being cost effective and remaining within the scope of the program. The electronic logic portion of the system was designed to be electrically compatible with the selected sensors. The packaging philosophy did not include miniaturization of the total integrated system since the packaging objectives were to provide flexibility and accessibility for assembly, disassembly, checkout, and testing. This philosophy was cost effective because the selected off-the-shelf miniaturized or compact subsystems did not require costly repackaging. However, the subsystems used were sufficiently small and their components are capable of being repackaged and directly integrated into a dense flight package. The packaging of the electronic logic portion of the system was predicated on the use of discrete components and integrated circuits mounted on standard logic cards. In addition, the materials, components, and subsystems were designed to be compatible with the long-term vacuum, vibration and temperature requirements associated with a space flight system. Also for cost effective reasons, ordinary MIL-standard parts are used in lieu of high reliability components.

The basic prototype design can be directly applied to the flight model. Only minor mechanical and electrical changes along with the repackaging and substitution of high reliability components and subsystems are required.

The Operation and Calibration Procedures are provided under separate cover. MDAC-W Drawing No. 1T19806, Operation and Calibration Procedure, provides the necessary information and procedures for operating, calibrating and troubleshooting the Pressurization System Controllers, P/N 1T38533, S/N 1 and S/N 2. Copies may be obtained from the MDAC-W Records Department or from the NASA LeRC Project Manager, Mr. R.E. Grey.

The total program was accomplished by performing three major tasks:

Task I: Analysis and Design

The objective of this task is to develop a design for the flight type cryogenic propellant tank pressure control system. This objective was accomplished by carrying out analytical studies, engineering evaluations, and breadboard testing to support the final detail design of the controller which includes the pressure sensors and electronic logic portion.

Task II: Fabrication

The objective of this task is to fabricate the two pressure control systems. This objective was accomplished by purchasing components and subsystems and by in-house construction of the enclosures and the internal wiring and assembly.

Task III: Testing

The objectives of this task are to determine: (1) the functional and operational capability of the controller to perform according to its design specifications, (2) the LF_2 propellant compatibility of the sensing portion of the system. These objectives were accomplished by performing vibration and shock tests, vacuum functional cycle tests, and LF_2 propellant compatibility testing of the pressure sensor.

This report describes the program effort and hardware developed under the contract. It includes data, analyses and its interpretation, as well as recommendations and conclusions based on the results obtained from testing.

SECTION 3

ANALYSIS AND DESIGN

This section describes the analysis and design efforts of the program. The analysis includes a study to evaluate and compare the two control approaches illustrated in Figure 2 along with a study for determining system accuracy requirements. A study for establishing the proper location for installing the sensors is also discussed. The design part of this section includes the logic, timing, and sequence of events for the controller operation. The controller's basic design features and capability along with a detail description of the integrated system is also discussed. The analysis includes the valve driver design and system reliability.

3.1 Control System Performance Analysis

At the outset of the program, the control system accuracy and performance analysis was conducted for the two basic control system approaches (true NPSP and fixed ΔP_T). This analysis was conducted to assess the benefits of the true NPSP control approach and to establish the accuracy required for the pressure sensing measurements.

Rather than conduct a complete parametric investigation, a limited study was performed for the two tank-pressure control approaches as applied to a vehicle and mission selected mutually by MDAC and NASA-LeRC. The selected mission is representative of a Mars Orbiter - Orbit Injection Stage with a mission duration of 205 days, with a 195 day interplanetary trip, and orbit trim after 10 days in orbit about Mars. Further a vehicle gross weight of 9,700 lbs (4400 kilograms) was assumed along with the following four engine firings and velocities:

a. First midcourse 164 ft/sec (50 m/s) at 2 days
b. Second midcourse 164 ft/sec (50 m/s) at 165 days
c. Orbit Insertion 6,295 ft/sec (1920 m/s) at 195 days
d. Orbit trim 328 ft/sec (100 m/s) at 205 days

These propulsive steps were conducted assuming that there is no staging between burns and that the nominal engine thrust is 5,000 lb (22,200 newtons). The propellants used in the investigation were fluorine (F_2) and hydrogen (H_2) with an oxidizer to fuel ratio twelve to one (12/1). The system analysis also assumes that the orientation of the spacecraft is fixed relative to the sun such that the environmental temperature outside the high performance insulation is 250°R (139°K) and that the fuel and oxidizer tanks are one each in tandem. The liquid hydrogen and liquid fluorine are at their normal boiling point temperatures at the start of the mission. Other assumptions and inputs applicable to the study and used in this investigation are:

a. Liquid fluorine system:

NPSP = 12 + 4 (LOSSES) = 16 psi (11×10^4 pascals)

Liquid hydrogen system:

NPSP = 8 + 4 (LOSSES) = 12 psi (8.3×10^4 pascals)

b. Maximum tank pressure for both LF_2 and LH_2 tanks = 120 psia (82.7×10^4 pascals)

c. On the hydrogen tanks, 300 layers of high performance insulation was used for thermal protection. (Thickness = 3.75 in. (9.53×10^{-2}m)

d. The fluorine tank used 100 layers of high performance insulation.

e. The outer hot side insulation temperature is at 250°R (139°K) throughout the mission. This condition provides an average heating rate of 1.7 Btu/hr (4.98×10^{-1} watts).

The conditions established for the pressurant were also mutually agreed to by MDAC and NASA-LeRC. The conditions established for each case used in the analysis are presented in Table 1. The three pressurization modes defined below were also investigated.

MODE

I Helium for prepressurization and autogeneous (vaporized) propellant for expulsion during the burn.

II He for both prepressurization and for expulsion during the burn.

III Autogeneous propellant for both prepressurization and for expulsion during the burn.

TABLE 1

SUMMARY OF PRESSURANT USAGE

Case No.	Pressurant/Temperature (°R) (°K)				Pressurant/Weight (lbs_m) (kg)			
	Prepressurization		Engine Burn and Expulsion		LH_2 Tank		LF_2 Tank	
	LF_2 Tank	LH_2 Tank	LF_2 Tank	LH_2 Tank	True NPSP	Fixed ΔP_T	True NPSP	Fixed ΔP_T
1	He/(154)(85.4)	He/(37)(20.6)	He/(500)(278)	He/(500)(278)	He(7.94)(3.59)	He(21.1)(9.57)	He(1.53)(0.695)	He(4.47)(2.03)
2	He/(154)(85.4)	He/(37)(20.6)	He(300)(167)	He/(300)(167)	He(8.69)(3.93)	He(23.8)(10.8)	He(2.05)(0.93)	He(6.03)(2.73)
3	He/(154)(85.4)	He/(37)(20.6)	F_2/(500)(278)	H_2/(500)(278)	He(8.80)(3.99) He(2.85)(1.29)	He(12.5)(5.66) H_2(4.26)(1.93)	He(1.24)(0.56) F_2(14.41)(6.52)	He(1.44)(0.65) F_2(21.6)(9.77)
4	He/(154)(85.4)	He/(37)(20.6)	F_2/(300)(167)	H_2/(300)(167)	He(8.65)(3.91) H_2(3.86)(1.75)	He(12.2)(5.50) H_2(5.78)(2.62)	He(1.23)(0.56) F_2(21.1)(9.55)	He(1.44)(0.65) F2(31.0)(14.0)
5	He/(500)(278)	He/(500)(278)	He(500)(278)	He/(500)(278)	He(6.44)(2.92)	He(7.46)(3.38)	He(1.52)(0.69)	He(2.49)(1.13)
6	He/(300)(167)	He/(300)(167)	He(300)(167)	He/(300)(167)	He(8.16)(3.70)	He(10.3)4.66)	He(2.07)(0.94)	He(4.71)(2.13)
7	He/(500)(278)	He/(500)(278)	F_2(500)(278)	H_2/(500)(278)	He(0.86)(0.39) H_2(2.96)(1.34)	He(0.90)(0.41) H_2(3.05)(1.38)	He(0.50)(0.03) F_2(14.39)(6.52)	He(0.54)(0.25) F_2(16.77)(7.58)
8	He/(300)(167)	He/(300)(167)	F_2(300)(167)	H_2/(300)(167)	He(1.37)(0.62) H_2(4.01)(1.82)	He(1.47)(0.67) H_2(4.25)(1.93)	He(0.72)(0.33) F_2(21.1)(9.55)	He(0.82)(0.37 F_2(26.25)(12.00)

The MDAC H109 Multistart Propulsion System Sizing Program (see Appendix B) was used with a given propulsion system and duty cycle, for determining tank pressure histories for the total mission (coasts + burns), pressurant and venting requirements, and payload capabilities.

The first step in the analysis was to determine the pressurant collapse factors (ratio of required pressurant mass to the ideal pressurant mass computed neglecting heat and mass transfer) for each engine burn. These calculations were performed by using the MDAC H370 (Ref. 1) pressurant requirements analysis computer code which has been correlated with experimental results to well within ±10%. These collapse factors are presented below and are used as basic inputs to the H109 program.

Case Numbers	Burn Number	Collapse Factors LF_2 Tank	Collapse Factors LH_2 Tank
1 and 2	1	1.5	1.14
	2	1.4	1.19
	3	1.37	1.71
	4	1.45	1.45
3 and 4	1	1.55	1.14
	2	1.55	1.24
	3	1.29	1.62
	4	1.80	1.37
5 and 6	1	1.25	1.03
	2	1.20	1.09
	3	1.14	1.32
	4	1.26	1.25
7 and 8	1	1.3	1.02
	2	1.3	1.12
	3	1.14	1.31
	4	1.42	1.26

Results

The inputs and vehicle operations were analyzed by the MDAC Space Propulsion System Sizing and Optimization Computer Program (H109), using the following sequence of events: coast, prepressurization, engine burn, and decay. In this multistart mission, the above sequence of events was repeated using the assigned inputs for coast and burn times for each restart.

Sixteen computer performance runs were made for obtaining pressure levels and pressurant usage for both the true NPSP and fixed ΔP_T control concepts. In each of these runs, helium was used for prepressurization. All of the helium was assumed to be stored in the LH_2 tank at the liquid hydrogen saturation temperature. The initial gross weight and the stage velocity increments were input while the performance was calculated in terms of the magnitude of payload weight capability of the stage.

The pressurization system weights calculated include the helium storage bottle weight, miscellaneous weights and the pressurant weight. Heat exchangers, pumps, gas generators, and high pressure bottles for storing or handling heated vaporized propellants are not included. The helium storage bottle weight is based on the quantity of the pressurant required. The miscellaneous weight is constant and accounts for valves, fittings, and plumbing. A spherical LH_2 tank configuration was assumed while the diameter is allowed to vary to accommodate the necessary LH_2 propellant load. The liquid hydrogen tank, as expected, showed the most significant performance difference and was, therefore, chosen to depict the tank pressure history.

The mission pressure histories for four selected cases shown in Figures 3 and 4 are based on the use of cold 37°R (20.6°K) helium for prepressurization, while Figures 5 and 6 are the results obtained when using helium at 500°R (278°K) for prepressurization. Both sets of pressure histories include the effects of heated helium and heated hydrogen vapor for pressurization during expulsion and firing. The total pressures are presented to show the effects of propellant heating, prepressurization required for the NPSP, pressurization levels during the burn, and the decay values after firing. The propellant vapor pressure equilibrium values are indicated by the dotted lines and the plotted points at the start and end of each burn. The effects of helium gas diluent from previous firings is illustrated by the divergence of the hydrogen vapor pressure and total pressure curves. The time scale has been expanded during the burn to show clearly the pressure levels that exist during the

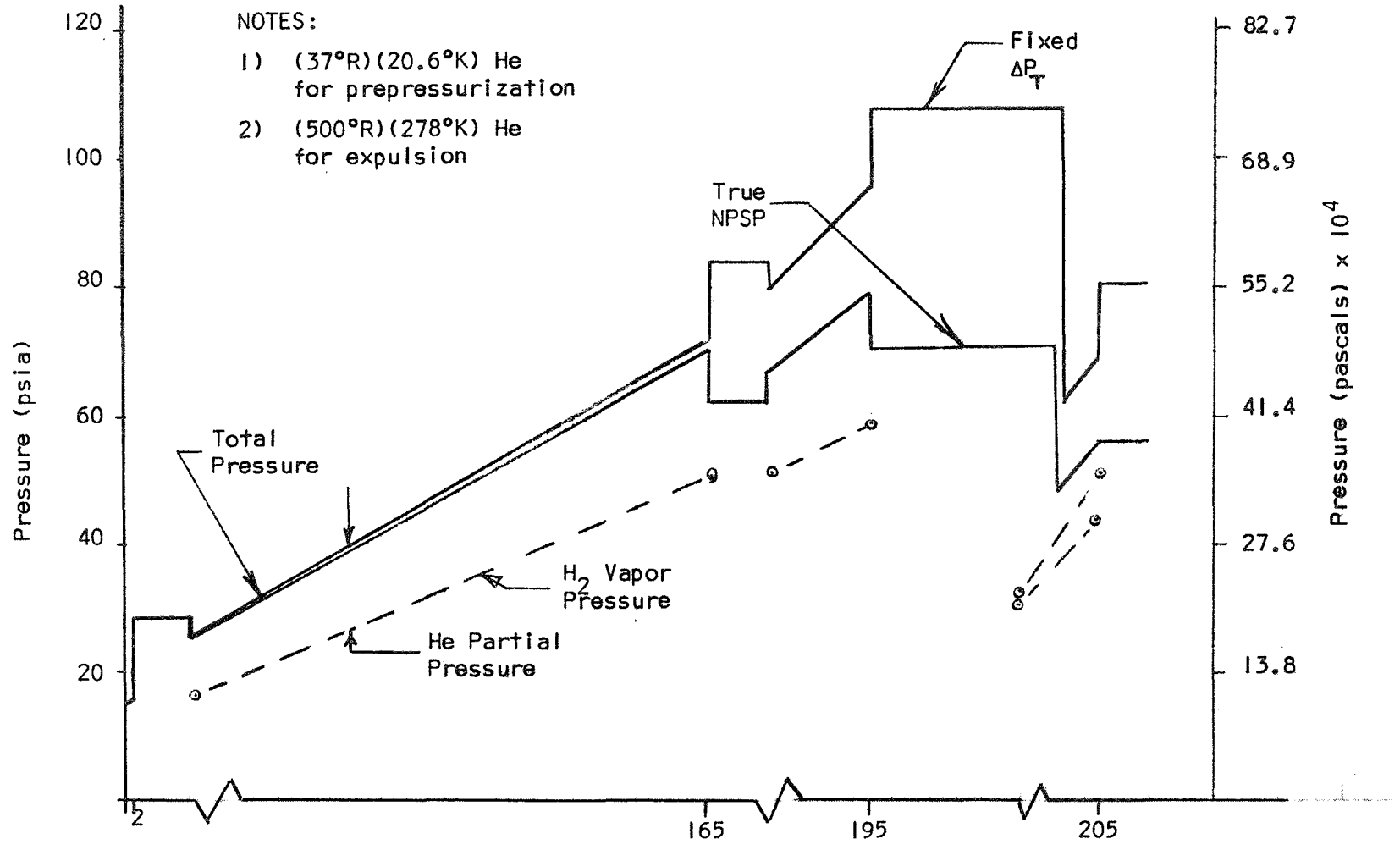

Figure 3 . LH_2 - Tank Pressure History - Case 1

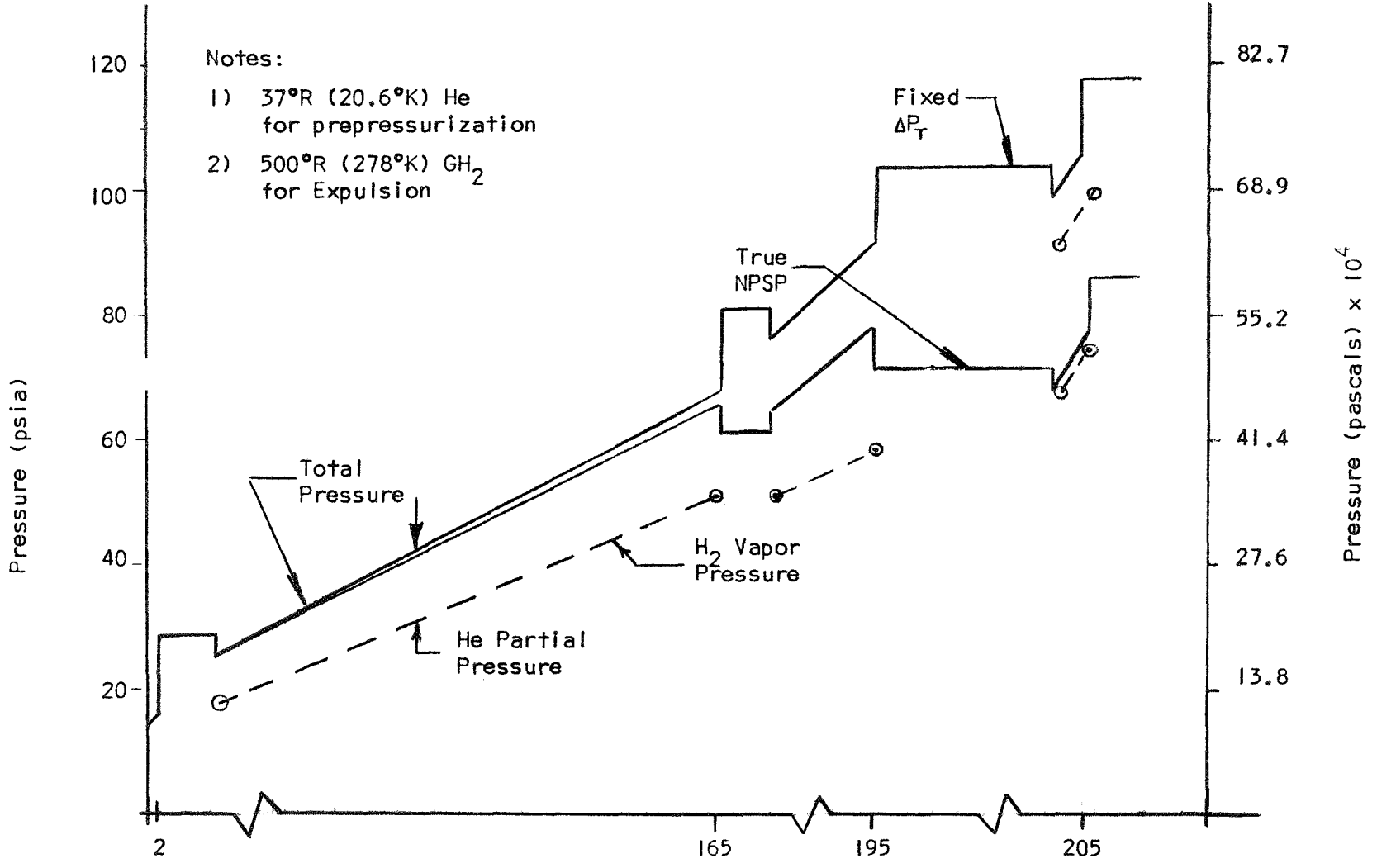

Figure 4 . LH_2-Tank Pressure History - Case 3

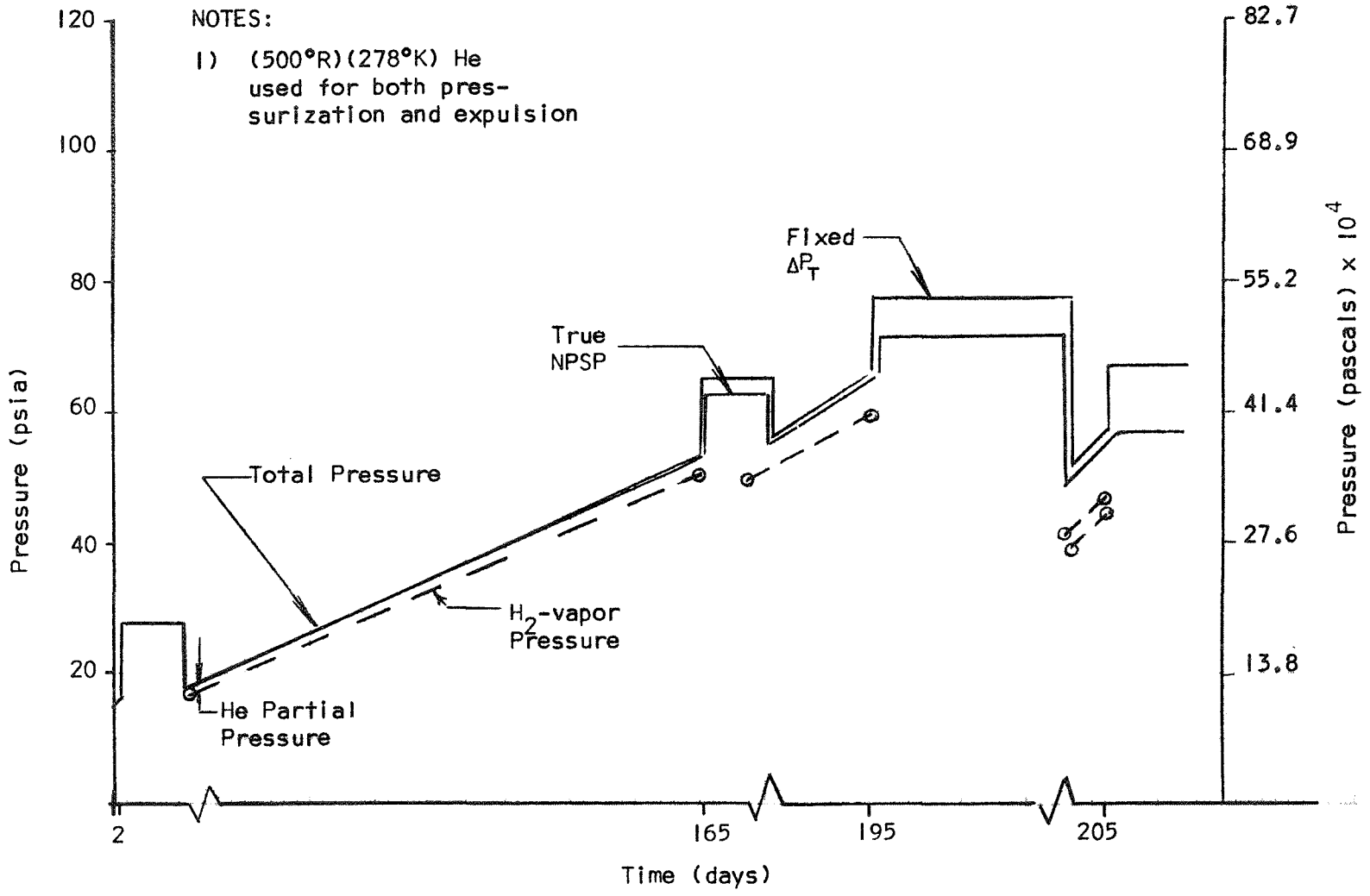

Figure 5 . LH_2-Tank Pressure History-Case 5

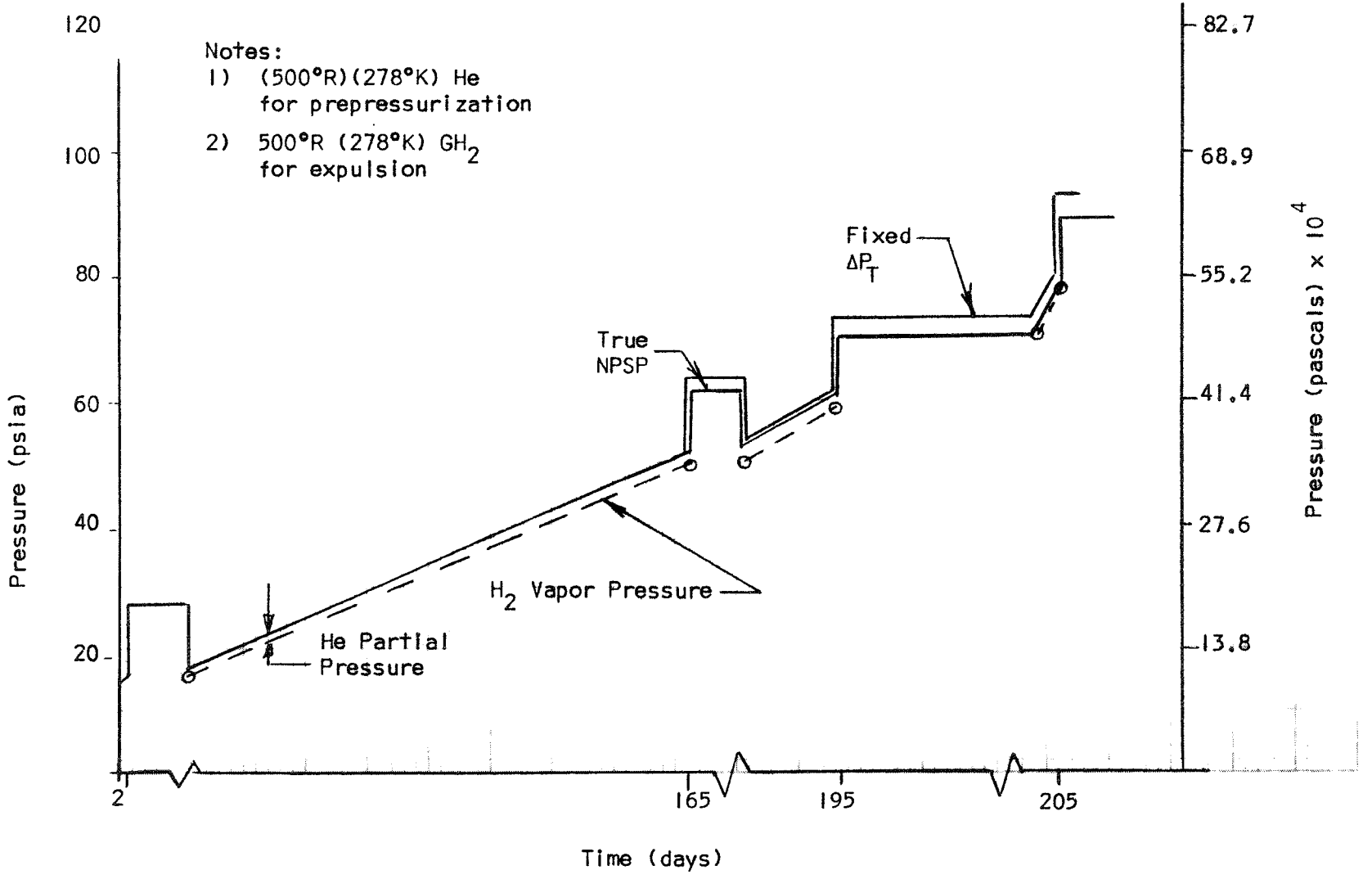

Figure 6 . LH_2 Tank Pressure History - Case 7

relatively short burn times. Figures 3 and 4 both show a significant condition existing at the second midcourse burn (165 days) and at the orbit insertion (195 days). Here the total pressure levels are sufficiently high, due to propellant heating during coast periods, that prepressurization was not required to supply the NPSP. In these cases the true NPSP tank pressure decayed during the initial expulsion to a level equal to the NPSP plus the liquid hydrogen vapor pressure, and the level was maintained during the remaining part of the burn.

Figures 3 and 4 also show marked differences in pressure level between the true NPSP and fixed ΔP_T control. The level in Figure 4 at the 205 day burn is 37% higher for the fixed ΔP_T control than for the true NPSP. In Figures 5 and 6 the helium partial pressures are small resulting from smaller quantities of heated helium required for prepressurization. In Figure 6 where the 500°R (278°K) GH_2 bleed is used, the pressurant requirements for true NPSP and fixed ΔP_T are nearly equal. Here a pressurant inlet gas temperature of 500°R (278°K) for the pressurant was used for expulsion and prepressurization.

For each case listed in Table 1, the total pressurant consumption was calculated by summing the pressurant weights computed for each of the four burns. These values are tabulated for both the liquid hydrogen and liquid fluorine tanks and for the true NPSP and fixed ΔP_T pressure control concept. The bar chart in Figure 7 compares the performance characteristics of the true NPSP and the fixed ΔP_T control concepts for four of the cases and conditions tabulated in Table 1. Here the performance is measured in terms of payload weight that varies over the range of 5100 lbs (2320 Kg) to 5300 lbs (2410 Kg). In Case 2, the conditions where cold helium 37°R (20.6°K) is used for prepressurization and 300°R (167°K) heated helium is used for expulsion, the true NPSP pressurization approach results in a payload performance gain of 2%. For the same above prepressurization conditions, but with 300°R (167°K) heated hydrogen used for expulsion (Case 4), the true NPSP approach results in a 1% increase in payload weight. In all cases, larger payloads result from using the heated vaporized propellants as opposed to heated helium for expulsion.

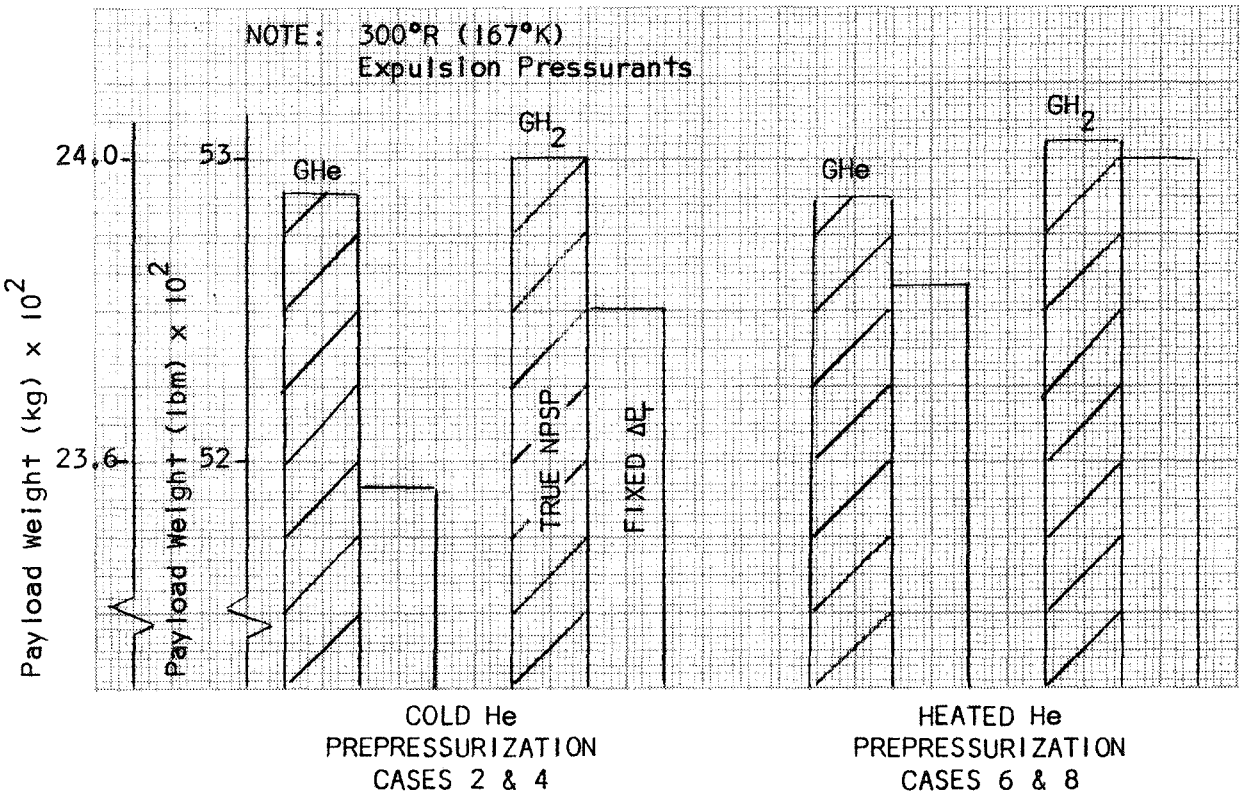

FIGURE 7. PERFORMANCE COMPARISON

Cases 6 and 8, show that the implementation of the true NPSP concept along with heating helium for prepressurization (using a gas generator system) does not increase the overall performance sufficiently to warrant the use of both systems simultaneously. For these cases, the pressurization systems requires further study to determine the component weight, reliability, development time, and cost tradeoffs between the gas generator/heat exchanger subsystem required to heat the prepressurant, and the subsystem required to implement the true NPSP control (e.g., vapor pressure sensor and electronic logic components).

The H109 computer program was also used for investigating the effects of control system accuracy on the stage performance. This investigation was accomplished by making computer runs identical to the runs made in the performance study except for the NPSP input. The NPSP input was varied in each run to simulate errors in sensing pressure during the mission. In the true NPSP case, errors can result from both total pressure and partial pressure measurements. Here the partial pressure is added by the controller to the NPSP, to obtain the tank run pressure levels. This level is then controlled by the total pressure measurement. In the fixed ΔP_T case, errors result only from tank total pressure measurement to which the NPSP plus losses are added to provide the tank pressure for each burn, while again the level is controlled by this same measurement. In both cases, the errors may be simulated by varying the NPSP using values greater than the minimum required. Figure 8 shows the payload variation over a pressure range from 0 to 5 psi (0 to 3.5×10^4 pascals) above the minimum NPSP, representing an error up to 2 1/2% of the full scale (200 psi) (138×10^4 pascals). Figure 8 shows the fixed ΔP_T concept to be more sensitive (8 lbs of payload per psi error (5.38×10^{-4} kg/pascal)) to pressure measurement errors than the true NPSP cases which is 4 lb/psi (2.69 kg/pascal).

When considering the accuracy of vapor pressure measurements, it may become important to distinguish between propellants (oxidizer and fuel), for the measurement of one of the propellants will have greater sensitivity to error than the other. Figure 9 shows how pressurant weights increase

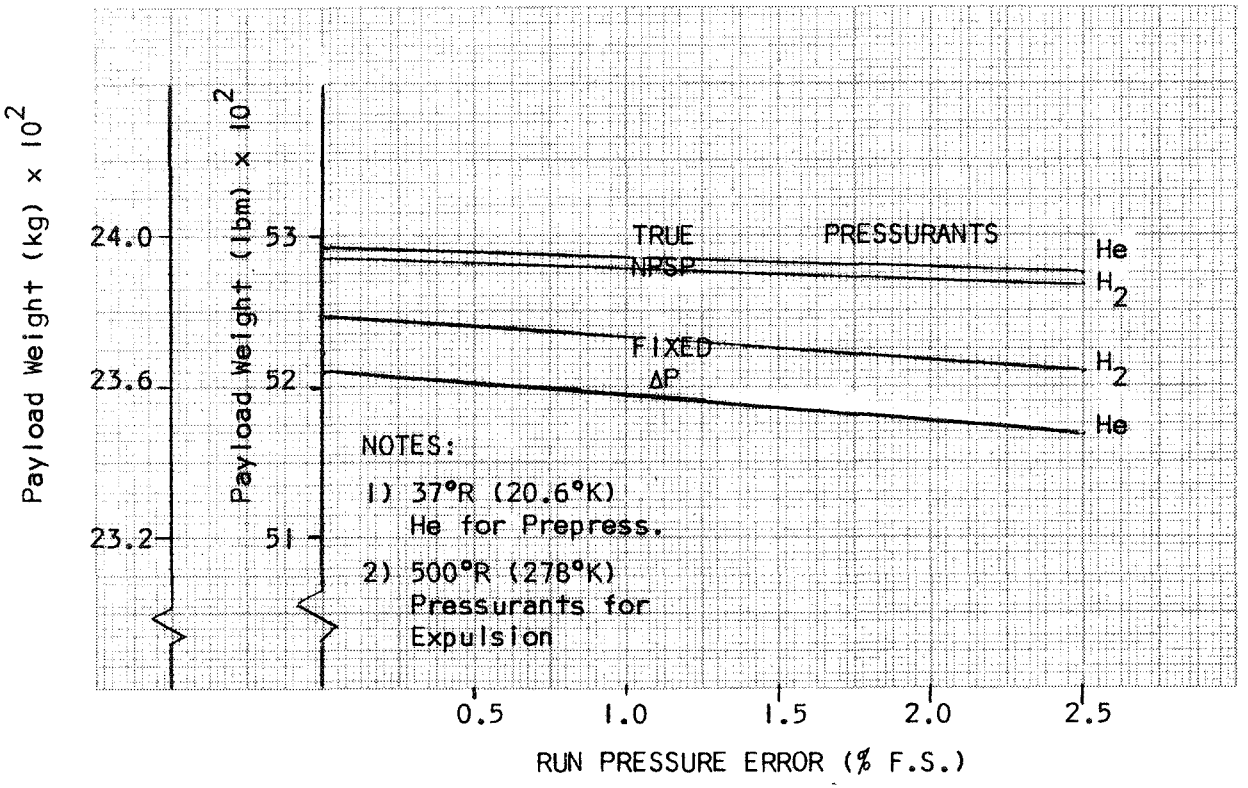

FIGURE 8. PRESSURE ERROR - VS - PAYLOAD WEIGHT

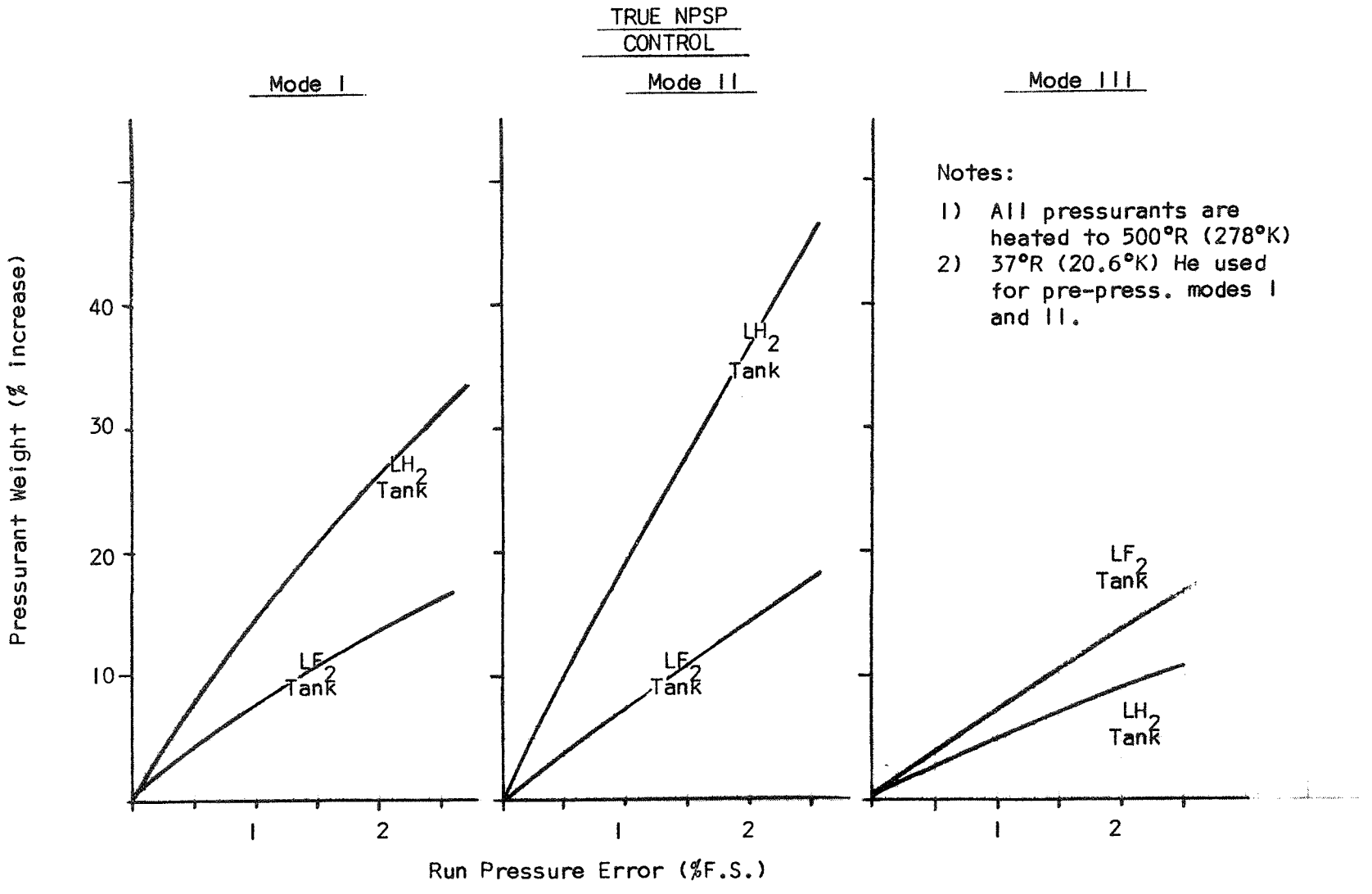

Figure 9 . Pressurant Weight Increase vs Run Pressure Error

in liquid fluorine and hydrogen systems as a function of error in pressure measurement for three modes of operation. Modes I and II show the hydrogen sensitivity to range from a 8 to 10% pressurant weight increase per psi error in pressure, while the sensitivity for the fluorine system is only 3 to 3.5% per psi. Furthermore, the weight ratio (hydrogen system pressurant weight to fluorine system pressurant weight) for these two modes of operation (I & II) are approximately 0.85 and 6.3, respectively. This further emphasizes the requirement that for the hydrogen tank the pressure measurement should be made more accurately than that of a fluorine system in order to provide a minimum pressurant weight for the overall system.

Three additional computer runs were made to generate accuracy data for the Mode III operation.

The Mode III operation resulted in the fluorine system having a greater sensitivity to pressure error than the hydrogen system and the quantity of pressurant required approximately 7 times that required for the hydrogen tank. In this case, the fluorine system accuracy is of greater importance, but the magnitude of the pressurant weight increase is small for both systems and should not penalize the total system to any great extent.

In summary, for systems that use helium pressurant, the true NPSP approach minimizes the amount of pressurant gas that must be added during the firing operation and it also maximizes the time that the feed system can be maintained in space until the tank vent pressure is reached. For some of the cases studied, a significant payload increase was obtained using the true NPSP approach. Based on the results of this limited study, it was concluded that the true NPSP control approach has sufficient merit to warrant its implementation. It should be noted however, that the actual differences in pressurant consumption and maximum orbit stay time will depend on the vehicle and mission requirements. Furthermore, if the reduction in pressurant weight plus the savings in venting losses are exceeded by additional hardware weight which may be required by a more complex system, the true NPSP system may not be warranted.

3.2 Pressure Sensor Evaluation

In the preceding section it was shown that pressure measurements could be in error by 1% to 2% of the full-scale (F.S.) without imposing a significant performance penalty . Therefore, the design target of 1% F.S. or better was established for pressure sensor accuracy. In evaluating accuracy, two factors were considered: (1) the inherent accuracy of the device, which includes repeatability and stability, and represents the best accuracy which can be achieved with the device under ideal conditions, (2) the inaccuracy of the actual measurement due to environmental effects, method of installation, and use.

The pressure sensor evaluation consisted of a literature search, concept and design study, vendor survey and the cryogenic testing of candiate pressure transducers. A summary of this evaluation is presented in the paragraphs that follow.

3.2.1 Literature Search

Some of the problems associated with pressure measurements in cryogenic systems were presented in Pressure Measurements in Cryogenic Systems, NBS paper and Temperature Response and Compensation for Pressure Transducers in Cryogenic Environments by Rocketdyne, Ref 2 & 3. In Ref 1, a few types of commercially available transducers were tested to determine their suitability for operation at temperatures down to 36°R (20°K). The results of this testing indicated that accurate measurements could be made using some of the types tested providing their calibration is checked each time they are cooled down. The types of transducers tested here encluded capacitance, potentiometer, and unbonded strain gage, and bonded strain gage. The capacitance type tested was found to be extremely sensitive to temperature requiring it to be re-zeroed at each temperature before calibration could be made.

All of the other instruments tested showed a deviation from their initial room temperature calibration when re-calibrated at liquid nitrogen and liquid hydrogen temperatures. This ranged from 2.7% of initial full scale

output for the instrument with the smallest deviation to a maximum of 16% for the instrument with the greatest deviation. These figures include any shift in the calibration which may have occurred during thermal cycling.

One of the unbonded strain gage types had the smallest error of any tested, and none of the three tested showed any tendency to develop marked non-linearity. However, some models showed large transient errors when they were subjected to severe thermal gradients during the thermal cycling process. The unbonded strain gage types were the most stable with respect to thermal cycling. However, of the three different ones tested, there were three different reactions to the low temperature environment.

Rocketdyne in Ref 3 evaluated a number of commercial cryogenic pressure transducers. This evaluation was made with the intent of improving transient temperature performance and adapting them for use with flowing liquid hydrogen under sudden exposure conditions. Three different transducer models were selected for experiments in liquid hydrogen. It was concluded that large massive transducers with diffuser protection were generally satisfactory for measuring the pressure of flowing liquid nitrogen or hydrogen for periods of few minutes of sudden exposure conditions. Flush diaphragm transducers were unsuitable for pressure measurements during transient cryogenic temperature conditions. Development of a new transducer was recommended for applications which cannot be met by heavy thermally protected units.

In the Instrument Society of America (ISA) transducer compendium, Ref 4 are over 300 models representing the various types of pressure transducers produced. In reviewing all these models, no unit had a specified operating temperature range extending to -423°F (-253°C). Five models had an operating temperature range that went as low as -300°F (184°C), however, the static error band was always greater than 1% of full scale, and in some cases as high as 10%. Kistler Instruments Corporation listed a piezoelectric type instrument rated for -400°F (240°C), but which was designed specifically for high pressure gas and dynamic conditions.

In reviewing available state-of-the-art transducers, it was found that accuracies of the order of .05% of full scale could be obtained under controlled laboratory conditions. However, the temperature variations, vibratory and/or static accelerations, instability, long-term non-repeatability, thermal hysteresis, and orientation changes encountered in flight environments will provide sources of additive errors. From the reference material studied, it was concluded that an error of 1% F.S. or slightly less represents an average for the degree of accuracy which can be "practically" realized with current state of the art transducers.

3.2.2 Concept and Design Study

In general, a pressure transducer consists of a force summing device and an electrical pickoff. The force summing device produces a displacement that is proportional to the pressure phenomenon being measured. The electrical pickoff produces a signal proportional to the displacment. Transducer design may be based on a wide combination of mechanical and electrical phenomena. The force summing devices include flat diaphragms, convoluted diaphragms, capsules, bellows, Bourdon tubes (circular and twisted), and ordinary tubes. Of all these mechanical devices, the flat diaphragm has the most desirable characteristics for the required pressure range and multi-propellant requirements of this program. Some of these desirable characteristics include:

a. Simplicity of design
b. Provides usable displacement and a bidirectional stress pattern
c. Provides small linear travel range; 1% linearly to 1/3 thickness
d. Low spring rate
e. Self protecting from overloads
f. Can be cleaned thoroughly for fluorine of FLOX service
g. Can be flush mounted

The MDAC laboratories are continually using and evaluating pressure instrumentation. Pressure transducers have been evaluated for both flight and ground testing on a number of programs. From this laboratory

experience, certain performance characteristics have been identified for the various types of pressure transducers and a discussion of the desirable and undesirable features associated with various types of pressure transducers follows:

Bourdon Tube/Potentiometer Transducer

This transducer exhibits many undesirable features which classify this design as not adaptable to this application. Some of these undesirable features included sensitivity to vibration and shock, and limited accuracy due to resolution and friction.

Bellows/Potentiometer Pressure Transducer

If this bellows type transducer uses a bellows manufactured from silver soldered nickel alloy (NI SPAN C) it will not be compatible with the corrosive medium F_2 or FLOX. If the bellows is manufactured from a corrosion-resistant metal such as stainless steel and the mechanical attachments are electron-beam welded instead of silver soldered, the repeatability and low hysteresis characteristic of NI-SPAN C alloy are not retained.

The bellows transducer, as with all potentiometric transducers, compromises accuracy, stability, and resolution for higher electrical output voltages.

Diaphragm/Potentiometer Pressure Transducer

This transducer is similar to the bellows/potentiometer; however, the diaphragm deflection is small, requiring additional linkage which results in poor repeatability. This type of instrument was judged to be inadequate for the control application.

Diaphragm Pressure Switch

Long-term error-band and lack of versatility eliminates the use of pressure switches in the design of a sophisticated multiple setting propellant pressure controller.

Electrical Capacitance Pressure Transducer

The electrical capacitance transducer was investigated and found to have several outstanding advantages. However, evaluation of this item was discontinued because of the parallel investigation of the capacitance digital transducer which offered even greater versatility and long term stability.

Piezoelectric Pressure Transducer

The piezoelectric (cystalline quartz) transducer and its man-made counterpart (polycrystalline) display excellent high-frequency pressure response. However, laboratory testing of a Kistler transducer for a previous program revealed that in the cryogenic temperature range, the transducer does not meet manufacturers claims for linearity, thermal zero shift, and long-term stability. The calibration factor (piezo-modulus) is not a constant under severe thermal-shock conditions.

A high rate of failure during thermal shock and acceleration testing, in conjunction with the low state of development in required accessory electronics, limits the use of this type transducer.

The piezoelectric pressure transducer was found to be more reliable in pressure ranges above 3,000 psi (2060×10^4 pascals).

Metal Wire or Strain-Gage Pressure Transducer

The strain-gage transducer was evaluated in both the bonded and unbonded configurations. Since this transducer design is the most widely used in cryogenic test and control technology, more data was available for this

type unit than for any other transducer investigated. The bonded strain-gage transducer was eliminated from further consideration because the epoxy bond becomes soft at elevated temperature (170°F) (57°C) and the long-term creep that results is excessive and beyond tolerance for accurate control. However, the vacuum film deposited strain-gage was further investigated because it was rated and recommended for cryogenic use. This type of transducer is small, relatively insensitive to vibration and acceleration forces, has relatively low spring constant and is sensitive to very small pressure fluctuations. Its compatibility with corrosive fluids is excellent and the instrument is capable of withstanding a great range of environmental extremes.

Capacitance/Digital Transducer

The capacitance digital transducer may incorporate a stainless steel diaphragm, electron-beam welded in position between capacitive elements. The deformation of the diaphragm by pressure causes a change of capacitance that is proportional to the pressure applied. As the diaphragm deforms, one oscillator increases in frequency while the other decreases. The output frequency of both oscillators is mixed and the resultant frequency is counted and converted to a digital output format that is analogous to pressure.

Such a unit would appear to be highly compatible with a digital controller and should have long term stability. Thus, this type of unit was a potential candidate in the program.

Inductance and Variable-Reluctance Pressure Transducers

All of the inductance variable-reluctance pressure transducers that have been investigated by MDAC utilize the same general principle; the sensor uses a flat diaphragm or twisted Bourdon tube whose deflection is proportional to pressure load. The force summing device is mounted between two magnetic pickups so that the gap between them is proportional to pressure. Ref 5 discusses the design of a variable - reluctance pressure transducer in some detail.

The variable reluctance transducer requires an excitation oscillator and demodulator as additional electronics. One very desirable characteristic of this unit is the relatively high level voltage signal delivered from the sensor to the remote electronic package which makes the system less sensitive to noise.

In summary, the piezoelectric potentiometer and the pressure switch were found to be unacceptable, in that they do not have the characteristics that are necessary to achieve the accuracy, long-term stability, and reliability required by this program. However, further consideration was given to the thin film strain-gage, the capacitance digital, the variable reluctance, and the variable impedence transducer types. These transducers represent the current state of the art, and appeared to have the potential for meeting the requirements of the program.

3.2.3 Manufacturer Survey

As a part of the sensor evaluation, a preliminary survey of a number of transducer manufacturers was conducted. The survey was accomplished by making direct contacts with the engineering departments of various transducer suppliers which could potentially satisfy program requirements.

It is desirable that the pressure sensing unit deliver a signal voltage to the electronics package in the controller that is as high as possible. This will minimize the effects of switching transients from the valve solenoids on the system that operates at cryogenic temperatures. Even the best diode suppression systems are not 100% failproof at cryogenic temperatures, and a switching transient could cause the controller to momentarily open the vent valve which would cause another transient and possibly start a chain reaction between solenoids and the controller which could deplete the tank pressure. The only failproof design is a transducer whose output signal could not be affected by extraneous voltage or transients from other systems. Of all the manufacturers surveyed, however, none could supply a pressure tranducer in a single unit package that would operate at as low as -320°F (-196°C), delivering 5 volts output for full scale pressure and maintaining an accuracy of 1% over a 2 to 3 year period.

However, four manufacturers agreed to submit their transducers for the engineering evaluation at cryogenic temperature in the McDonnell Douglas Meteorology Laboratories. Three of these four transducers meet the design criteria of high voltage output but only two, the Statham and Whittaker, were advertised as cryogenic instruments. All four transducers have "split-package" configurations with a portion of the electronics remotely located from the pressure sensor unit, so that the electronics may be located in a more suitable temperature environment. The transducers furnished for the cryogenic evaluation are described in detail below.

(1) Thin Film Strain-Gage Pressure Transducer

Statham Instruments, Inc., manufactures a vacuum-deposited, fully active strain gage bridge transducer made for operation at cryogenic temperatures. (Model number is PA 822). The transducer uses a flat diaphragm assembly made of 17-4 PH stainless steel. A ceramic film is deposited on this diaphragm to provide electrical insulation for the bridge elements. Four strain gages all vacuum deposited onto the insulator and are electrically connected to the bridge circuit. The instrument is excited with 10 VDC and the output, at full-scale is 34 millivolts. A certified 200 psia (138×10^4 pascals) transducer (Serial No. 504) was checked out of the McDonnell Douglas instrumentation pool for the testing.

(2) Capacitance/Digital Transducer

The CEC transducer division of Bell and Howell manufacture a digital pressure transducer. This instrument employs a dual capacitor primary sensor as a means of generating a frequency which is in turn applied to an integrated circuit counter and presented to a register for readout in a digital format. A conductive flat diaphragm is placed between two fixed insulated conductive flat diaphragm is placed between two fixed insulated conductive plates so that two capacitors are created.

The diaphragm is deflected by pressure in a bellows. The capacitances between the diaphragm and the fixed plates vary with diaphragm deflection. Each capacitance is the primary frequency determining element of an oscillator, giving two frequencies which are combined in a mixer to yield a highly linear FM output. The FM output from the mixer is then digitized by an integrated circuit counter.

The existing transducer described above is fully developed and in production however, it is designed for an operating temperature range of -65°F (-54°C) to 212°F, (135°C). These operating limits are imposed by the associated electronics (oscillator and mixer). This electronic package is an integral part of the sensor portion of the transducer and may not be separated. CEC furnished to MDAC a breadboard model for testing. The model was tailored for the cryogenic application by using standard button and platinum wire heaters to warm four critical transistors in the electronic package. Prior to delivery to MDAC the breadboard model was placed in a plastic bag and submerged in liquid nitrogen at the CEC facility. The instrument with its heated electronics was soaked for two hours and continued to function.

(3) Variable Reluctance Pressure Transducer

The Dynasciences Corporation (a Division of the Whittaker Corporation) produces a variable reluctance transducer that has a welded, twisted Bourdon tube sensing element combined with a variable reluctance pick-off and a miniaturized electronic package. Model P2-5000A was recommended by the Dynasciences Corp. This transducer was qualified by and was used on the LEM program. This transducer requires that the sensor portion be separated from the electronics which will not operate below -65°F (-54°C). This electronic change plus other material changes (change sensor element material to stainless steel, change glass seals to ceramic seals, etc.) will be required to enable the transducer to work in a continuous -320°F (-196°C) corrosive environment. The standard model P2-5000A (0-300 psia) (0-207 x 10^4 pascal) with the electronic package split was furnished to MDAC for the cryogenic testing.

(4) Variable Impedance Pressure Transducer

Kaman Nuclear recommended and furnished to MDAC for the cryogenic testing, their Model K-1500 (0-200 psig) (0 - 148 x 10^4 pascals) variable impedance transducer and their laboratory electronics. The basic sensor consists of an active and an inactive (compensating) coil assembly mounted in the same housing. The coil assemblies are mounted with the inactive element behind the active element, and a flat diaphragm is the only moving part.

The diaphragm is made of beryllium copper (nonmagnetic metal) and the coils are formed from ceramic-insulated magnet wire, wound on ceramic forms. The coil assembly is embedded with a special boron-free encapsulant in a beryllium copper transducer case. (See Figure 20).

The active and inactive coils are electrically connected to form two arms of a four-arm bridge circuit which is energized by a 1.0 MHz source. The other two arms of the bridge are contained in the matching network. When the diaphragm is exposed to a change in pressure, it becomes displaced into the magnetic flux lines that are emanating from the active coil. This action produces eddy currents which cause the bridge to become unbalanced. The sensing head is operated remotely from the oscillator-demodulator. Kaman recommended the use of their Model K-5500 aerospace electronic package in the final design (oscillator-demodulator). (The variable impedance principle is further described in Reference 6.)

3.2.4 Cryogenic Evaluation Testing

The object of the evaluation testing was to determine, under cryogenic and static conditions, the following performance characteristics of each of the four candidate transducers.

a. Pressure sensitivity
b. Linearity and hysteresis
c. Repeatability and zero drift
d. Temperature effects, zero drift and sensitivity

The test setup, procedure and results are presented in the paragraphs that follow:

3.2.4.1 Test Setup & Procedure

The evaluation test were performed in the McDonnell Douglas Metrology Laboratory. Figure 10 shows the four transducers installed in the Missmer chamber where the temperature was controlled and maintained at -320°F (-196°C) ±0.5°F (±0.3°C) for the duration of the test. Figure 11 shows the test equipment used in support of the testing. This equipment is also listed in appendix A. A Heise pressure gage (accuracy = 0.1% of full-scale [300 psig] (217×10^4 pascals) was used as a standard for the 10-point calibrations. The Datran electronic system was used for excitation and readout of the Statham transducer. The CEC's frequency output was monitored by the Hewlett Packard electronic counter and the oscilloscope. Volt meters and power supplies were also used for supplying energy for the heaters and the necessary excitation voltage. The Whittaker and the Kaman Nuclear transducer were both read out on the digital voltmeter. Kaman Nuclear laboratory electronics were used to supply the power, modulation, and demodulation required for the sensor. The electronics for the Whittaker transducer is not shown in Figure 10 but its small flight type package is located outside the Missmer chamber.

The sensors are connected to the electrical and pneumatic systems and helium is used as the pressurant. The procedure adapted in this testing consists of calibrating the test instruments at ambient and at liquid

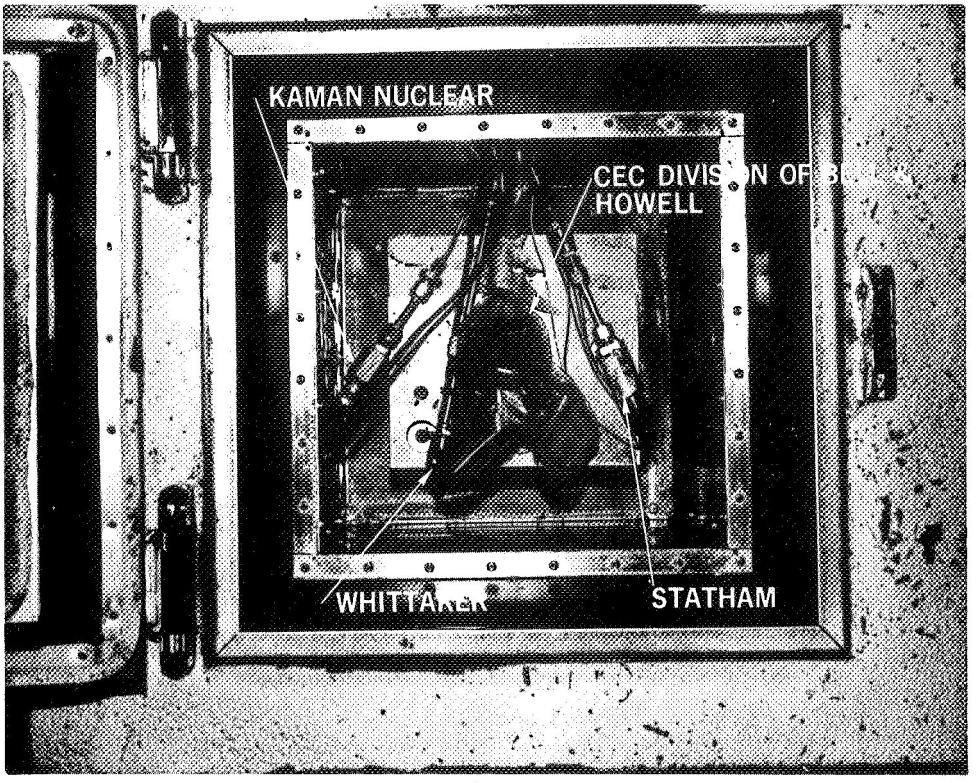

Figure 10. Transducer Installation—Missmer Chamber

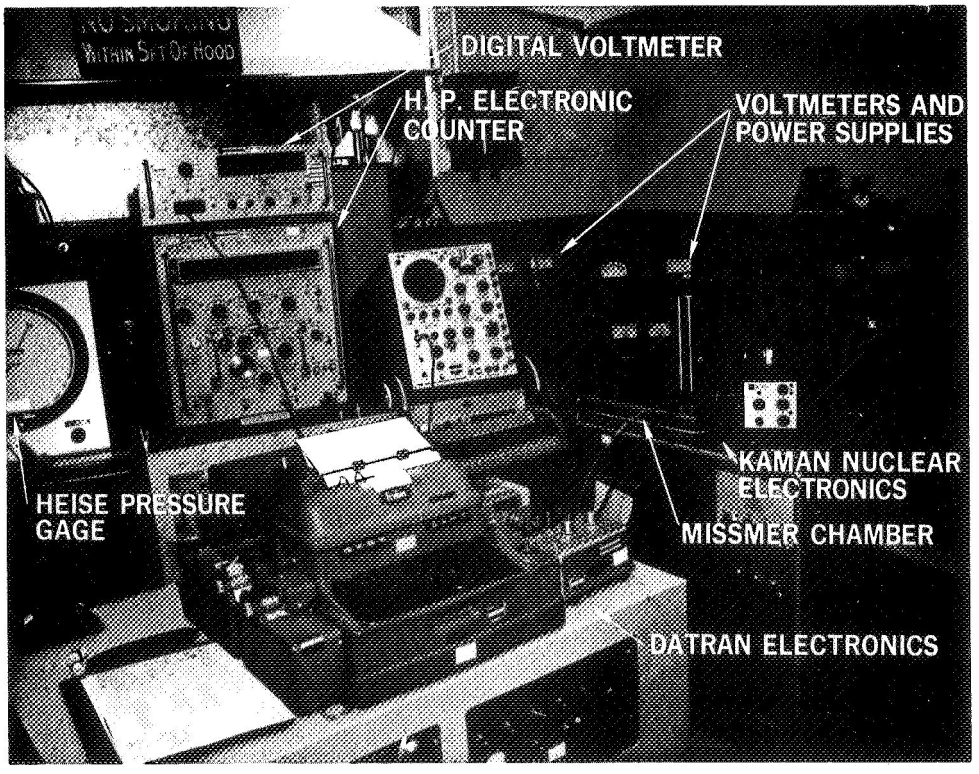

Figure 11. Test Equipment—Transducer Evaluation

nitrogen temperature. The instruments were cooled slowly at atmospheric pressure and the cryogenic calibration were not attempted until the sensors appeared to be at thermal equilibrium as indicated by both stable temperature measurements and stable zero output. Voltage outputs were measured in 25% FS pressure increments in both increasing and decreasing steps. Stability testing was conducted and calibration data were taken two times each day for a total of 96 hours in which the sensor environment temperature was maintained at -320°F ±4°F. (-196°C ±2°C).

3.2.4.2 Results

The results of the tests are plotted in Figures 12 through 15. Figure 12 shows the maximum pressure deviation for the Statham PA 822 transducer. These deviations were measured at the indicated times during the 96 hour testing. They are referenced to the initial calibration that was taken after 6 hours of soak at -320°F (-196°C). Each calibration was made using the Datran electronic system. However, this standard equipment nulls the DC output at the beginning of each calibration and therefore did not allow for zero drift data to be obtained. A maximum deviation of 2% FS occurred at 60 hours, however, the deviation from 72 hours to 96 hours remained at an acceptable level.

Figure 13 shows the zero drift data obtained from the CEC transducer. This transducer was in a plastic bag, installed by the manufacturer, without provisions for pressurizing. The manufacturer would not recommend pressurizing this instrument because they claimed the bellows used in the breadboard model was not representative of the 200 psia (148×10^{-4} pascals) used for our application. Therefore, zero drift data were all that was obtained for this instrument. At approximately 24 hours into the test, the sensor failed to show any output on the H.P. Electronic counter. At about 50 hours it came back on, for no apparent reason, and continued to function for the rest of the test. The maximum frequency drift, while in operation, was 0.04 MHz representing less than 1% of full-scale. The CEC design engineer was on hand at the end of the test, and while the chamber was warming up, the transducer again stopped. The CEC

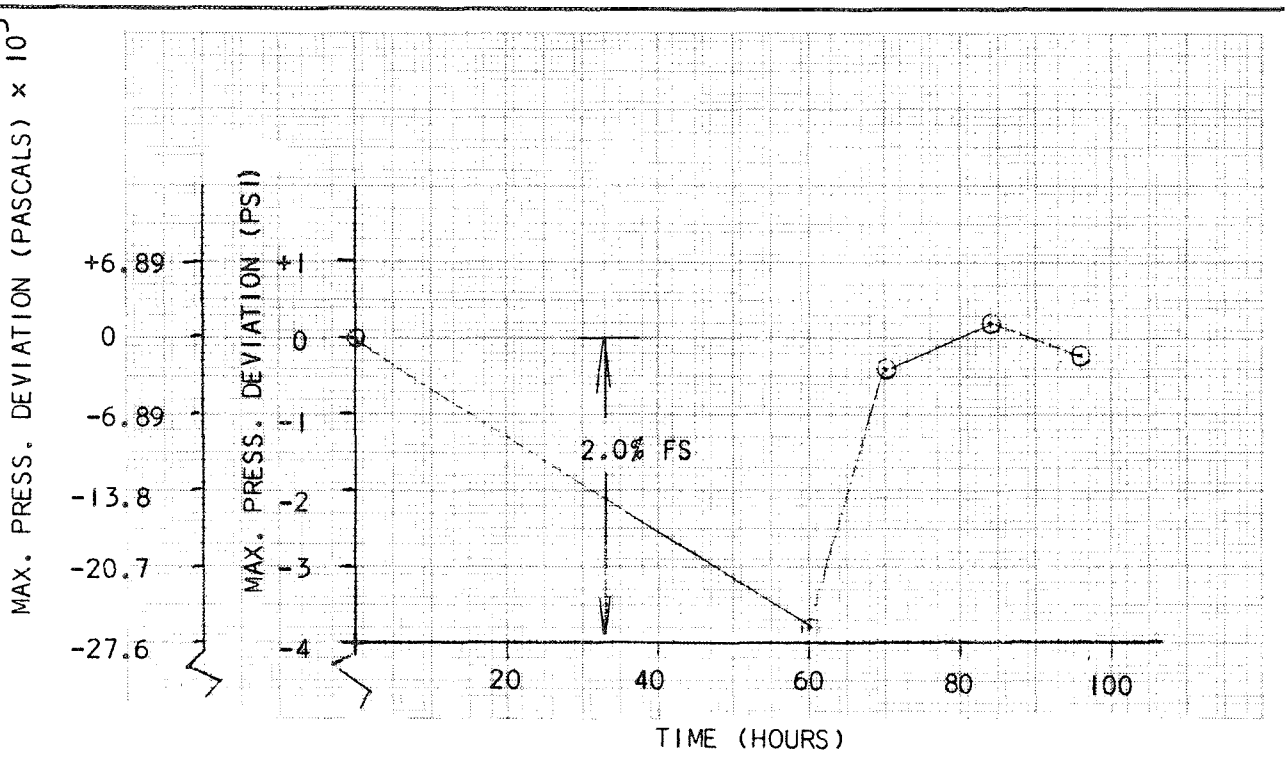

FIGURE 12 LONG TERM DATA - MODEL PA822

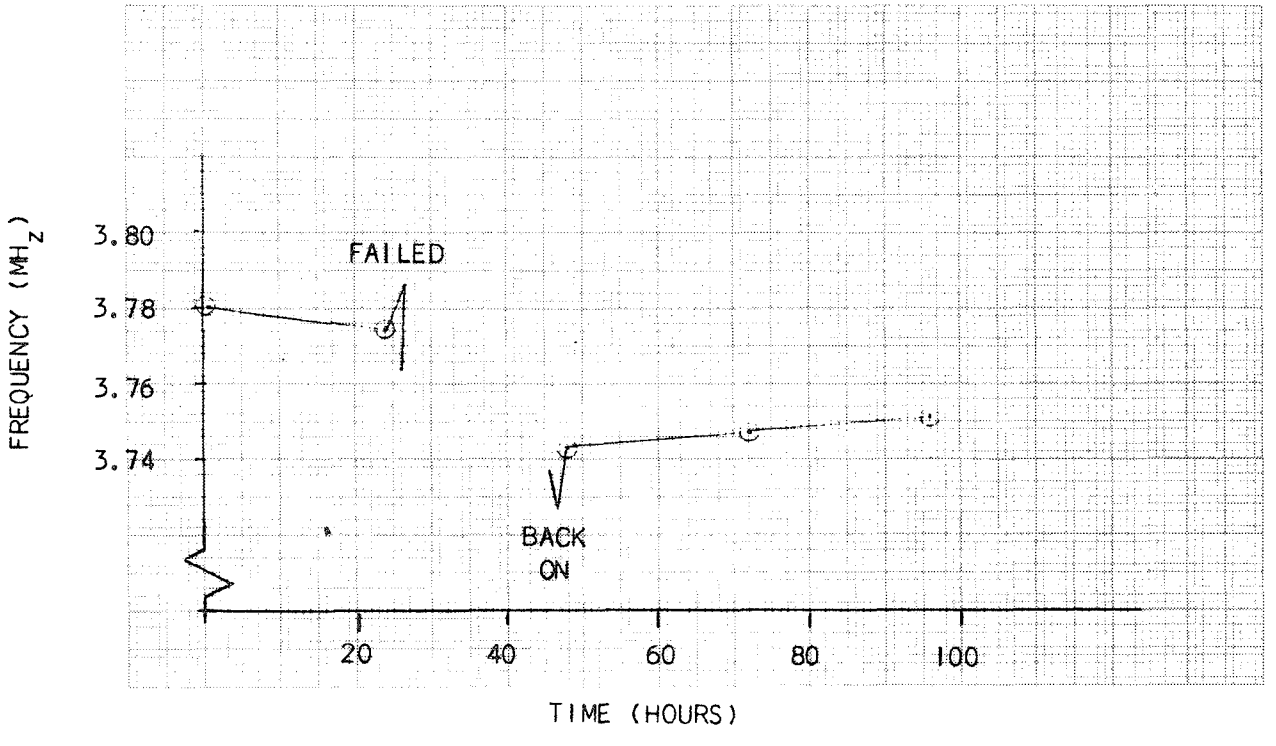

FIGURE 13 ZERO DRIFT DATA - CEC BREAD BOARD MODEL

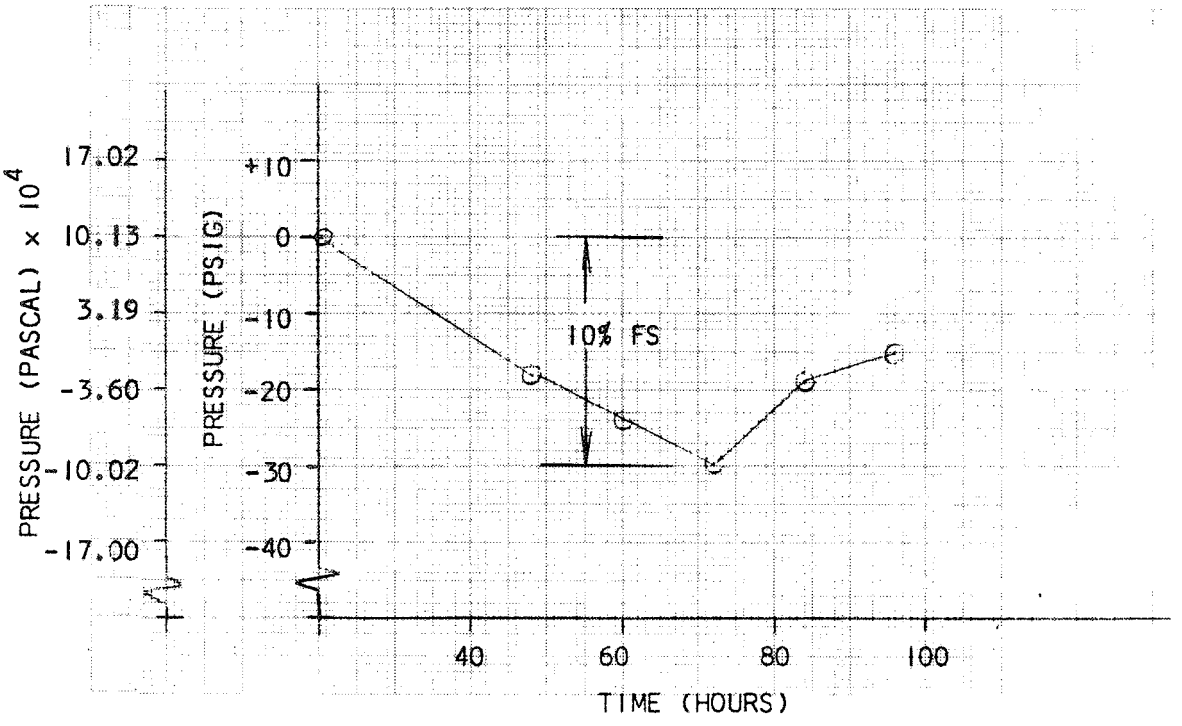

FIGURE 14 ZERO DRIFT DATA - MODEL P2-5000A

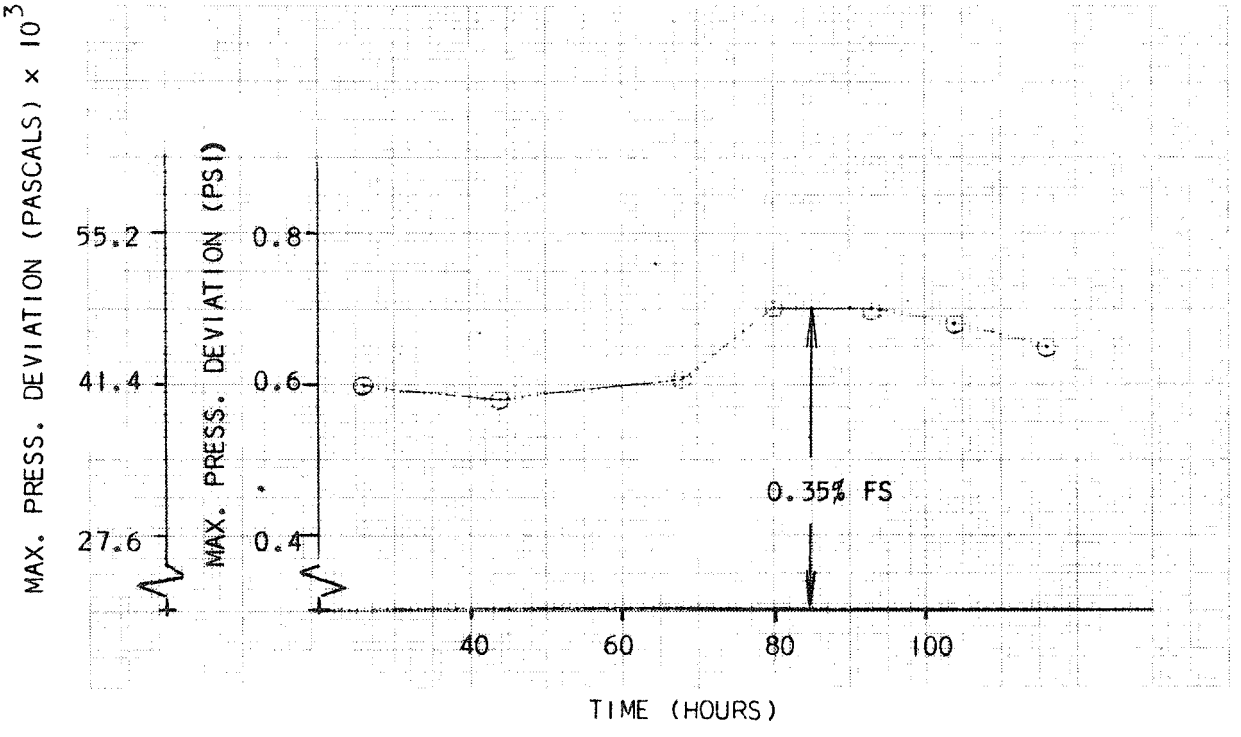

FIGURE 15 LONG TERM DATA - MODEL K1500

engineer examined the instrument and found that the capacitor had shorted out. It was assumed that dirt or moisture was the cause of failure. The distance between the capacitor plate and the flat diaphragm is about .002 inches (5.08×10^{-3} cm) so that even a very small ice or dirt particle could lodge between them and short out the capacitor.

Figure 14 shows the zero drift data taken from the Dynasciences Model P2-5000A variable reluctance transducer. This instrument was calibrated at 24 hour increments, however, only the zero drift data is reported here because of its overwhelming significance. At 72 hours the zero had drifted 10% of full-scale. There was some recovery at 96 hours, but still not to an acceptable level. A post-test analysis was made by the manufacturer and it was found that a welded electrical joint was open in the electronic package, which was outside the cryogenics. The long term zero drift was attributed to this condition.

The data taken for the Kaman Nuclear pressure transducer is presented in Figure 15. The ten-point calibrations were made at 24-hour increments and the maximum deviation was only 0.35% of full-scale. This maximum deviation occurred at the 200 psia (137×10^{-4} pascals) end point. These deviations were also referenced to the original calibration taken after the 6-hour soak at -320°F (196°C). There was virtually no zero drift over the 96-hour test. These most favorable results were encouraging and promoted testing at -423°F (-253°C). The transducer was submerged in 20 inches (0.51m) of LH_2, soaked at -423°F (-253°C) for one hour, and calibration tests were performed. Ten-point calibrations were made, pretest and post-test, at ambient temperature and at -423°F (-253°C). The change from 70°F (24°C) to -423°F (-253°C) resulted in both a sensitivity change of 11% FS and a zero shift of 16% FS, as expected. The repeatability, linearity, and hysteresis at -423°F (-253°C) totaled less than 1.1% of full-scale.

Based on the pressure sensor evaluation that includes the limited test results, the following conclusions were made for each of the instruments evaluated:

a. Statham PA822 - The maximum deviation (2% F.S.) measured in our lab is not acceptable by the 1% full-scale or less established requirement. Furthermore, the system accuracy that includes the signal conditioning (flight electronics Model No. CA17-0) was not guaranteed by Statham to be better than 2%. The reliability of this instrument is questionable because of the high incidence of failure reported by the Saturn S-IVB program. The low level voltage output (34 mv at F.S.) of the transducer further limits its reliability. This instrument relative to other candidates evaluated fails short of providing the necessary accuracy and reliability for the control system.

b. CEC - The CEC breadboard capacitance digital transducer did not perform satisfactorily in the long term test performed, however, the instrument, when tested at the CEC facility worked without interruption and showed a remarakably small deviation from the terminal straight line that is drawen through the zero and the maximum output points. A deviation of less than 0.2% full-scale was measured in this two hour -320°F (-196°C) soak test. In order for this instrument to be made reliable for operation in a cryogenic and fluorine environment both electronic and material changes are necessary. These changes would involve considerable risk and be out of scope.

c. Whittaker Model P2-5000A Variable Reluctance Transducer - The initial ten-point calibration taken in our labs at -320°F (-196°C) was extremely linear however, the long term -320°F (-196°C) data taken showed the instrument to drift from the initial zero point quite drastically. A post test examination was made by the manufacturer and revealed that an electrical connection had broken in their electronic package and that this was the reason for the zero drift. Unfortunately there was not time to re-evaluate the sensor in our laboratory. However, the vendor repaired the electronics and tested the instrument at -320°F (196°C) for 30 hours. The manufacturer reported the instrument to be stable with virtually no zero drift. This instrument, like CEC, also requires a material change. The Bourdon tube is made of Haynes 25, an alloy containing 14 to 16% Tungsten. Such alloys containing appreciable amounts of tungsten, are not recommended for fluorine service. The Bourdon tube material would have to be changed to stainless steel and the existing glass seals changed to ceramic. These changes will change the instrument's performance, which implies certain development risks associated in using this transducer, that make it undesirable for adapting for use in this program.

d. Kaman Nuclear - The performance of this instrument was proven to be more than adequate from the -320°F (-196°C) cryogenic testing performed in both the MDAC and Kaman Nuclear laboratories. Tests performed in liquid hydrogen further proved the instrument capable of making accurate measurements at -423°F (-253°C). There are no material changes required for the instrument to be fluorine compatible and the flight electronics with the sensor are guaranteed to deliver a static error band of less than 1% of full-scale at -320°F (-196°C). Furthermore, the instrument has a simple, rugged construction, fabricated entirely from corrosion resistant metals and ceramics. This transducer and its associated flight electronics was selected as the total tank pressure measuring device because of its superiority in terms of reliability, accuracy, and minimum development risk. The manufacturers specifications can be found in section 3.5.

3.2.5 Pressure Sensor Location Study

Pressure measurements in cryogenic systems are generally made by running pressure sensing tubing from the point where the pressure measurement is desired to a suitable pressure sensor located at a point where the temperature is near ambient. This technique of locating the body of the transducer slightly away from the low temperature region to achieve a more favorable environment is used on the Saturn S-IVB and many other applications. There are, however, some possible disadvantages associated with this approach such as:

a. Reduced frequency response
b. Thermal oscillations
c. Heat leak
d. Fatigue failure of lines
e. Temperature excursions which effect accuracy

With some pressure transducer installations, the limiting factor is frequency response in the connecting tubing. This is especially true if the lines are long and of small diameter, as they often are in an attempt to minimize heat leak in cryogenic applications. The best frequency response for a given type of transducer, is, of course, obtained when a flush diaphragm instrument is installed directly into the system. The

importance of this consideration in this controller application cannot be assessed at this point because it will depend on the requirements for dynamic response and stability of the total pressurization system that includes the pressurization and expulsion valves and tankage.

Lines that run from some relatively "high temperature" [250°R (139°K) in the Baseline Study] location into a cryogenic liquid can give rise to pressure pulsations unless care is taken to fix the liquid-vapor interface in the line. This phenomenon is caused when liquid is suddenly forced into a transducer line to a point where the temperature is above the saturation temperature of the liquid. The resultant pressure rise forces the liquid back in the line, causing a drop in pressure which again allows the liquid to move into the high temperature region starting a new cycle. This problem is especially severe with liquid hydrogen because of the low viscosity and low volumetric latent heat of vaporization. However, in a low g (.01 g's) environment, the sensing tube diameter required for allowing liquid hydrogen to be forced to the sensor would have to be approximately .785 in. (2 cm) in diameter. This is much larger than what would be used, from a practical standpoint, in attempts to minimize heat leaks while obtaining the required frequency response. Thus, this would not appear to be a significant problem.

The use of a sensing tube would at first seem to represent another source of heat leakage into the cryogenic tank. To evaluate this, a comparison was made of the possible conduction heat leak through an equal length 5/16 (0.79 cm) x 0.01 (2.54×10^{-2} cm) in. stainless steel tube and a four conductor bundle of No. 30 (very fine) electrical wires (to supply signal and excitation power to the direct tank mounted transducer) over a temperature difference of 500°R (278°K) to 40°R (22.2°K). It was found that the heat conduction through the wire bundle is about three times that through the steel tube, primarily because of the high conductivity of the wire at low temperatures. This also does not take into account the heat which is generated by the transducer while ON, and which goes directly to the propellant heating when the transducer is mounted directly on the tank. Thus, from propellant heating considerations, the

stand-off transducer is preferred. Assuming a 5/16-in (0.79 cm) diameter by 2-ft (0.61 m) long stainless steel sensing tube, the heat leak to the LH_2 with a ΔT = 460°R (256°K) would be less than 0.1 Btu/hr (0.029 watts).

The above considerations of reduced frequency, thermal oscillations, and heat leak, along with fatigue failure in lines, appear to be small factors influencing the selection of the sensor location in this application. The temperature excursions, however, will contribute largely to the pressure sensor accuracy. In a space mission typical of the 205 day trajectory to Mars, the environmental temperature external to the propellant-tank-mounted high performance insulation will vary with time due to space vehicle orientation and changes in solar flux between Earth and Mars. The ambient temperature span may be 2 to 3 times larger than the liquid propellant temperature. These changes will result in a thermal shift in zero, sensitivity, and nonlinearity. To obtain the most accurate possible measurement with a given pressure sensor, the sensor should be placed in the most constant and stable temperature environment.

In an effort to obtain a near constant and stable temperature, it was recommended that the sensor portion of the pressure transducer to be placed beneath the high performance insulation and mounted directly to the tank wall with the sensing diaphragm exposed to the liquid propellant. The associated electronic package will be remotely located with the controller. This was also the design approach used in the evaluation of the sensors.

3.3 Partial Pressure/Vapor Pressure Measuring Techniques Evaluation

Techniques and devices for measuring the liquid propellant vapor pressure and the propellant vapor and helium partial pressures were evaluated and compared. The measuring concepts and techniques considered include:

a. Polarographic
b. Gas Chromatograph and Mass Spectrometer
c. Propellant Sampler
e. Temperature Transducer

3.3.1 Polarographic Sensor

Beckman Instruments, Inc. has developed a miniaturized Polarographic Oxygen Sensor. The sensor and its associated electronics measures oxygen partial pressure. This sensor was developed for the United States Air Force Manned Orbiting Laboratory (MOL), and was used as a part of an Oxygen Partial Pressure Monitoring system which provides output signals to control the precise quantity of oxygen in the MOL two-gas life support systems.

The sensor body is 1.0 inch (2.54 cm) in diameter and 1.3 (3.31 cm) inches in length containing a gold cathode and a silver anode. These electrodes are mounted behind a thin FEP Teflon membrane which permits diffusion of oxygen for the electrochemical measurement. Potassium chloride gel is used as the electrolyte between the electrodes.

This oxygen sensor is linear throughout its entire range. The output current depends on the permeable membrane used. In this application, current was generated using 1-mil (2.54×10^{-3} cm) thick FEP Teflon membrane.

The current produced at the sensor passes through a load resistor; the voltage developed is amplified by a low-power, differential, DC amplifier. The output of the amplifier (0-5VDC) is used for telemetry and meter readout.

Temperature compensation is required for the sensor because the membrane permeability changes with temperature. The amplifier also requires a controlled temperature environment. The performance characteristics for the MOL sensor include:

Mission Life (Hrs)	1,000
Accuracy % (F.S.)	$\pm$ 1.5
Storage Life (months)	9
Operating Temperature (°F)(°C)	40-110 (4.5 - 44.5)
Stability % (F.S)	
(1000 Hr Tests)	
Min. drift instrument	< 1.0
Max. drift instrument	> 7.0

The Polarographic Oxygen Sensor has been used successfully with an oxygen supply control system to maintain oxygen partial pressure, however, the flexibility of this program requires the control system to be compatible and capable of measuring fluorine, FLOX, hydrogen, and methane as well as oxygen. Based on the technical discussion and the data furnished by Beckman engineers, the following conclusions were made:

a. The oxygen sensor is highly reliable, stable and sufficiently accurate for the NPSP application.

b. A modest study could be made to prove the sensor for use with fluorine, however, certain material changes will be required. The electrolyte, potassium chloride may have to be replaced with potassium fluoride.

c. An extensive development program would be required to sense hydrogen. Changes in the cathode material from gold to platinum will be required. Hydrogen sensors have been built for the space program but have never flown, and in those built there was difficulty in maintaining a constant sensitivity in low concentration hydrogen environments.

d. The Polarographic sensor is not universally adaptable to all the required propellants.

e. Difficulty may result in supplying a representative sample of the ullage gas. This difficulty arises from the necessity of locating the sensor in a remotely controlled temperature environment where the gas sample must be plumbed to the instrument.

f. Partial pressure measurements, even if measured accurately, are not ideal because the measurements are made within ullage gases that are at a different temperature than the liquid propellant that enters the pump due to non-equilibrium and thermal stratification in the tank.

g. Based on the above conclusions, a large development program will be required to qualify the three polarographic sensors, for Hydrogen, fluorine, and methane.

3.3.2 Gas Chromatograph and Mass Spectrometer

These two techniques for measuring partial pressure require that a gas sample be analyzed. Similar to the Polarographic Sensor, a representative sampling is required, and again, partial pressure is measured which is not ideal for true NPSP control. Other conclusions based on an investigation of these techniques as applied to the true NPSP control operation include the following:

a. These instruments are inherently large
b. They are very sensitive to both shock and vibration.
c. They are both extremely complex and costly.
d. Low level signals are generated as output.
e. It is doubtful if these instruments could provide sufficient accuracy for control.

Therefore, such concepts were eliminated as candidates.

3.3.3 Propellant Sampler

One of the most frequently used techniques for measuring vapor pressure in the laboratory is a method that places the propellant in an evacuated container where temperature is controlled and vapor pressure is directly measured. Figure 16 shows the conceptual design of a device for sampling and measuring the vapor pressure on board the spacecraft. The design consists of all metal parts, a body, poppet, bellows, and seats. The

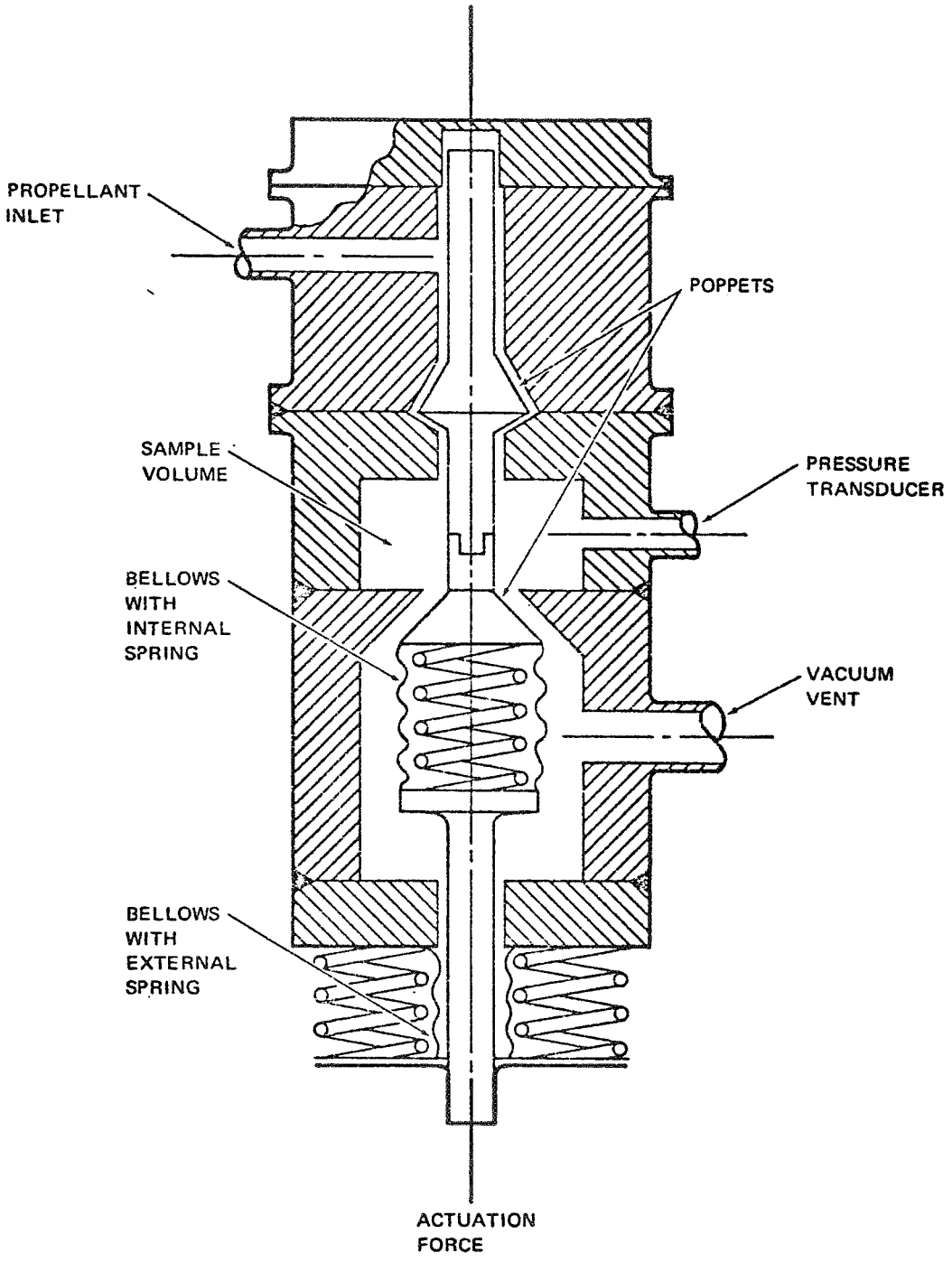

FIGURE 16. PROPELLANT SAMPLER CONCEPT FOR DIRECT VAPOR PRESSURE MEASUREMENT

propellant sample is made available at the inlet side of the sampler valve while the other side, including the sample volume, is evacuated to space. To obtain a propellant sample, the valve is actuated to move the poppet and allow the liquid propellant to enter the sample volume, partially filling it with vapor and liquid, before the poppet seats to seal off the flow from the inlet. At the same time, the poppet seats in the bellows and traps the liquid and vapor in the sample volume. The sampler is submerged in the propellant tank as near to the pump inlet as possible, to assure that there will be no significant temperature change in the propellant being sampled. One obvious advantage of this technique is that the vapor pressure is measured directly by a pressure transducer which, in turn, provided a signal to the controller.

This design should be accurate and have a high degree of adaptability. The sampler can be designed to work with all the required propellants providing the materials selected are compatible. In addition, the following conclusions can be made for this technique.

a. In obtaining a propellant sample it is required that both liquid and vapor be trapped in the sample volume. Proper sizing of the poppets and seats and timing for the sampling cycle will be necessary to obtain the required sample.

b. Very low leak rates are required for the long term mission, and may represent a development problem.

c. For the liquid hydrogen tank the actuating force can be supplied by a solenoid submerged in the tank. The electrical leads and a small 1/16" .159 cm OD tube for vacuum venting will penetrate the tank wall. The vapor pressure line can be plumbed to a tank wall mounted pressure sensor.

d. The liquid fluorine tank may require a pneumatic actuator, since a submerged solenoid would be incompatible.

e. The vapor pressure measurement is not continuous and will require a number of cycles of operation during engine burn and expulsion in order to account for the time variation in propellant partial pressure that results from the thermal stratification in the tank.

Based on the above findings, considerable design, analysis and testing will be required to develop a sampler of this type. The effort required was judged to be beyond the scope of this program in terms of dollars and development time, however, this concept may have future potential.

3.3.4 Temperature Transducer

The vapor pressure of the liquid propellant can also be determined by measuring the liquid-propellant temperature. However, the vapor pressure-temperature function for typical cryogens is generally nonlinear over the pressure range from 14.7 to 100 psia (10.1 to 68.9 x 10^{-4} pascals). A platinum resistance temperature transducer and its associated signal conditioning unit were considered here. The signal conditioning unit consists of a low gain differential DC amplifier with a constant current transducer excitation supply and platinum resistance vs. vapor pressure linearization.

The platinum resistance vs. temperature curve is nonlinear, as well as the vapor pressure vs. temperature function. Low gain differential DC amplifiers have been designed and built for Agena and Apollo. They provide platinum vs. temperature linearization with 0 to 5 volts DC output. This linearization was less than 0.5% of full-scale deviation from the best straight line for the 0 to 5 volts output. It was believed that the manufacturer would be able to do as well linearizing the vapor pressure function. Additionally, the following conclusion were made regarding the temperature transducer and generation of the vapor pressure-temperature function.

a. For the system that uses a platinum temperature probe with remote signal conditioning, tailoring of the signal conditioning amplifier will be required for the fuel and oxidizer to provide the necessary accuracy. This is a result of the different temperature range and the nonlinearity differences associated with each propellant.

b. The accuracy for the probe and linearizing amplifier system should be adequate for measuring vapor pressure.

The platinum sensor technique was selected for the propellant temperature/vapor pressure measurement because it was the most practical of the methods investigated and the cost and development time were within the scope of the program.

Four manufacturers' system designs for the vapor pressure measuring system were evaluated on the basis of accuracy, cost and reliability. The sensors and signal conditioning systems proposed by manufacturers are listed below along with their predicted total system accuracy:

	ROSEMOUNT ENGINEERING	THERMAL SYSTEMS	RDF WEST	MDAC-WD
LF_2 System	$\pm$3.0%	$\pm$1.5%*	$\pm$1.6% to 2.6%	$\pm$1.8% to 3.0%
LH_2 System	$\pm$1.5%	$\pm$1.5%	$\pm$2.6% to 4.6%	$\pm$1.0% to 1.5%

*NOTE: This value was assumed because data were not available.

MDAC-WD investigated the possibility of linearizing the fluorine vapor pressure vs. platinum resistance curve for pressures from 0 to 180 psig (10.1 to 134 x 10^4 pascals). Specifically, a digital computer program was used to analyze the effect of gain $(\frac{R_1 + R_2}{R_2})$ on the linearity of the output voltage as a function of vapor pressure (indirectly measured by the platinum resistance R_T) for the network shown in the sketch below. R_i, E_s, and R_f were arbitrarily set to 5 K ohms, 10 volts, and 10 K ohms, respectively.

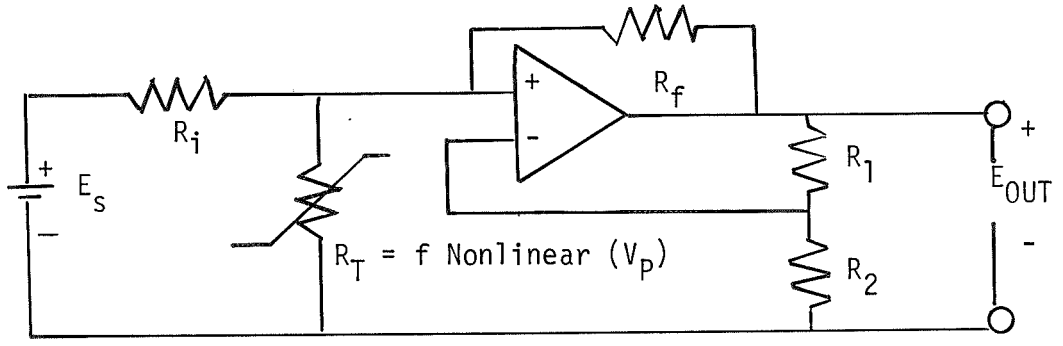

A gain choice of $\frac{R_1 + R_2}{R_2} = 25$ resulted in a reduction in nonlinearity of the subject curve from an uncompensated value of 16.8% to a compensated value of 2.4%. A 1% nonlinearity was observed over most of the curve and it was 2.4% only at the extreme end points. Thermal Systems proposed a design similar to the MDAC design. Both systems would have required development since they are completely new designs. These systems theoretically have a better accuracy; however, it is believed that this small accuracy advantage over the Rosemount and RDF-West systems would not warrant the risk of development. Rosemount Engineering Company's proposed systems was selected primarily because of accuracy and reliability. The liquid hydrogen tank pressurization system accuracy was of particlar importance as shown earlier in Figure 9. The specifications for the instrument can be found in Section 3.5.2.

Ideally for the space vehicle application, the platinum probe should be located at the pump inlet. However, if conditions are such that this is not possible the probe should be located in the propellant tank sump area or wherever the propellant temperature is representative of that which will enter the pump.

3.4 Controller Logic and Timing

Figure 17 shows the controller block diagram which includes all the essential elements of the system and how they are related. ΔP_2, ΔP_3, P_4 and P_5 are the preset reference points analogous to pressure. ΔP_2 is the minimum net positive suction pressure (NPSP) also defined by $P_2 - P_1$. Similarly, ΔP_3 is defined by $P_3 - P_1$. These values are also defined below and illustrated in Figure 2. The run pressure dead band is $\Delta P_3 - \Delta P_2$ and P_4 and P_5 are the upper and lower limits of the vent pressure respectively. These preset reference points have the following range capability:

ΔP_2	1.48 to 46.1 PSID (1.02 to 31.7 x 10^4 pascals)
ΔP_3	1.48 to 46.1 PSID (1.02 to 31.7 x 10^4 pascals)
P_4	1.48 to 188.6 PSIG (11.15 to 139 x 10^4 pascals)
P_5	1.48 to 188.6 PSIG (11.15 to 139 x 10^4 pascals)

Two analog measurements are provided to the control logic, P_T and P_V (propellant total pressure and vapor pressure). After power turn on, the system operates on these measurements and controls valves in accordance with the following:

Standby

if $P_T \geq P_4$ open vent valve(s)

if $P_T \leq P_5$ close vent valve(s)

if pre-fire signal on, start P_T signal conditioning warm up

if firing signal on, go to pre-calculation

Firing

Pre-Calculation

if $P_1 + \Delta P_3 = P_3' < P_4$ go to pre press.

if $P_1 + \Delta P_3 = P_3' \geq P_4$ open vent valve(s) and go to venting mode

if firing signal off go to standby

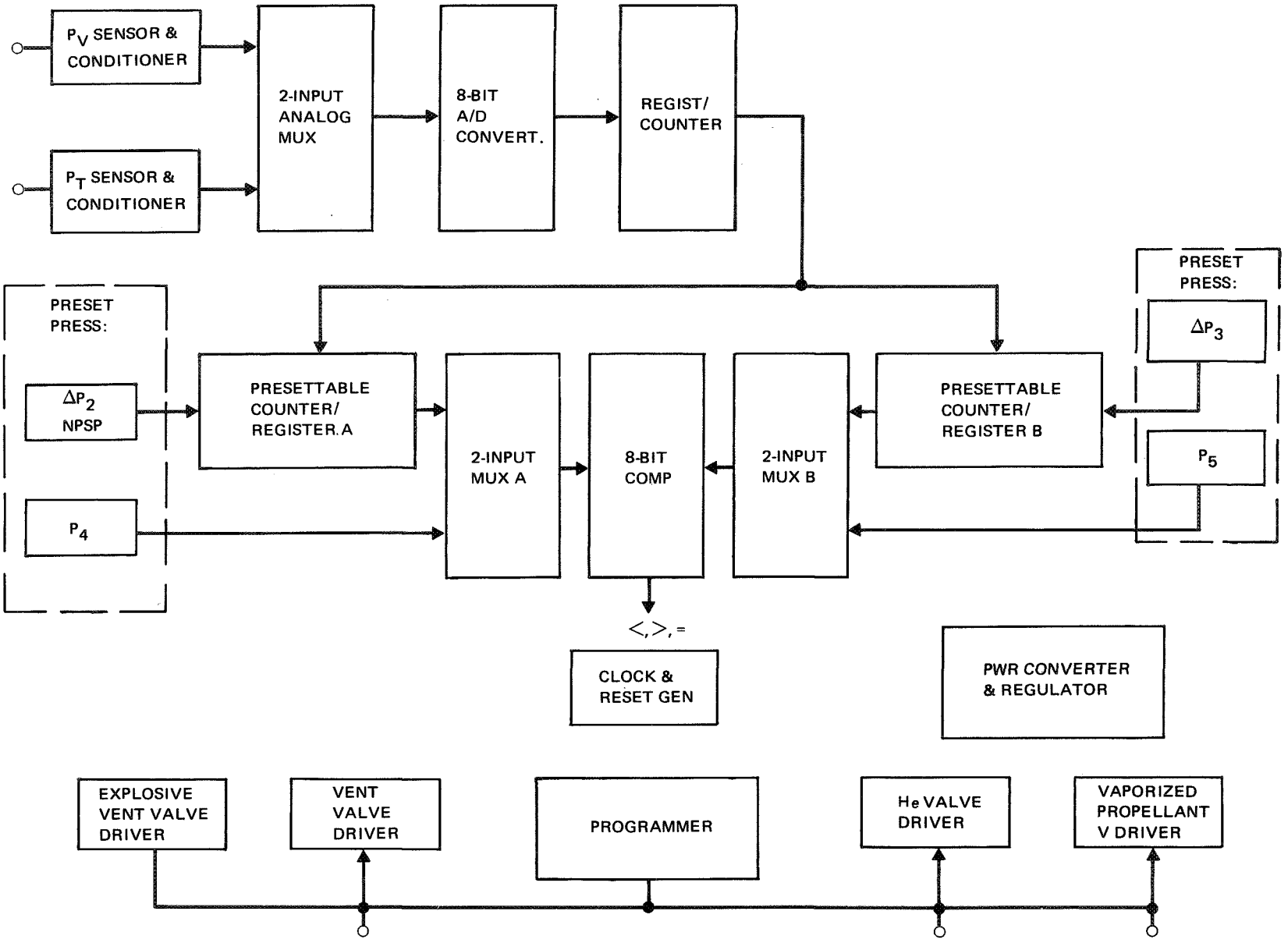

Figure 17. Controller Block Diagram

Firing (Continued)

Venting

if $P_T \leq P_5$ close vent valve and go to precalculation

if firing signal off go to standby

Pre-Press and Firing

Open pre-press. valve

If $P_T \geq P_3$ close pre-press. valve and generate pre-press. complete signal

then

if $P_T \leq \Delta P_2 + P_V$ open press. valve

if $P_T \geq \Delta P_3 + P_V$ close press. valve

if firing signal off return to standby

NOTE:

1. P_1 = initial propellant vapor pressure
2. P_2 = lower limit of the control band during pressurization and expulsion and $P_V + \Delta P_2$
3. P_3 = upper limit of the control band during pressurization and expulsion and $P_V + \Delta P_3$
4. P_4 = vent valve open pressure
5. P_5 = vent valve closed pressure
6. P_V = instantaneous vapor pressure

   P_T = instantaneous total pressure
7. The following limitations to the operation of the controller should be observed.

   a. The output from the P_T and P_V signal conditioners should not be allowed to go negative or to exceed + 5V. These cases represent an under or over range condition at the sensors (Range: 0-190 PSIG (10-141 x 10^4 pascals) alternately, faulty system calibration may cause either of these conditions to occur. If an over-range condition occurs during standby, all valve drivers are disabled and the vent valve is closed. If an under range condition occurs during either standby or firing, unpredictable valve driver response will result.

   b. During the firing precalculation, P'_3 should not be allowed to exceed +5V or 190 PSIG (141 x 10^4 pascals) since it will result in an over-range condition with unpredictable valve driver response.

From Figure 17 it can also be seen that the digital counting output from the 8 bit A to D converter is routed to either presettable counter/registers A or B. For example, in the firing mode and at the appropriate time, the prewired NPSP (ΔP_2) is preset into counter/register A. The A to D converter output (P_V) is then added also by counting it into counter/register A. This operation yields the sum of preset pressure ΔP_2 and the counting output of the A to D converter (P_V). The sum may be routed to the 8 bit comparator by enabling the 2 input multiplexer A at the appropriate time. The sum is routed through multiplexer B into the 8 bit comparator where it is compared against P_T. The resultant comparison determines whether one quantity is larger than, smaller than, or equal to the other. The programmer then advances the controller to the next operation.

The time required to complete a given sequence can be determined by multiplying the sampling rate of the A to D converter by the number of operations. The A to D converter requirements can be found in paragraph 3.5.3.

Figure 18 shows a representation of controller timing and events. The controller functions appear at the center of the diagram while corresponding input and output signals are shown at the top and bottom, respectively.

After 28 volts power input is provided to the controller, all bistable elements are reset. The reset period $t - t_0$ is approximately 3 seconds which includes the total time required for controller warmup. This period coincides with the turn-on time constant of the voltage converters and regulators.

The standby cycle $t_3 - t_1$ occurs when neither firing nor reset signals are present. During standby, P_T is monitored and the vent valves are opened when required by the tank pressure. A one-shot circuit is incorporated into the explosive vent valve driver which generates a pulse of approximately 0.9 seconds width. This pulse width is sufficient to open the explosive vent valve, while power consumption during the subsequent venting is reduced.

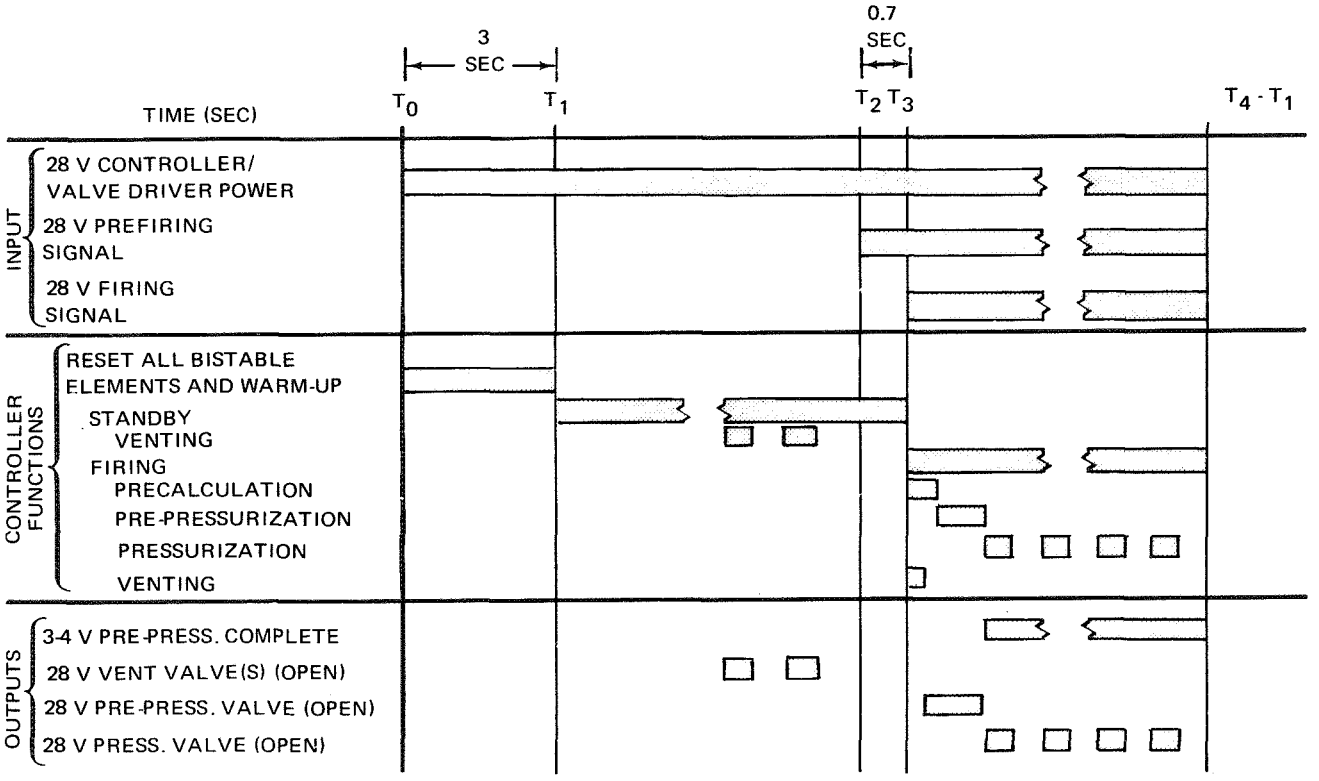

Figure 18. Timing and Events

At time t_2 the prefiring signal is applied to the controller. The sole function of this 28 volts signal is to turn the P_V signal conditioner on and to allow a minimum of 0.7 seconds for its warmup prior to initiating the firing cycle. An alternate delayed firing signal generator circuit, which is discussed in Appendix C, eliminates the need for the pre-firing signal. This delay generator was not furnished with the controller.

When the firing signal is input to the controller, the standby cycle is terminated and the firing cycle starts. Initially a precalculation is performed, to determine whether the prepressurization would result in $P_3' = P_1 + \Delta P_3 \geqq P_4$. For this condition, the system is vented to P_5 before prepressurization takes place. When prepressurization is complete, an appropriate "pre-press complete" signal is output until the firing signal terminates. The system is pressurized during the remainder of the firing cycle. At time t_4, the firing signal terminates and the controller switches to standby operation shown at t_1.

3.5 Subsystems

The section discusses the specifications and requirements for the controller subsystems. All the components and materials selected in the design are compatible with the long-term vacuum requirements for a space flight model. In addition, all the integrated circuits and discrete components used in the digital logic portion of the controller are military parts designed to operate over the temperature range -65 to +170°F (-54 to 77°C). Where possible, all other selected subsystems, power regulators, A-to-D converter, and the analog signal conditioning units were designed or modified to meet the vacuum, vibration and temperature environmental requirements of the actual flight model (see system specifications in Appendix D).

For cost effective reasons, ordinary military parts are used in the prototype instead of the costly high reliability components that will be required for the long-term flight model. A reliability analysis is presented in paragraph 3.6 where the reliability of each subsystem is discussed.

3.5.1 Total Pressure Measuring System

The Kaman Nuclear sensor, Model No. KI501-2, and Flight Electronics Model No. K5500 were used and incorporated with the controller for the total pressure measurement. This system was described also in some detail in Section 3.2.3. The manufacturers' drawings associated with this subsystem are listed below:

DRAWING NO.	TITLE
800466	DIMENSION DRAWING AEROSPACE MODEL K5500
830155	SCHEMATIC AEROSPACE MODEL K5500
810942	ADAPTER FITTING

This system is also supplied with mating connectors and are furnished with 20 feet of flexible coax cable. Figures 19 and 20 are exploded views showing the adapter, "O" ring, Raco seal, sensor and retaining nut assembly. The sensor diameter is 0.687 inches (1.74 cm). The manufacturer specification for the electronics and sensor are listed below; and the initial calibration data furnished by the manufacturer is given in the Operation/Calibration Procedure (1T19806).

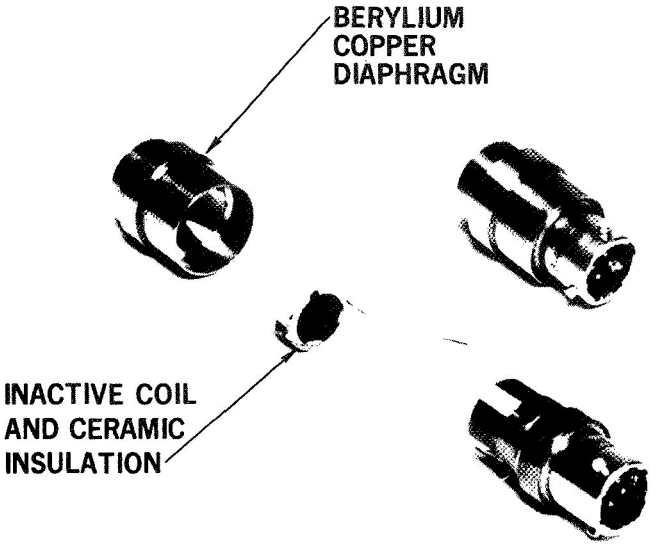

Figure 19 Pressure Sensor Exploded View

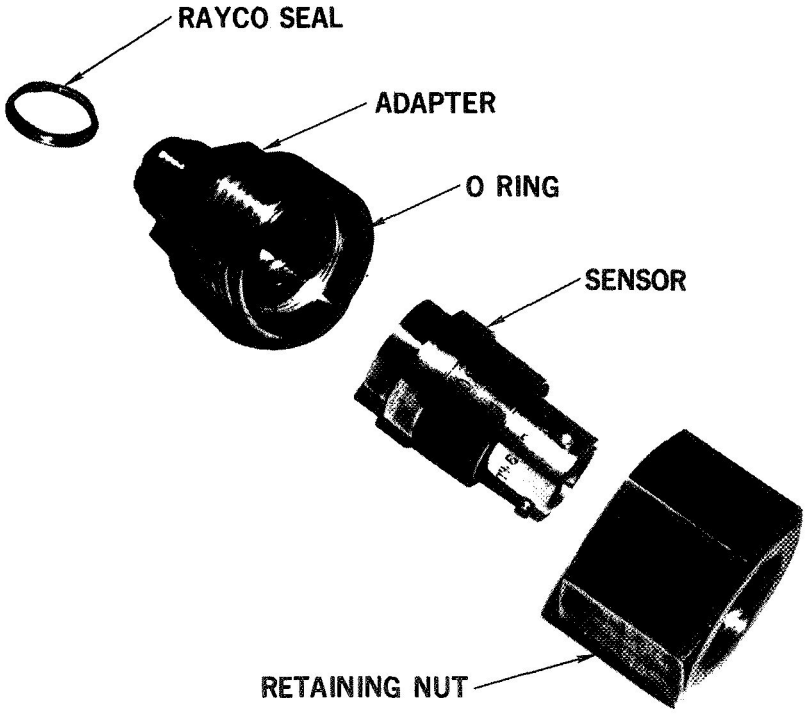

Figure 20 Pressure Sensor and Adapter Exploded View

KAMAN NUCLEAR, SPECIFICATIONS FOR THE MODEL K-5500 ELECTRONIC PACKAGE

Output voltage:

0 - 5 Volts DC proportional to measured range. Limited at +6V, -1V DC.

Output Impedance:

1000 OHM's.

Maximum Linear Output Current:

.2 Ma into 25 K OHM's.

Maximum Output Noise:

Less than 5 millivolts peak-to-peak.

Input Power:

21 - 32 Volts DC unregulated.

60 Ma Maximum current drain (without degradation).

(Capable of withstanding $\pm$ 50 V transients 10 milliseconds duration.)

Electromagnetic Interference:

Within requirements of MIL-STD-826 Class A_U for both conducted and radiated interference.

Isolation, Power and Ground:

Greater than 50 Megohms @ 50 V (non-operating)

Environmental:

Survival:

Temperature:

-30°F to +185°F (-36°C to 85°C)

Humidity:

0 - 100% relative humidity over temperature range.

Shock:

18 shocks 50 g, 11 millisecond duration.

Vibration:

Random 20 - 2000 Hz, density 0.16 g^2/Hz peaks to 3 times RMS value, 5 minutes, 3 axes

KAMAN NUCLEAR, SPECIFICATIONS FOR THE MODEL K-5500 (Con't)

Acceleration:

25 g 10 min. 3 axes.

Operating:

Temperature:

+30°F to +130°F (0°C to 54°C)

Humidity:

0 - 100% relative humidity over temperature.

Thermal 0 Shift:

Less than ± .03%/°F.

Thermal Sensitivity Shift:

Less than ± .03%/°F.

Weight:

K-5500 - 12.6 oz.
Interconnecting Cabling - .088 oz./ft.

Case Materials:

Aluminum, Anodized, or Nickel Plated.

KAMAN NUCLEAR, SPECIFICATIONS FOR MODEL K-1501-2 PRESSURE SENSOR

Pressure Range:

0-190 PSIG (10 to 141 x 10^4 pascals)

Overload Pressure:

295 PSIG

Leak Rate (Adapter Assembly):

$<1 \times 10^{-9}$ scc/sec, He at 70°F

Operating Temperature:

-423°F to +170°F (-253°C to +77°C)

Zero and Full Scale Output
(0 to 5 volts)

Adjustable:

-320°F and -423°F

Linearily (Best straight line):
at -320°F (-196°C)
$\pm$0.5%

Hysteresis (Ref. to F.S.):
at -320°F (-196°C)
0.1%

Acceleration Sensitivity:
0.05% F.S./g max

Thermal Zero:
0.02% F.S./°F

Thermal Sensitivity:
0.02% F.S./°F

Transducer Case and Adapter Assembly Material:
Berylco - 10

Cable Length:
20 feet (6.096 meters)

Reference Pressure:
The reference side of the sensor is back filled and sealed up with dry helium to a pressure of 1 atmosphere (10.13 x 10^4 pascals) or less.

3.5.2 Vapor Pressure Measuring System

The Rosemount Vapor Pressure Measuring System provides a 0 to 5 volt DC output signal from a platinum resistance temperature sensor. The vapor pressure is sensed in terms of temperature and the system internally, within the signal conditioning, linearizes the inherent vapor pressure/ temperature and temperature/resistance anomalies. A bridge network accepts the remote probe signal and together with the linearization circuitry provides a signal to the amplifier. (See Block Diagram, below.) The Model 510BF is built around a carrier type amplifier which has much better stability than straight DC amplifier over the wide ambient temperature variations and long periods of time. The unit also contains voltage regulation output, supply voltage, isolation, internal resistance for 50% F.S. calibration and output limitation and protection circuitry. All circuitry is solid state.

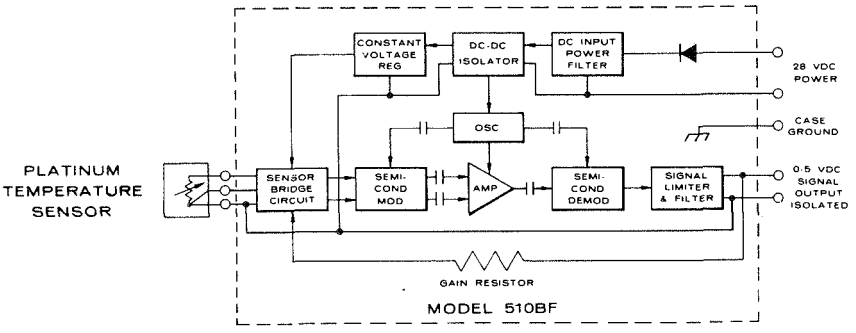

ELECTRICAL BLOCK DIAGRAM

The specifications and requirements defined for each system are listed below:

a. SYSTEMS

LF_2 SYSTEM	LH_2 SYSTEM
176 HY 24 Transducer	133 CC 24 Transducer
Specification Drawing	Specification Drawing
510 BF Signal Conditioning	510 BF Signal Conditioning

b. OPERATING TEMPERATURES

LF_2 Transducer = -306 to -249°F [-188°C to -156°C]
H_2 Transducer = -423 to -402°F [-253°C to -241°C]
Signal Conditioning Amplifier = -65°F to +170°F [-54°C to +77°C]

c. TOTAL SYSTEM ACCURACY

H_2 System = ±1.5% F.S.
F_2 System = ±3.0% F.S.

d. SYSTEM CONFIGURATION

The transducers are supplied with mating connectors. The transducers and their mating connectors are assembled with 20 feet 6.096 meters of flexible double shielded cable and a jam nut receptacle. The jam nut connector is assembled with 8-1/2 inches 0.216 meters of flexible double shielded cable and the mating connector for the signal conditioning. The above assembly is typical for both fluorine and hydrogen systems. The 176HY24 transducer receptacle was changed to incorporate a receptacle like that of the 133-CC-24 transducer probe.

e. CALIBRATIONS

The calibration data furnished by the manufacturer is given in 1T19806. The special calibration data was also furnished by Rosemount and is presented below.

LH_2 SYSTEM

TEMPERATURE				OUTPUT VOLTAGE (VOLTS)		
°K	°R	°C	°F	(ACTUAL)	(IDEAL)	DEVIATION
20.6	37	-253	-423	0.012	0.013	-0.001
24.4	44	-249	-416	0.734	0.684	+0.050
26.6	48	-244	-412	1.351	1.316	+0.035
30.0	54	-243	-406	2.673	2.658	+0.015
32.2	58	-241	-402	3.933	3.908	+0.025

LF_2 SYSTEM

85.5	154	-188	-306	-0.139	0.013	-0.126
93.8	169	-180	-291	0.617	0.566	+0.051
97.7	176	-175	-284	1.027	0.961	+0.066
103	185	-170	-275	1.6577	1.631	+0.027
108	194	-165	-266	2.445	2.500	-0.055
113	202	-161	-258	3.444	3.474	-0.030
117	21	-156	-249	4.8671	4.868	+0.003

The liquid hydrogen calibrations show the maximum deviation from the ideal linear function to be +50 millivolts. The liquid fluorine system data show the deviation from ideal to be -126 millivolts at the zero point (85.5°K); however, the data at 21.5 psig (24.9 x 10^4 pascals) and for values up to 185 psig have a maximum deviation of 66 millivolts. Added to the nonlinearity are the inaccuracies associated with zero shift, temperature sensitivity, repeatability and input supply all of which in the worse case add up to 0.8% of full scale. Therefore, the liquid hydrogen system should have an accuracy of better than 1.8% and the LF_2 system should prove to be better than 2.1% over the greater part of the pressure range (20-190 psig) (23.9 to 141 x 10^4 pascals).

3.5.3 Analog to Digital (A-to-D) Converter

The A-to-D converter selection also resulted from a thorough search. The Analogic system was chosen from a number of preferred models. Its selection was based on the following considerations:

a. A counting output to facilitate system interfacing and possible substitution of digital pressure sensor.

b. A low speed conversion rate (characteristics which increases noise rejection).

The following components were selected:

ANALOGIC DRAWING NO.	TITLE
5-1010	SCHEMATIC HI-Z MULTIPLEXER AN 4110
5-1141	SCHEMATIC VOLTAGE TO COUNT CONVERTER AN2317
5-1014	OUTPUT REGISTER SCHEMATIC AN 300 SERIES

The 2 channel multiplexer accepts signals from either temperature or pressure transducers after these signals are conditioned to yield 0 to 5 volt outputs which are proportional to propellant vapor pressure and total pressure. The multiplexer routes either signal to the A to D converter when commanded by the programmer.

The A-to-D converter and multiplexer evaluation was further based on the following requirements:

Multiplexer

a. Input Signal: 0 to +5 VDC, unipolar

b. Input Impedance: larger than 100 K ohms

c. Combined Effect of Offset Voltage and On-Resistance: less than 0.1%.

d. Switching Rate: less than 1 msec.

A to D Converter

a. Compatible with multiplexer containing internal reference source

b. Input Signal: 0 to +5 VDC, unipolar

c. Resolution: 8 binary bits

d. Accuracy: less than ±1% for combined effects of operating temperature range, extrapolated 2 year drift, initial and linearity errors.

e. Output: parallel or preferably pulse train

f. Sampling: Initiated by external trigger or internal presettable clock

g. Sampling Rate: 20 msec or less

Environment

a. Operating Temperature: -65°F (-54°C) to +170°F (+77°C)

b. Other Environmental Conditions: according to Specifications in Appendix D.

c. If compliance cannot be assured, unit(s) must be suitable to be potted, foamed, and/or conformally coated by MDAC.

The temperature and total pressure sensors yield low-level analog voltages which are amplified in their respective conditioners to the 0 to 5 volt level. In conditioning, the temperature is converted into equivalent vapor pressure. These two 0 to 5 volt analog outputs are multiplexed to the 8 bit A to D converter by an analog multiplexer. The A to D converter is of the dual-slope integrating type. Its internal sample rate adjustment is presently set to 1.2 per second, while the aperture time is less than 20 milliseconds. The sampling rate of the A to D converter can be readily changed by changing the external RC components. The procedure to change the sampling rate can be found in the "Operating and Calibration Procedures" MDAC-W Drawing No. 1T19806.

3.5.4 Valve Drivers

The valve driver circuit converts a 0-3 VDC logic level signal to a 0-28 VDC power signal to be used for valve actuation. Three amperes were selected as a maximum valve load as specified in Table 2.

Circuit Configurations

Several circuit configurations were considered prior to selection of the circuit shown in Figure 21.

The first choice to be made was whether to use a grounded transistor or a grounded load. It was decided that the grounded load configuration provided practical advantages with respect to valve maintenance and repair since otherwise an additional power switch would be necessary to eliminate hazards at the valve interface.

The next selection to be made was whether the output transistor (Q2, Figure 21) should be a PNP or NPN device. PNP material was selected as the most economical choice in the desired power dissipation range.

TABLE 2

VALVE
ELECTRICAL REQUIREMENTS

The following solenoid valve requirements shall be met throughout any combination of the environmental and operating conditions.

a. Wiring

All external wiring of the solenoid shall be AWG 22 or larger. Internal wiring shall be insulated from case ground.

b. Current Draw

The current draw, at operating pressure and temperature shall not exceed 3.0 amperes.

c. Continuous Duty

The valve must be capable of continuous excitation at 30 VDC with no failure or degradation in the electrical properties.

d. Pull in Voltage

The solenoid shall not be pulled in at a voltage less than 18 VDC.

e. Interference Circuity

The internal electrical circuitry of the valve is required to contain a transient suppression system.

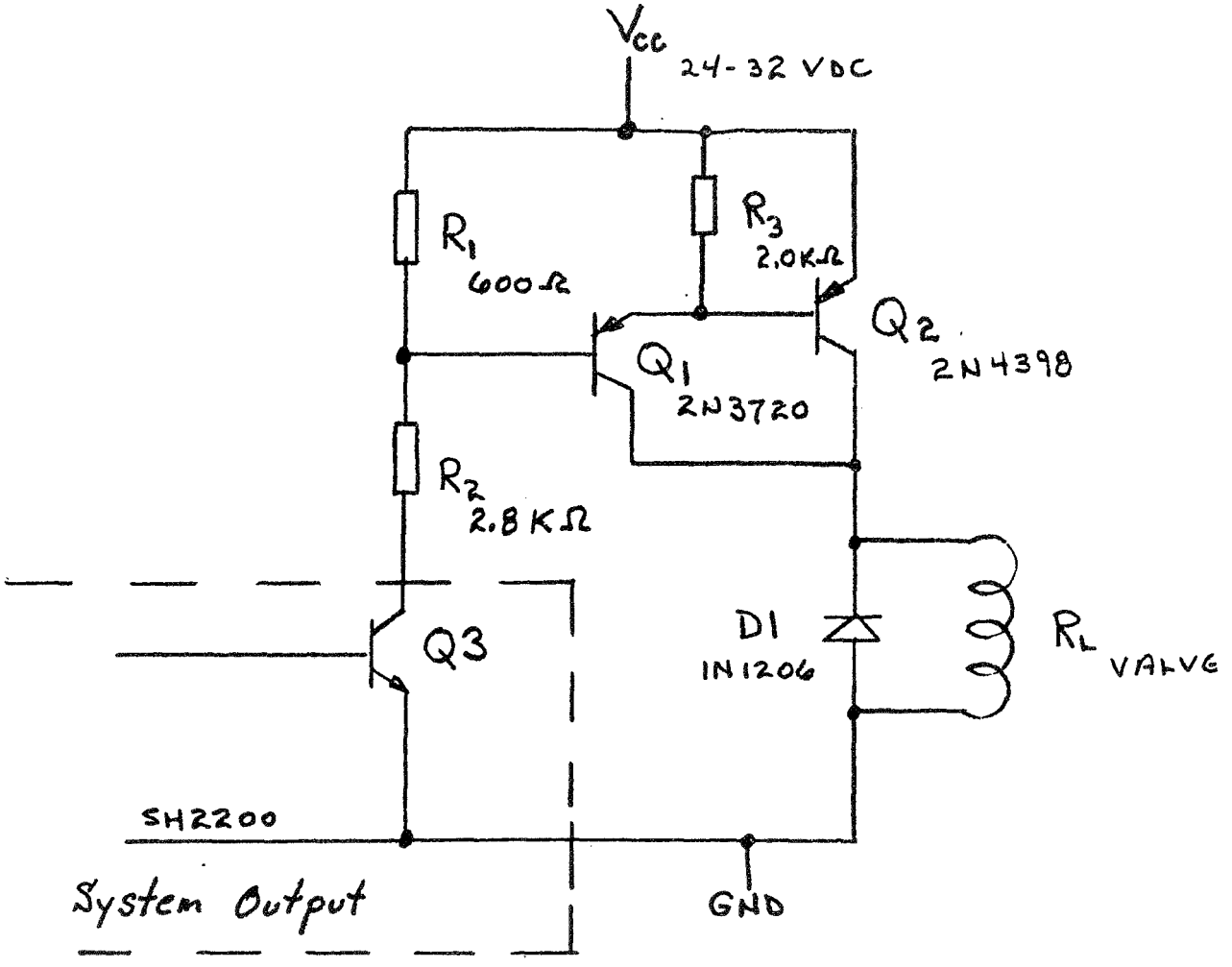

FIGURE 21
VALVE DRIVER SCHEMATIC

The Q2 base drive must be approximately 0.150 A. This current may be sunk in the load, or through some other component to ground. The latter choice would necessitate dissipation of approximately 5 watts steady state during valve energization while the former choice only requires a peak of 5 watts dissipation during valve switching. The former alternative was selected.

If an NPN transistor were selected for this task (Q1), its base would be near 28 V and additional circuitry would be necessary to provide the drive current. A PNP transistor in this position can sink its drive current (7mA) to ground through an appropriate 5 V logic element; hence, a PNP transistor was selected. R_1 and R_2 are provided to limit the forward bias on Q1 and Q2 when Q3 is off, and R_2 provides a voltage drop to set the base drive in Q1. Q3 is the output stage of an integrated circuit element compatible with the other system circuitry. D1 provides a current path for the solenoid discharge, thereby preventing high voltage "inductive kicks" across Q2.

Analysis and Component Selection

a. Q2 Selection

1. Steady State Current

Q2, by specification, must deliver a maximum of 3 amps to the inductive load over the total operating temperature range (-55°C to +77°C).

2. Steady State Power

The steady state power dissipation will be the product of 3 amps, and the saturation V_{CE}, approximately 6 watts.

3. Peak Power

Since the load is inductive and the L/R ratio is unknown, the load line could approach the worst case shown in Figure 22 at point 3, e.g., 32 V x 3 amp. = 96 watts.

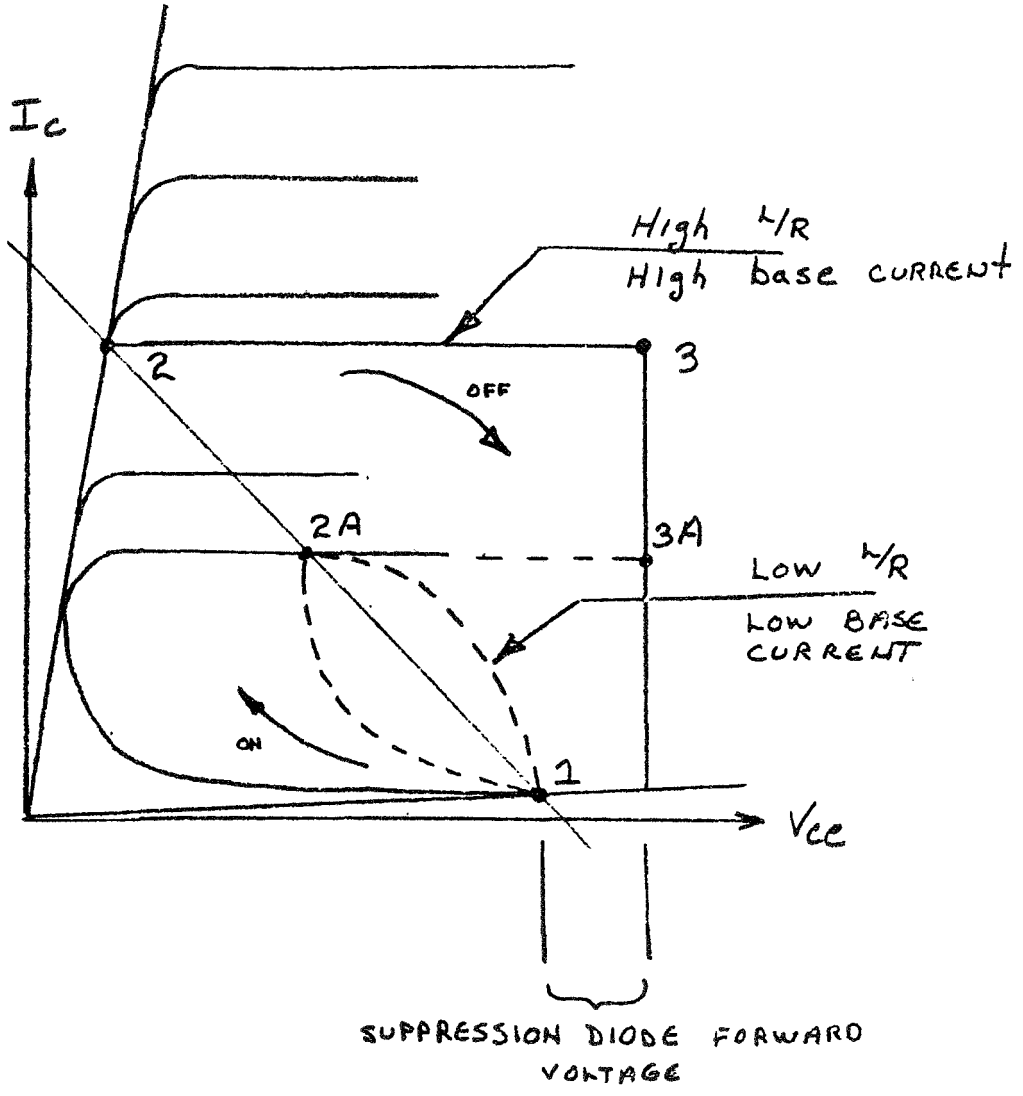

FIGURE 22

TYPICAL INDUCTIVE LOAD LINE

At point 1, Q2 is off, $I_C = 0$, $V_{CE} = 32$ VDC worst case. When Q2 is turned on, V_{CE} quickly drops to zero and the current rises exponentially to point 2, or 2A. Point 2 will be the "on" state if adequate base drive is available; Point 2A is the point if the base drive is limited. Since 2A is a high steady state power dissipation state, adequate base drive over the temperature range must be guaranteed.

At turn off, the operating state moves to Point 3, at which time D1 becomes forward biased and begins to conduct. D1 continues to conduct while the inductive field collapses and state 1 is reached. To achieve maximum reliability, Point 3 should be well within the D.C. safe operating region of Q2.

4. Worst Case Average Power - Repetitive Operation

Q2 could conceivably be required to operate at a 50% duty cycle. Under this condition the average power dissipation would be 50 watts or less.

5. Voltages

V_{CC} is 28 to 32 VDC, V_{CEO} = 40 VDC was chosen as the specification.

6. Selection

The 2N4398 transistor was selected for Q2. Its characteristics are as follows:

(a) PNP, Silicon, TO-3 case

(b) 50 watt at 130°C Air

(c) 6 amp at 32 VDC peak

(d) Minimum h_{FE} (-55°C) = 15 @ 3 amp.

(e) $V_{CEO_{max}}$ = 40 VDC

(f) I_C = 30 amp. at V_{CE} = 4 VDC

b. Q1 Selection

1. Steady State Current

Q1 must pass enough current to nearly saturate Q2. From the 2N4398 Spec. Sheet, this value is .06 amps[1] at 25°C. typical.

2. Steady State Power

.06 x V_{CE} (Sat) = approx. .12 watt

3. Peak Power

.06 x 32 VDC = 1.98 = approx. 2 watts

4. Worst Case Average Power - Repetitive Operation

50% x 2 = 1 watt

5. Voltage

$V_{CEO_{max}}$ = 40 VDC

6. Selection

The 2N3720 transistor was selected.

Its characteristics are as follows:

(a) PNP, Silicon, TO-5 case

(b) 1 watt cont. at 25°C AIR

(c) H_{FE} min (25°C) = 20 at I_C = 500 mA

(d) $V_{CEO_{max}}$ = 60 VDC

(e) I_C = 3 amp. at V_{CE} = .6 VDC, I_B = 100 mA

---

[1] The 2N4398 gain, at 25°C (Spec. Sheet, Fig. 10), V_{CE} = 2 VDC, is approximately 100.
I_C = 3.0, I_B = .03, I_{C/I_B} = 100

The normalized gain at I_C = 3A, V_{CE} = 2 V, 25°C is .7

The normalized gain at I_C = 3A, V_{CE} = 2 V, -55°C is .4
therefore, the gain at -55°C, V_{CE} = 2V is approximately 57 and a V_{CE} vs. I_B, curve for 3 amps at -55°C can be approximated. This curve shows approximately 60 mA drive required to saturate Q2.

c. R_1, R_2, R_3 On-State Analysis

if $V_{CC} = R_1 I_1 + R_2 (I_1 + IB_1)$, Q3 shorted, I_1 flows thru R_1

and

$$V_{CC} = V_{EB_1} + V_{EB_2} + R_2 (I_1 + I_{B1})$$

$$\text{let } V_{EB_1} + V_{EB_2} = V_{EB}$$

then:

$$I_1 = \frac{V_{EB}}{R_1}$$

$$I_B = \frac{V_{CC} - V_{EB} (1 + R_2/R_1)}{R_2}$$

if I_{B_1} must be 4 mA or more

$$R_2 = \frac{V_{CC} - V_{EB}}{I_{B_1} + \frac{V_{EB}}{R_1}}$$

A plot of this relationship is shown in Figure 23. R_2 = 2.8 KΩ, R_1 = 600Ω was the selected operating point.

R_3 was selected by test to provide .001 VDC forward bias on Q_2 at 90°C. The 2N4398 Spec. Sheet shows that Q2 transconductance is negligible at any forward bias less than .1 volts at 100°C.

SUMMARY

Q2 = 2N4398		
Q1 = 2N3720		
R1 = 600 ohms	1/4 watt	
R2 = 2.8 K ohms	1/2 watt	
R3 = 2.0 K ohms	1/4 watt	
D1 = 1N1206		

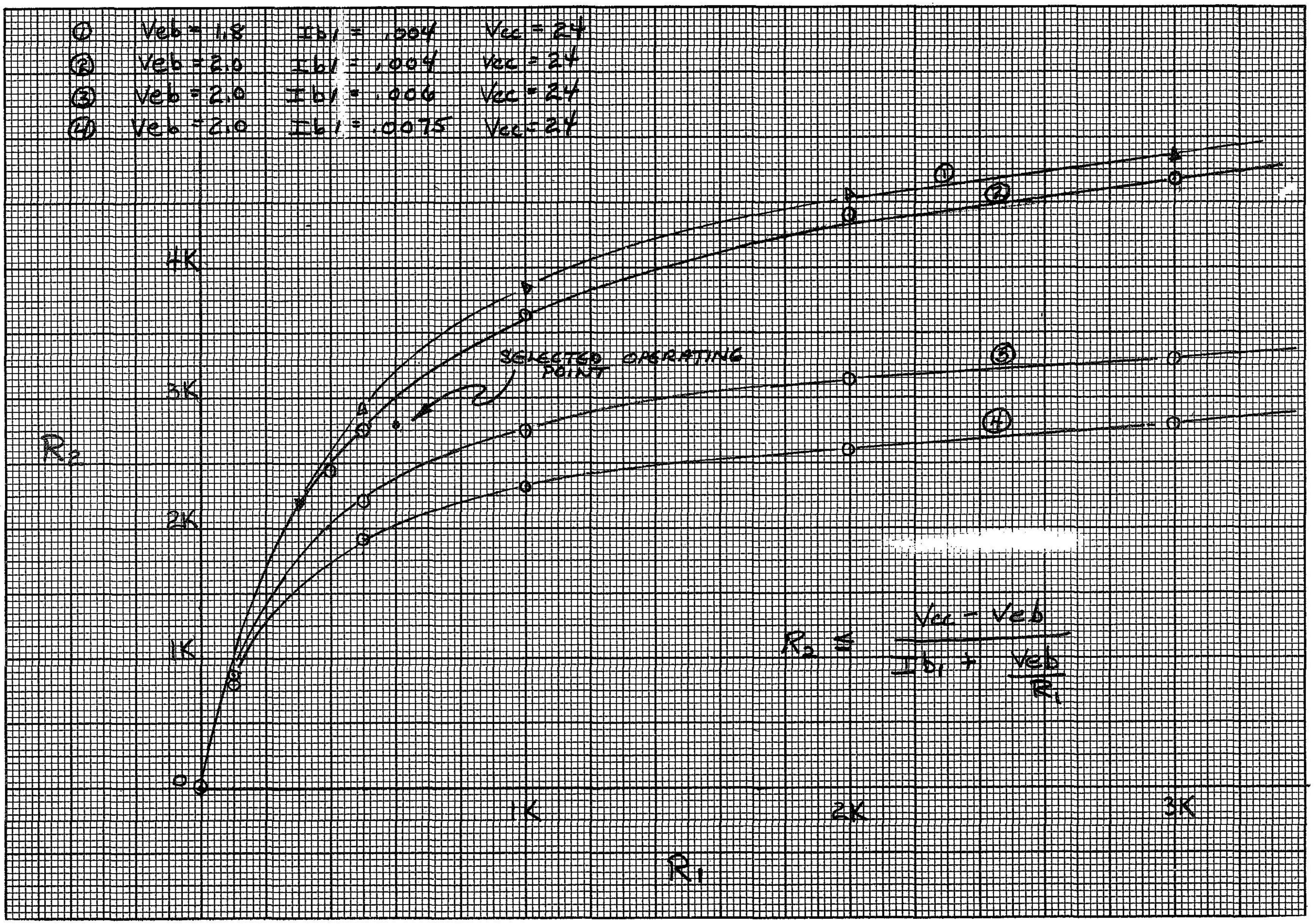

Figure 23. R_1 vs R_2 Relationship

3.5.5 Power Converters and Regulators

Two modular power supplies were selected for incorporation into the controller design. The guidelines for selection of the two power supplies were as follows:

a. Power Supply for the A to D Converter

1. Input voltage 24 to 32 volts D.C.
2. Output will be fixed to ± 1% setting accuracy.
3. Output ± 15 VDC @ 100 ma.
4. Line regulation (10% change) ± 0.0005%.
5. Load regulation (no load to full load) ± 0.002%.
6. Temperature coefficient per °C ± 0.001%.
7. Stability over 40 hours ± 0.0025%.
8. Ripple (RMS) 0.0005% or .262 MV peak to peak.

The above specifications will apply over the entire temperature operating range of (-65°F to -170°F) -55°C to +80°C. The total accumulative error over the entire temperature range will be:

(55° + 77°) x 0.001/°C	= .132
Line, Load, + Stability	= .005
TOTAL DEVIATION	= .137%

b. Power Supply for Logic Circuitry

1. Input voltage 24 to 32 volts D.C.
2. Output fixed ± 1% setting accuracy.
3. Output +5 volts @ 2 to 2.5 amps.
4. Line regulation (10% change) ± 0.002%.
5. Load regulation (no load to full load) ± 0.008%.
6. Temperature coefficient per °C ± 0.005%.
7. Stability over 400 hours ± 0.01%.
8. Ripple (RMS) 0.001% or .175 MV peak to peak.

The above specifications also apply over the entire temperature operating range and the total accumulative change will be:

$$(55° + 77°) \times 0.01/°C = 1.32\%$$
$$\text{Line, Load, + Stability} = \underline{.02}$$
$$\text{TOTAL CHANGE} = 1.34\%$$

The transformers will have 100 db of shielding from the input line.

3.6 Reliability Analysis

The pressure sensing control system was analyzed using MIL-Handbook 217A Failure Rates for a laboratory environment and at temperatures of 77°F (25°C) and (170°F) 77°C. The results indicate for continuous operation a MTBF (mean-time-between-failures) of 33,000 hours at 77°F (25°C) and 14,500 hours at 170°F (77°C) for the system as delivered. The use of high reliability (Hi-Rel) parts would be required for the real flight system in order to provide a reasonable chance for a 2 to 3 year successful mission. Hi-Rel parts are normally MIL-Standard parts which have been subjected to 100% acceptance testing and have been burned-in for 100 hours at rated load.

Using Hi-Rel type of parts for the flight controller would result in a system having a predicted MTBF of 240,000 hours at 77°F (25°C) and 125,000 hours at 170°F (77°C). This corresponds to reliabilities for 3 years (continuous operation) of .896 at 77°F (25°C) and .811 at 170°F (77°C).

The total pressure and vapor pressure signal conditioning subsystem represents a contribution greater than 40% of the total systems failure rate. Furthermore, a large portion of the system is not required to function except at engine firing. If this equipment were shut off during most of the three year period, a significant reliability improvement would be made. For instance, when the vapor pressure signal conditioner is off except when required at engine firing, the reliability is increased to .916 from .896 for 77°F (25°C). The actual requirements are for a continuous sensing and control of the tank total pressure for the venting

operation that occurs only under emergency conditions. This continuous operation also penalizes the system reliability. If the total system were non-operative except at monthly intervals during the mission, the controller reliability would be further increased. For a 3 year period, a reliability of .9948 can be realized using Hi-Rel parts at 77°F (25°C) in this nearly non-operative condition.

Table 3 contains a three part summary of the reliability predictions on the pressure sensing control system. The first part lists reliability values for the controller with sensors turned on and operating continuously for the periods indicated. The other two parts show reliability values associated with the controller operating continuously without the total pressure and vapor pressure signal conditioning units in operation and the total system (controller and sensors) not in operation continuously but for only 5 minutes per month. Table 4 lists the failure rates for each subsystem which indicates their relative reliability.

TABLE 3

SUMMARY OF RELIABILITY PREDICTIONS

Total Control System (Continuous Operation)

PERIOD OF OPERATION (YEARS)	MIL-STD PARTS		HI-REL PARTS	
	25°C(77°F)	77°C(170°F)	25°C(77°F)	77°C(170°F)
1	0.763	0.549	0.964	0.932
2	0.583	0.299	0.930	0.870
3	0.444	0.164	0.896	0.811

Controller Operating Continuously Without the P_T and P_V Signal Conditioning

PERIOD OF OPERATION (YEARS)	MIL-STD PARTS		HI-REL PARTS	
	25°C(77°F)	77°C(170°F)	25°C(77°F)	77°C(170°F)
1	0.868	0.719	0.978	0.958
2	0.754	0.517	0.958	0.914
3	0.657	0.370	0.932	0.880

Total Control System
(Non-Operating Except for 5 Minutes Per Month)

PERIOD OF OPERATION (YEARS)	MIL-STD PARTS		HI-REL PARTS	
	25°C(77°F)	77°C(170°F)	25°C(77°F)	77°C(170°F)
1	0.9972	0.9938	0.9983	0.9965
2	0.9945	0.9877	0.9965	0.9930
3	0.9917	0.9817	0.9948	0.9896

TABLE 4

SUMMARY OF SUBSYSTEM FAILURE RATES

SUBSYSTEM	FAILURES PER MILLION HOURS (λ) = $\frac{1}{MTBF}$			
	MIL-STD PARTS		HI-REL PARTS	
	25°C(77°F)	77°C(170°F)	25°C(77°F)	77°C(170°F)
Vapor Pressure Signal Conditioner	7.386	15.55	.7386	1.5553
Total Pressure Signal Conditioner	7.386	15.55	.7386	1.5553
Analogic Multiplexer	0.589	1.250	Typically the Hi-Rel Part Provides a Ten Fold Improvement Over MIL-STD Parts ↓	
Analogic Voltage-to-Count Converter	4.954	10.105		
Analogic Output Register	0.469	1.310		
+ 5 Volt Power Supply	1.211	2.658		
± 15 Volt Power Supply	2.622	5.996		
Card Cage	4.757	13.016		
Valve Drivers	0.80	3.24		
Connectors	0.316	0.316		
Junction Modules	0.28	0.28		
Sensors	0.60	0.60		

SECTION 4
FABRICATION AND ASSEMBLY

After design approval by NASA-LeRC, two complete tank pressure control systems were fabricated and assembled. All the basic electrical components of the units, including some spares were purchased. Certain electrical components were installed and wired to standard Information Control Corp. (ICC) logic cards and the entire internal wiring including the wire wrap in the logic plane was performed by MDAC-W. The nonpurchased parts which required MDAC-W fabrication include the enclosure, chassis plate, valve driver power transistor circuits and their heat sinks, the A to D converter enclosure, special test hardware, and test equipment. During the fabrication task, limited breadboarding of the electronics was performed to assure that the final units would satisfy all the required functions for the controller.

A rather extensive effort was required in the procurement of major subassemblies. Each of the available off-the-shelf subassemblies: sensors, signal conditioning, multiplexer, Voltage-to-count converter, output register, +5 volt power supply, and ±15 volt power supply required some degree of modification in order to meet the controllers interfacing, environmental and performance requirements. To assure that these requirements be provided, procurement specifications were written for each subassembly which included, where necessary, the requirements for:

a. Environmental conditions covered in Appendix D
b. Special circuits for linearizing outputs
c. Component substitution
d. System burn-in
e. Special calibrations and adjustments
f. Special connectors, (adapter fittings, and support hardware)

Table 5 lists the numbers and titles of those drawings prepared for fabrication of the total control systems. Figures 24 through 28 show external and internal views of the controller, subassemblies, and the chassis plate. All subassemblies are removable and can be interchanged between S/N1 and S/N2 controllers with the exception of the signal conditioners and their associated cables and sensors.

TABLE 5

LIST OF DRAWINGS

NUMBER	SHEET	TITLE
1T38533	1	Pressurization System Controller (Top Assembly Drawing)
1T36163	1	Position 1 Connector Card and Internal Wiring Diagram
	2	Position 2 Connector Card and Interconnection Diagram-Analog MUX, Voltage-to-Count Converter, Output Register
	3 to 21	Circuit Cards in Positions 3 to 19
	22 to 26	Parts List - Circuit Cards
1T36165	1 to 4	Logic Diagrams
NPN	1 to 5	Wiring Lists and Fan-In, Fan-Out Calculations for Logic Diagram, (Sheet No. 1 of 1T36165)
NPN	1 to 4	Wiring Lists and Fan-In, Fan-Out Calculations for Logic Diagram, (Sheet No. 2 of 1T36165)
NPN	1 to 5	Wiring Lists and Fan-In, Fan-Out Calculations for Logic Diagram, (Sheet No. 3 of 1T36165)
NPN	1 to 5	Wiring Lists and Fan-In, Fan-Out Calculations for Logic Diagram, (Sheet No. 4 of 1T36165)
1T19806		Operation and Calibration Procedure

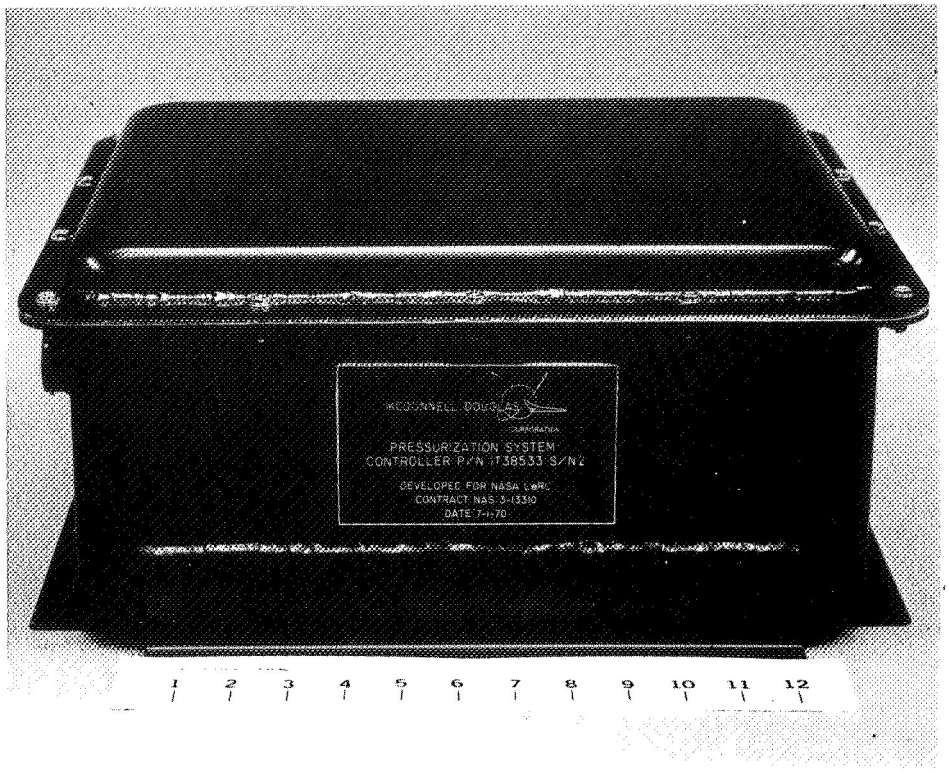

a. FRONT VIEW

b. OBLIQUE VIEW

Figure 24. Assembled Controller

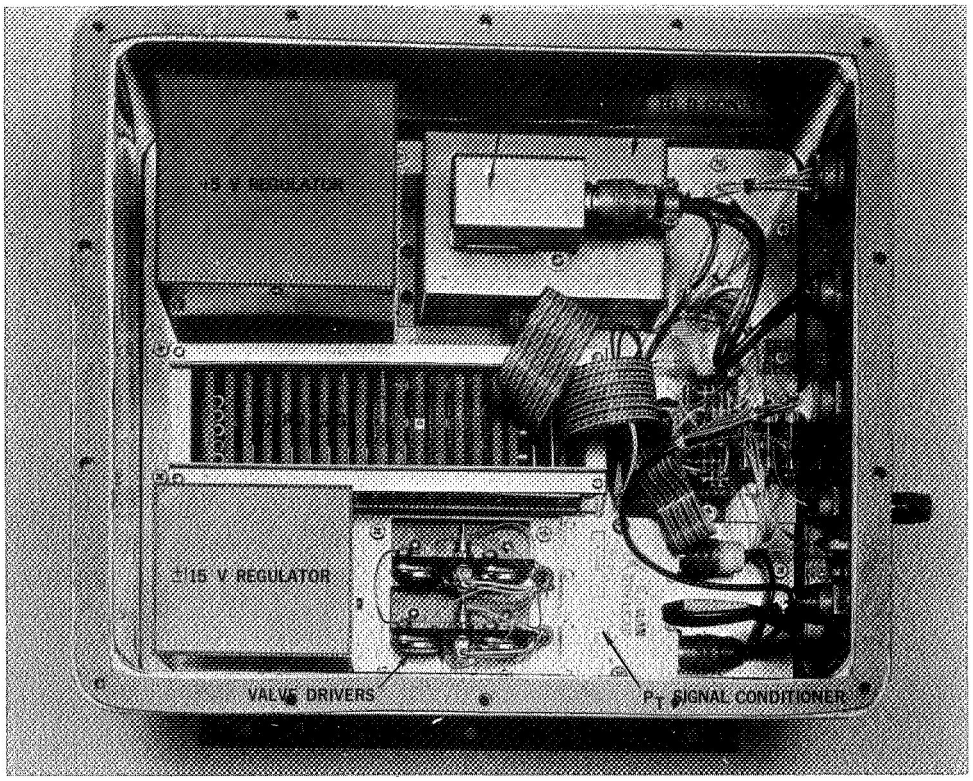

a. WITH CHASSIS PLATE

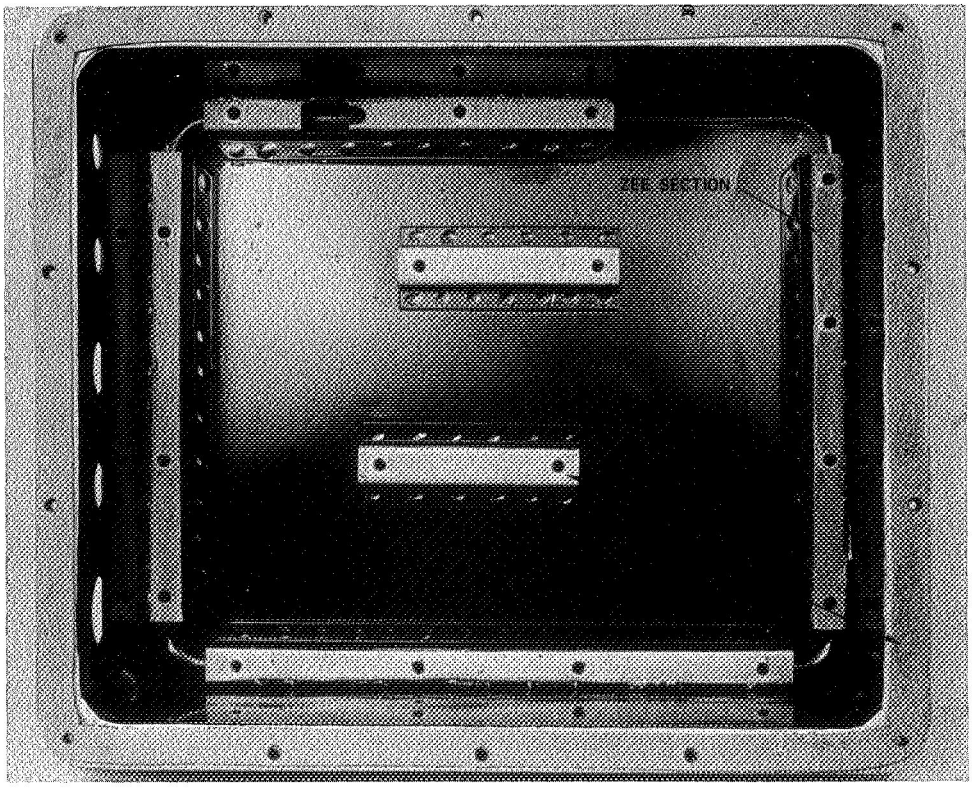

b. WITHOUT CHASSIS PLATE

Figure 25. Enclosure, Cover Removed

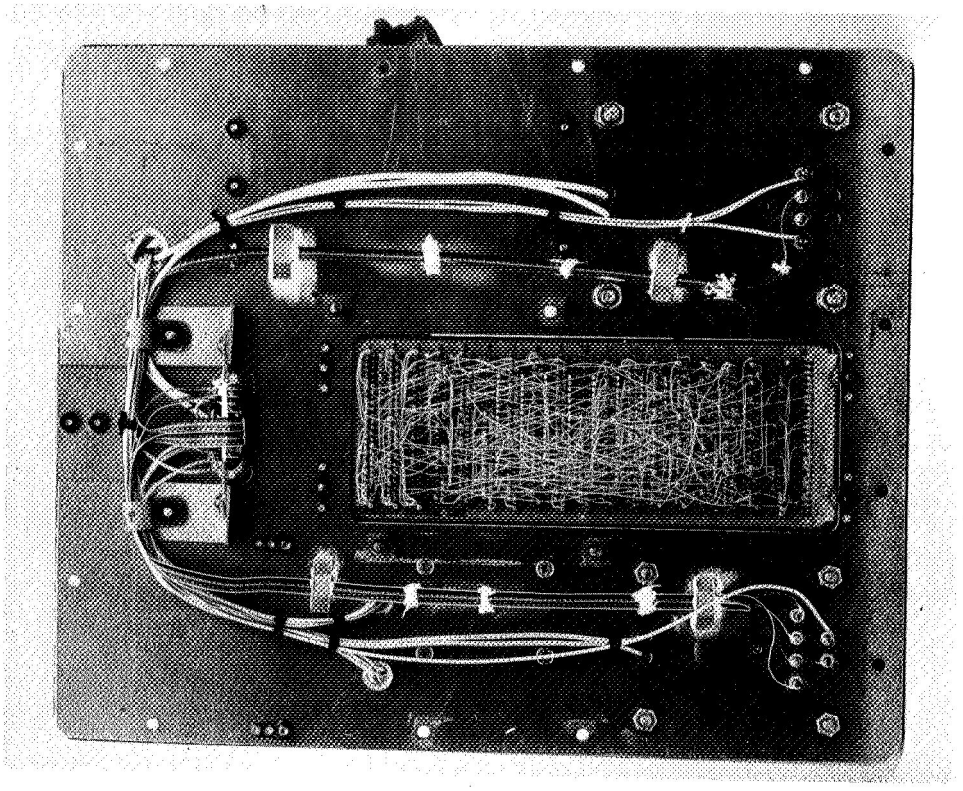

a. ENTIRE CHASSIS

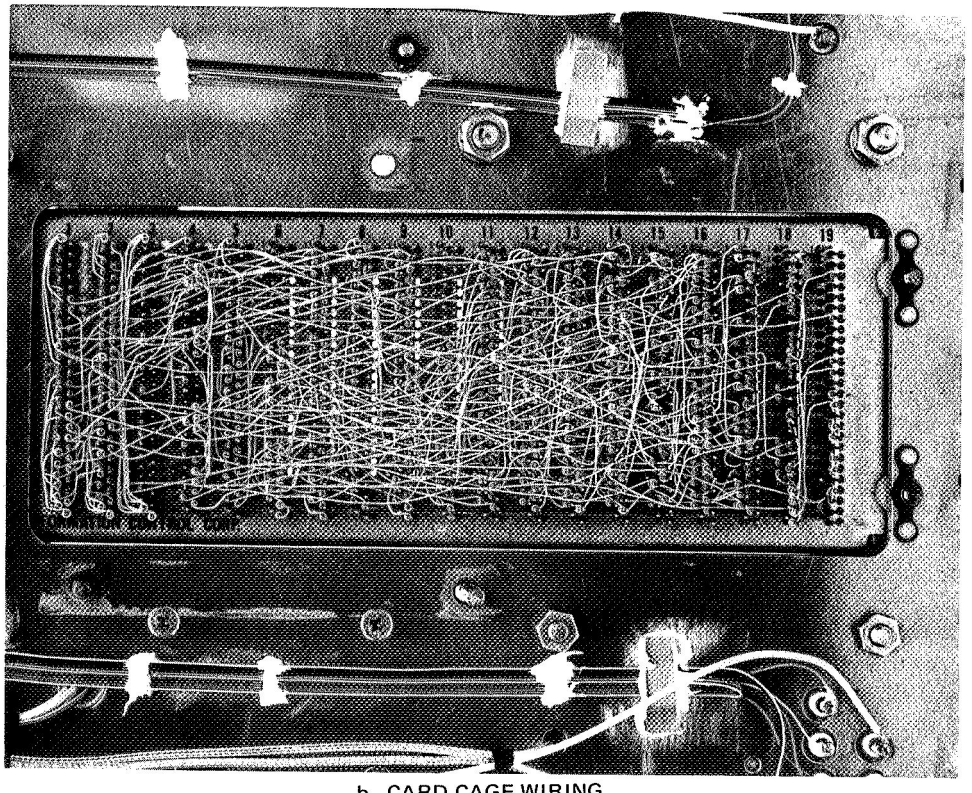

b. CARD CAGE WIRING

Figure 26 . Chassis Plate, Bottom Views

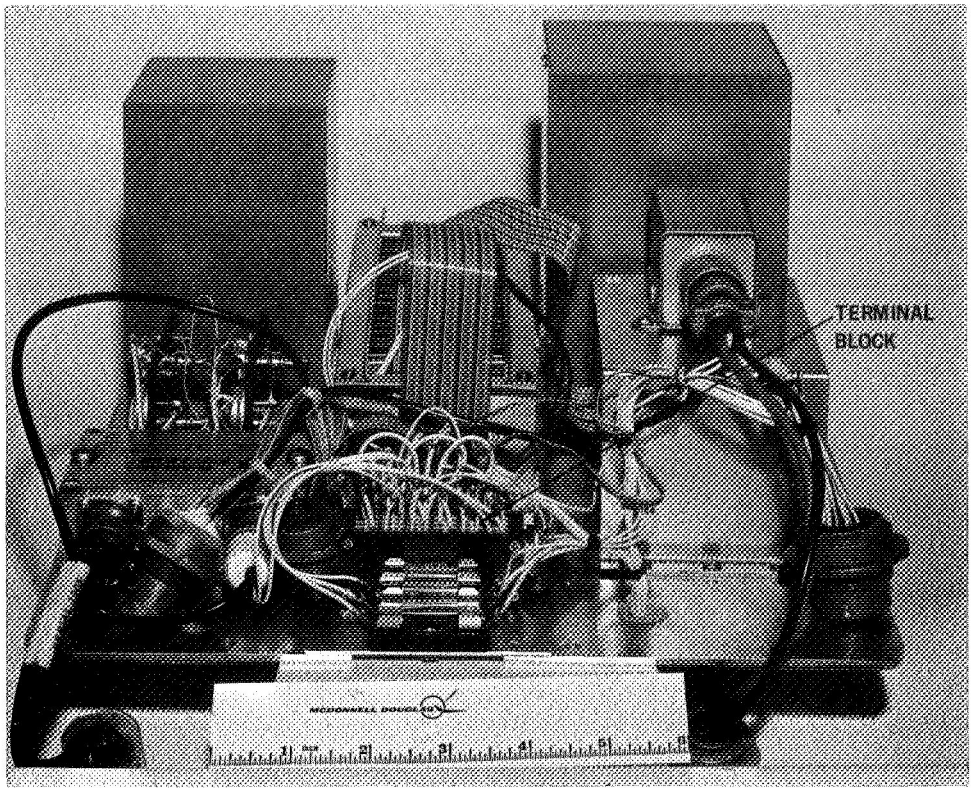

a. FACING FUSES

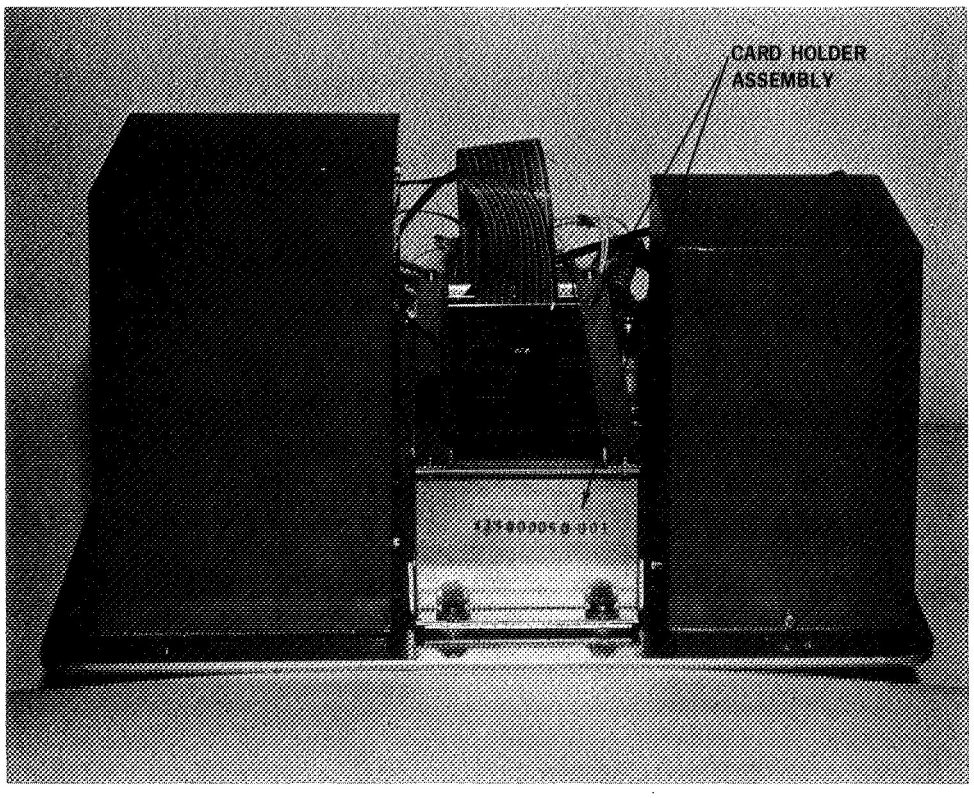

b. FACING CARD CAGE

Figure 27. Chassis Plate, Oblique Side Views

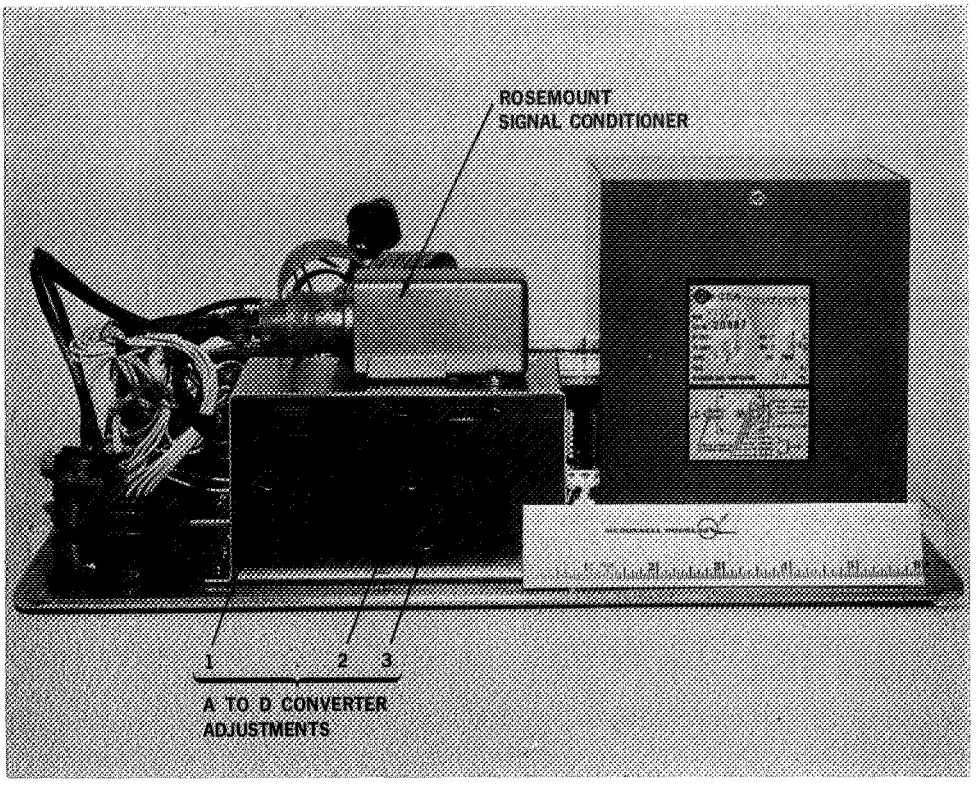

a. FACING A/D CONVERTER

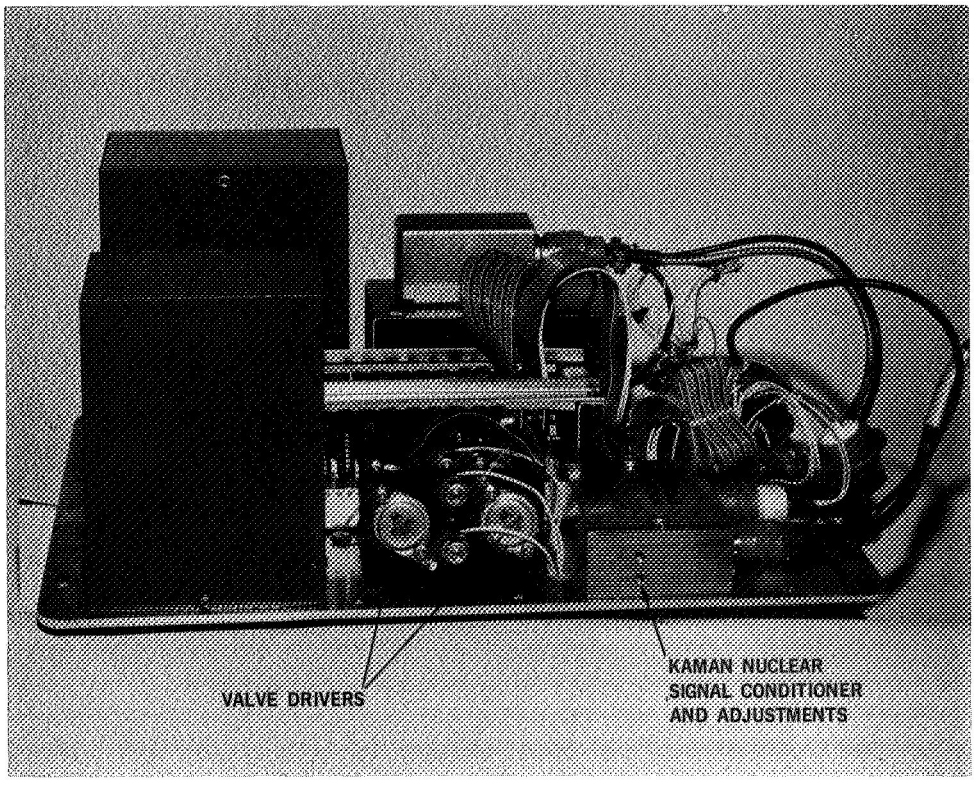

b. FACING VALVE DRIVERS

Figure 28. Chassis Plate, Oblique Side Views

These items are tailored and precalibrated for use with either the liquid hydrogen or fluorine propellants. Figure 27 shows the Matrix Corporation terminal block. This terminal block is resistant to vibration and pins are removed easily with a special pin removal tool. The ground configuration wired into this terminal block may be changed to suit system application. The chassis plate supporting all major components and subassemblies is attached to channels located at the bottom of the enclosure. This chassis plate may be removed by removing the screws along the inside edge of the enclosure. The bulkhead connector nuts also have to be taken off prior to removal of the chassis plate and the connectors pushed to the inside of the enclosure. Captive nuts have been employed wherever possible to facilitate the removal of individual subassemblies. (The controller enclosure is approximately 14 x 16 x 8 inches high (36 x 41 x 20 cm high) and weighs 29.5 pounds (13.4 Kg).) The power consumption of the controller is nominally 30 watts when operating in either standby or firing modes.

4.1 Enclosure Assembly Fabrication

The enclosure was fabricated from a standard 6061-0 aluminum box and cover supplied by Zero Manufacturing Co. The box and cover is 0.063 in. thick, and is furnished with 1/8 inch thick mating flanges. The enclosures were further fabricated in the MDAC-W Experimental/Development Operations Department and in the Applied Research Laboratory Shop Facility.

The four right angle mounting brackets are shown welded to the box exterior in Figure 24. The chassis plate in Figure 26a and its supports (zee and hat sections) shown in Figure 25b were cut to length and drilled to accommodate the assembly of components, subsystems, and their fasteners. The zero box and cover flanges along with the internal zee and hat sections are drilled to accommodate the captive nuts and their rivet fasteners. Self locking, floating type captive nuts were riveted to the box flange and on the under side of each zee and hat section. Two hat sections were then spot welded to the center portion of the box while the four zee sections were butted against the box wall where they were intermittently fusion welded. These zee sections were also spot welded to the bottom of the enclosure.

A 5/8 x 1/8 thick gasket strip for EMI/RFI and environmental sealing was procured from Primec Corporation. The gasket strips were corner spliced, butt jointed, and holes cut out to match the box flange hole pattern and contour. The gasket was then spot bonded under pressure to prevent the formation of a non-conductive adhesive film between the gasket and metal surface. The gasket material is a solid silicone rubber with monel wires aligned perpendicular to the sealing surface. Dow Corning silastic RTV adhesive was applied, in spots, to the cleaned and primed box flange surface.

Five holes of various sizes were drilled through the front of the enclosure to accommodate the Bendix connectors. The enclosures were then cleaned and masked for the undercoat primer and the top coats of paint. All surfaces were painted except those requiring good electrical and thermal contact such as: the gasket sealing surface, the bottom side of the mounting flanges, the tops of the internal supports for the chassis plate, and where the name plate is bonded to the side of the controller.

4.1.1 Chassis Plate Assembly

The chassis plate, shown in Figure 26 was milled to fit inside the enclosure and to accommodate the card cage and its wire wrap pins. Holes were provided for fastening the chassis plate to the enclosure and for assembling subsystems and components. Holes were also provided for the power supply terminals and leads and for the 28 volt valve driver leads. A silicone compound was used at the interface between the enclosures brackets and the chassis plate to provide optimum heat transfer to the mounting structure. This is important especially during operation of the unit in a vacuum. Similarly, power supplies and valve drive transitors which must dissipate heat were also heat-sinked with silicone compound to the chassis plate. The following miscellaneous items were provided in this assembly:

a. Nylon grommets in the chassis plate for routing wiring from top to bottom.

b. Cable clamps for wiring and epoxy for bonding the ribbon cable to chassis plate.

c. Heat sink and mounting plate for driver power transistors.

4.2 Electrical Components and Subsytems

The two controllers with exception of welding and painting were constructed, assembled and wired in the R&D laboratories. Qualified engineers/technicians performed all fabrication steps.

4.2.1 Breadboarding

Critical portions of the control system were breadboarded prior to freezing the electronic design. The standby portion of the programmer and arithmetic unit were breadboarded on Augat wire wrap planes for dual-in-line I.C. packages. During this design evaluation phase, partial and total pressure inputs were simulated with digital thumb wheel switches and BCD-to-binary code converters.

4.2.2 Circuit Cards

Several blank circuit cards were obtained from ICC and subsequently assembled and wired by MDAC-West. All MDAC designed circuits except the valve drivers were packaged in this fashion. Similarly, medium scale integrated circuits which were not available from ICC were mounted on blank cards.

Interchangeable matrix cards were utilized to program different combinations of preset pressures and pressure differentials. The presetting was accomplished by hard-wiring jumpers into the required logic locations. The binary equivalents of ΔP_2, ΔP_3, P_4, P_5 were marked on the cards by a silk screening process.

Two connector cards provide ribbon-cable interconnections to the main chassis and the A/D converter.

4.2.3 A/D Converter

The A/D converter was supplied by Analogic and modified to meet the environmental specification. Certain parts were substituted as requested by NASA LeRC for preferred component types and manufacturers.

At MDAC-W, the three circuit boards comprising the A/D converter and the analog multiplexer were hard-wired with color-coded multiconductor ribbon cable to an ICC connector card. Logic and power supply leads were alternated to reduce signal crosstalk.

The three circuit boards were then inserted in a spacer jig and potted in silicone rubber. The potting compound was poured into a five-sided aluminum sheet enclosure which became an integral part of the A/D converter assembly.

4.2.4 Card Cage

In the card cage, #30 gauge high temperature insulated wire, consistent with the wire wrap pin size and spacing, was utilized. Due to the large number of wires and close pin spacing, the pin matrix numbering was covered by wiring. Numbered templates were used to facilitate wiring and checking.

All interconnections to and from the wire wrap plane are achieved through 2 connector cards. This construction maintains the modular approach used throughout the controller allowing interchangeability of most subassemblies.

A special holder assembly to retain the circuit cards during shock and vibration testing was procured.

4.3 Test Apparatus Fabrication

4.3.1 Environmental Test Fixture

Figures 29 and 30 show the test fixture base plate and cover that was fabricated for the vibration and functional testing. Two holes were drilled and tapped to the AND 10050-4 configuration to accommodate the transducer adapter fittings and the Rayco metal seals. A pressure port 1/8 inch in diameter was also drilled in the side of the flange for the simultaneous pressurization of both pressure transducers. Four 5/16 inch diameter holes were tapped for bolting the fixture cover to the base

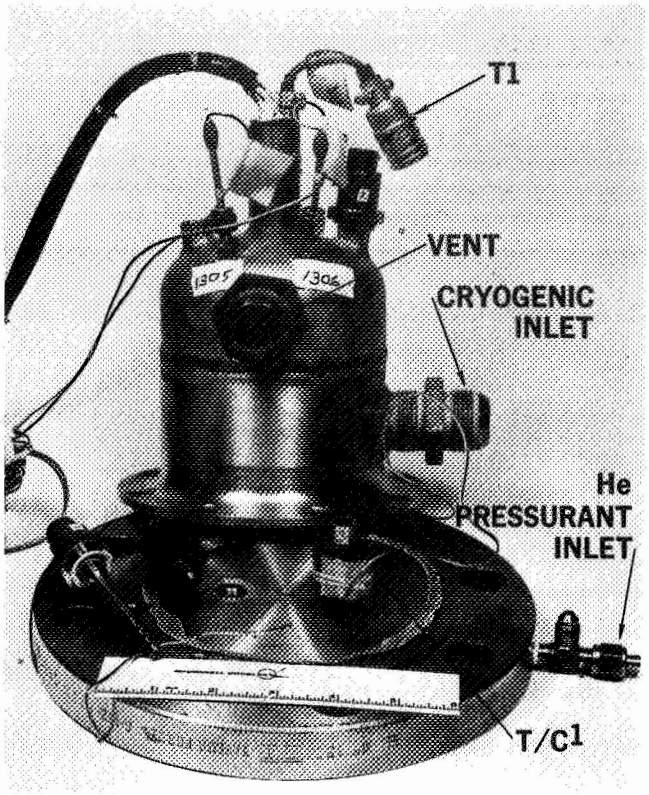

Figure 29 Test Fixture – Sensors and Instruments

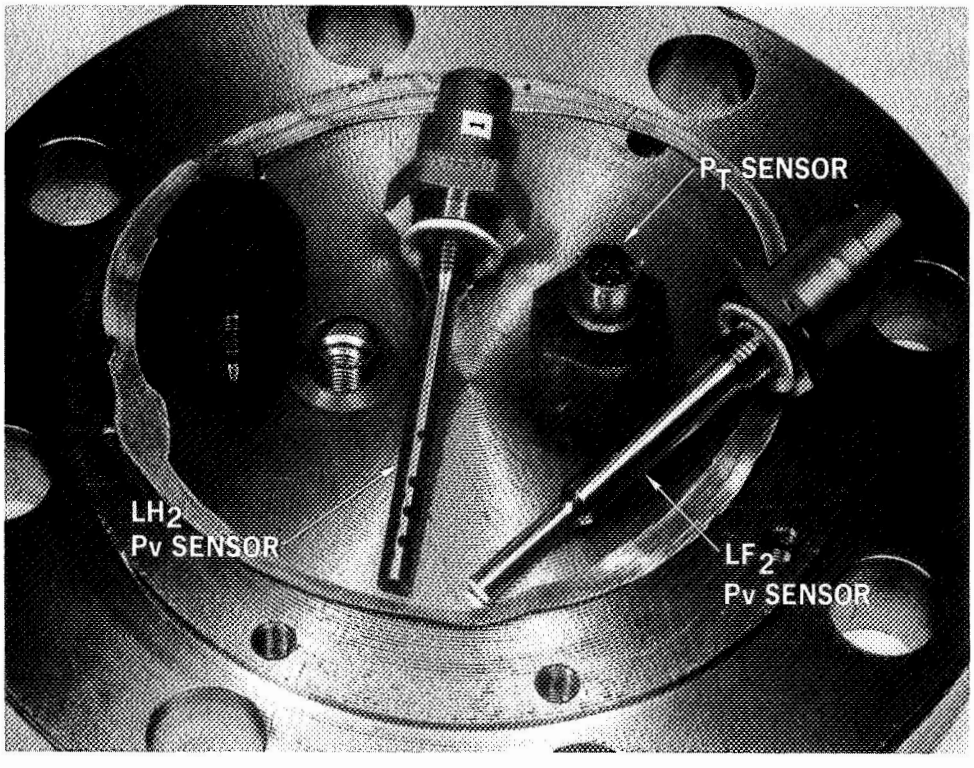

Figure 30 Test Fixture Base and Sensors

plate. The cover was sealed to the base plate using an Armalon gasket. The 7/8 inch diameter holes were for mounting the test fixture. A micarta block was fabricated to provide insulation between the fixture mounting flange and the vibration shaker mounting plate. The cover has two AN 815-16C inlet and outlet ports welded on it for the coolant supply. A 1-inch diameter tube was welded to the top. It penetrates the top where two chromal constantan thermocouples and two Kaman Nuclear sensor cables are fed through and potted in place. Attached to the Kaman Nuclear adapter fittings were two chromel-constantan thermocouples. Three AN 818-40 fittings were welded on the fixture cover for the installation of the two Rosemount vapor pressure sensors (temperature probes) and the temperature monitoring probe.

4.3.2 Vacuum Chamber

Figure 31 show the 14 x 24 inch vacuum chamber that was fabricated. The chamber accommodates the controller in the functional testing. Welded to this chamber was a 6-inch flange for mounting on the larger 5 x 7 foot Bemco vacuum chamber that is equipped with a diffusion vacuum pumping system located at the liquid hydrogen facility. The controller lid was removed and the bulkhead connectors unfastened from the controller and mated to the five holes provided in the vacuum chamber cover.

4.3.3 Pressure System

This pressure system was fabricated for use in both the vibration and functional testing. In the functional testing, the system was used to simulate the tank pressurization, expulsion and venting. This system was also used to calibrate the Kaman Nuclear total pressure measuring system. Three 1/4 inch solenoid valves were acquired and used to simulate the helium pressurization valve, the vaporized propellant valve and the venting and tank expulsion valves. Two hand valves were also used to regulate the rate of pressure rise and decay. These valves were all mounted off the 2 1/2-inch diameter by 36-inches long accumulator and all the attaching plumbing was fabricated from 1/4 inch stainless steel tubing.

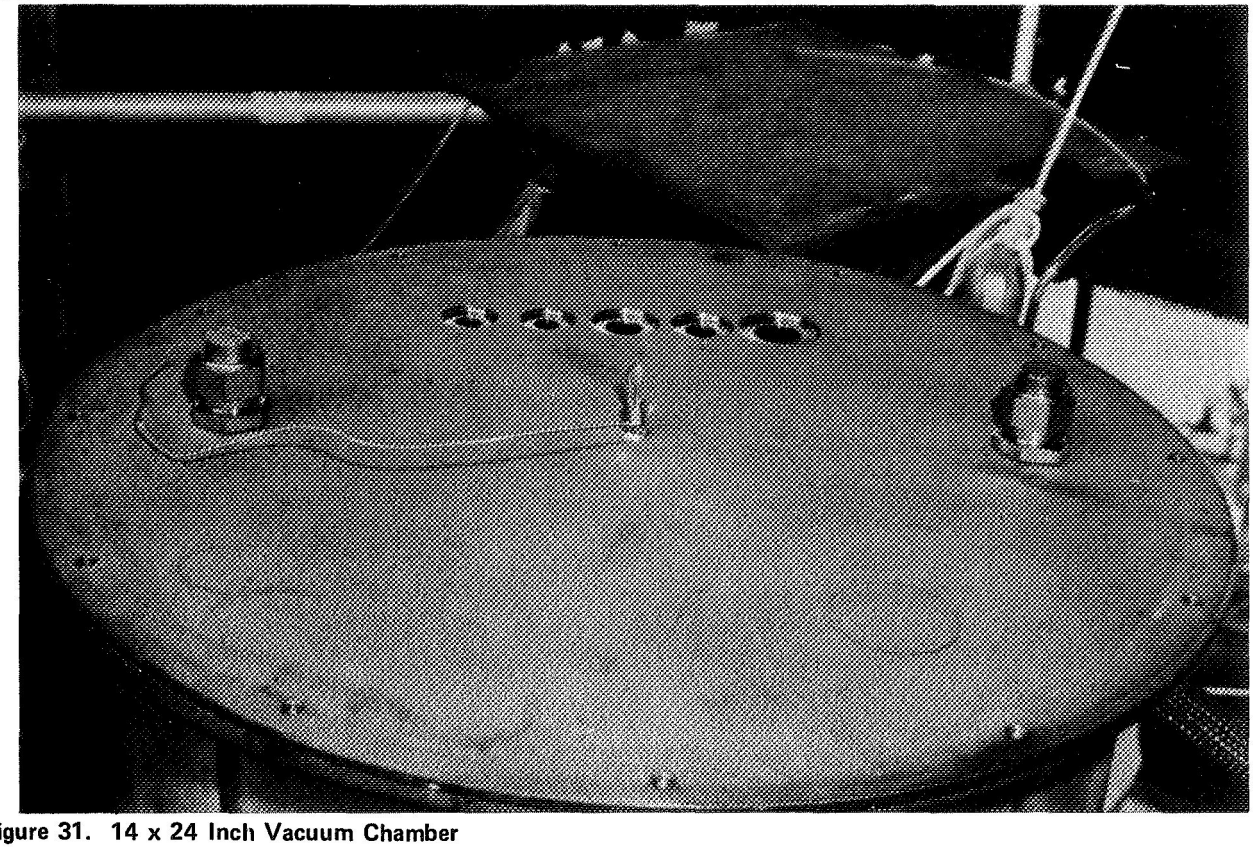

Figure 31. 14 x 24 Inch Vacuum Chamber

4.3.4 Control and Calibration Unit

A control and calibration unit shown in Figure 32 was constructed to aid in testing and calibration of the controller. It is enclosed in an aluminum box and is mated to the controller through two 3-foot cables. A number of binding posts were mounted on the unit to provide accessible input/output connections. Visual indication of the status of the four valves, the firing signal and the pre-press complete signal was given by appropriately marked pilot lights that were installed.

A number of switches were also installed for control valve functions, simulating prefiring and firing signals, and to connect the analog P_V and P_T 0-5V inputs to either the calibration sources or the signal conditioner.

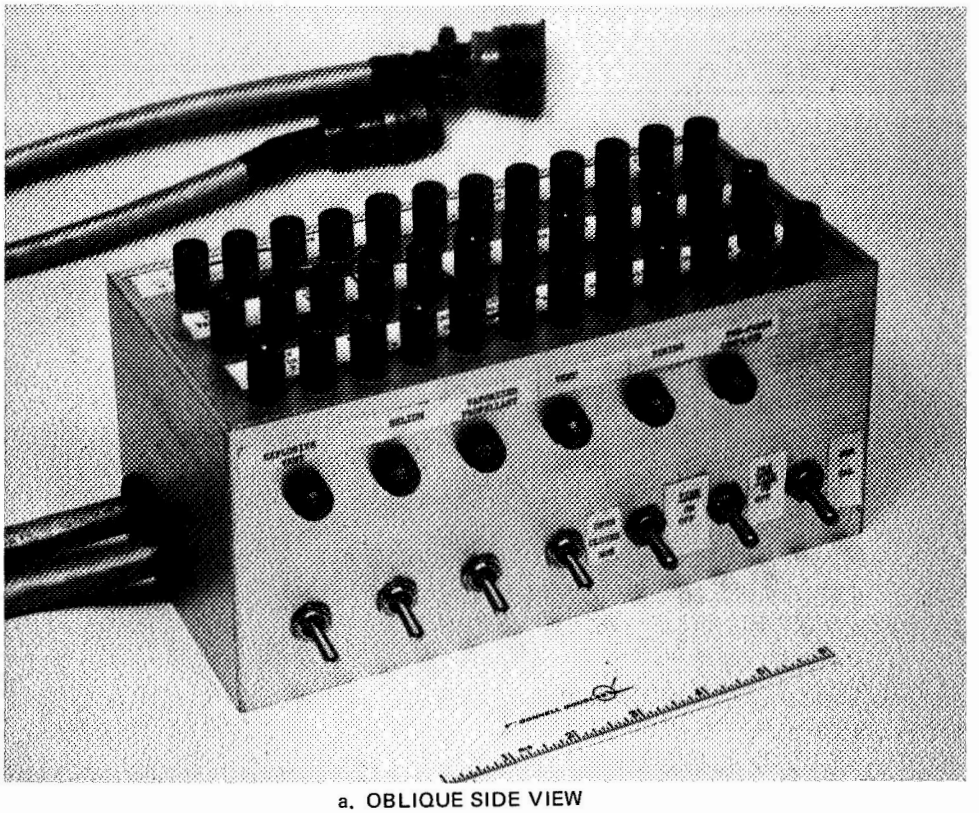

a. OBLIQUE SIDE VIEW

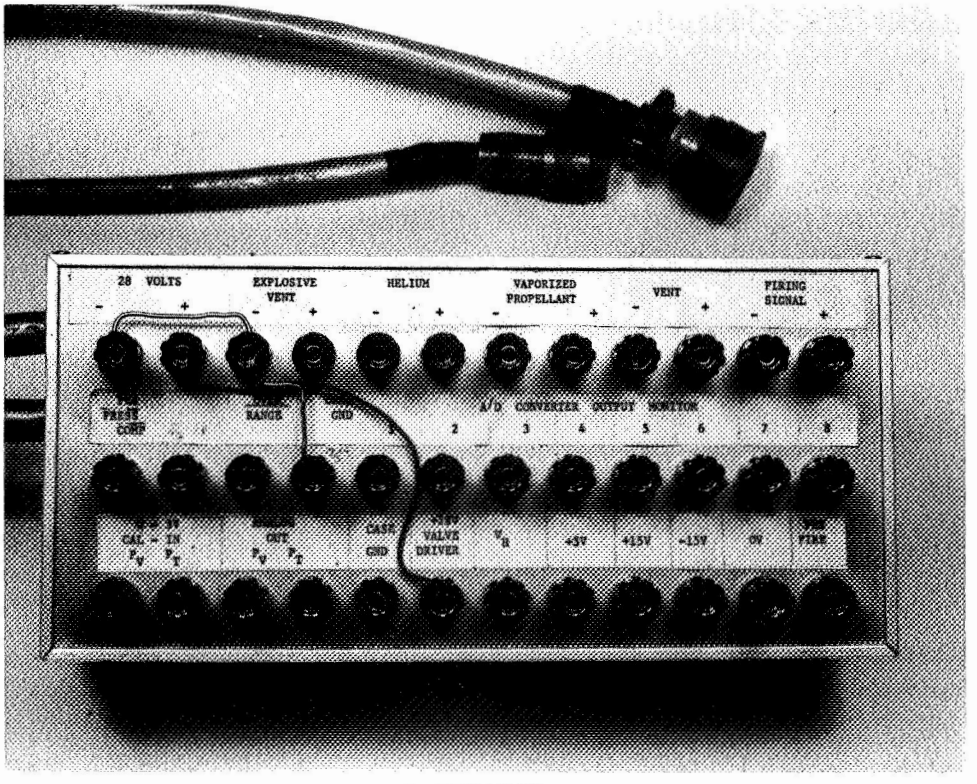

b. TOP VIEW

Figure 32. Control and Calibration Unit

SECTION 5

TESTING

After the fabrication of the two controllers, a series of comprehensive functional and operation tests were conducted on both units to demonstrate their capability to perform according to the design specifications. The testing includes: proof and leak tests of the pressure sensors, calibration tests of controller and sensors, vibration and shock tests, vacuum functional cycle tests, and fluorine compatibility tests.

5.1 Liquid Fluorine Compatibility Test

The objective of this test was to demonstrate the adequacy of the total pressure sensor portion of the Pressure Sensing Control System for LF_2 or FLOX use. The total pressure transducer and its adapter assembly were subjected to LF_2 while undergoing pressure calibrations.

The LF_2 compatibility test was performed at the McDonnell Douglas A-12 Gypsum Canyon Test Area.

5.1.1 Test Setup and Procedure

Figure 33 shows schematically the test setup. The setup includes the electrical hookup, the fluorine/vacuum flow system, and the Varian flange apparatus. The sensor was installed in the Varian flange assembly as shown in Figure 34. Here, the interconnecting cable is seen which mates with the electronic package. A 28 volts D.C. power supply was used to energize the electronics, while a H.P. digital voltmeter was used to measure the output voltage of the Kaman Nuclear pressure transducer system. A 0-300 psig (10 to 217 x 10^4 pascals) Heise gage was used during the chilldown of the test appartus for condensing and collecting liquid fluorine.

The Kaman Nuclear sensor and adapter assembly were unpacked in the clean room and visually inspected. There were no signs of any damage to any of the parts. The sensor, seal, adapter assembly, and Varian flange assembly were all cleaned for fluorine service and inspected with black light to verify cleanliness.

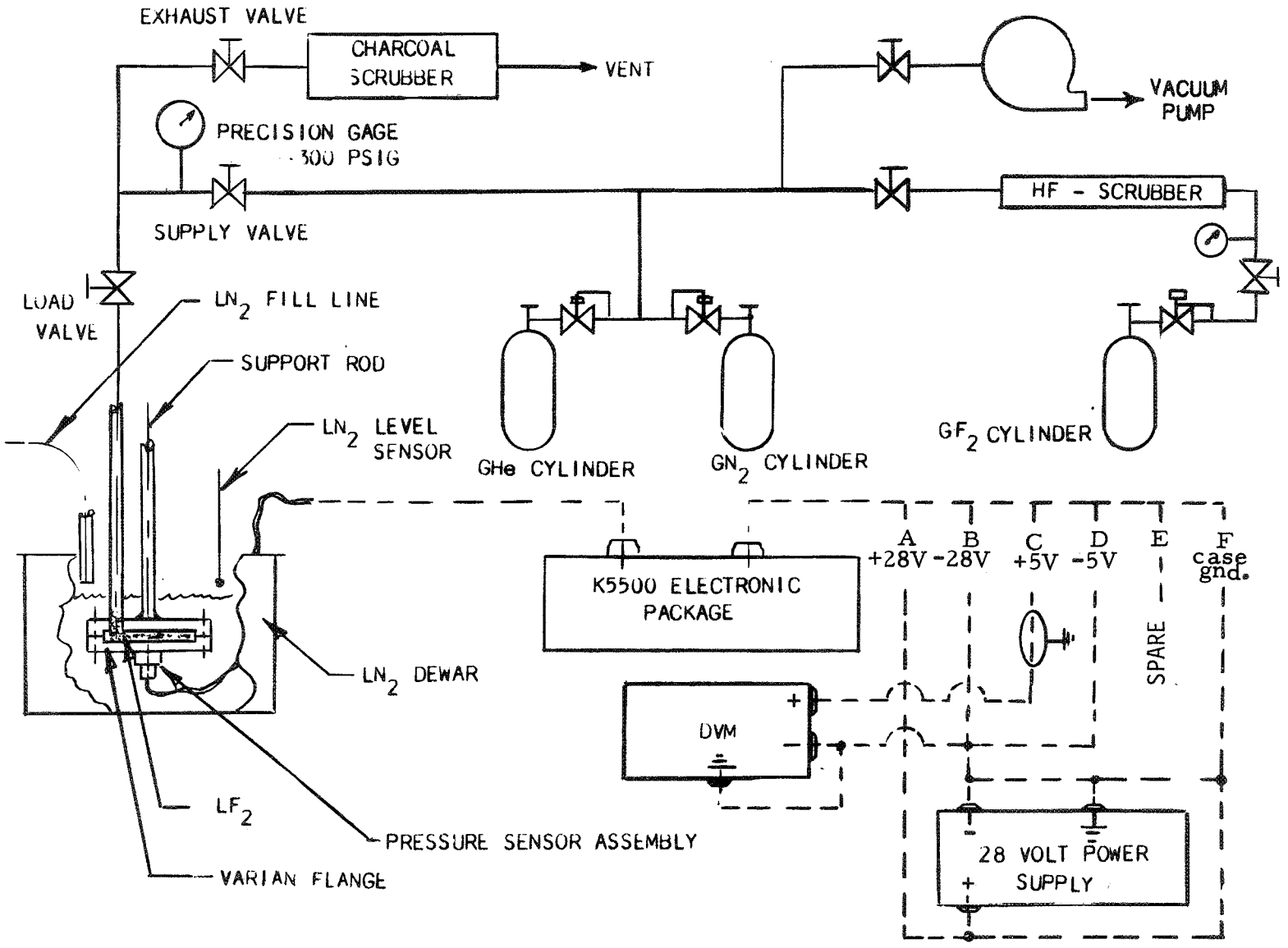

FIGURE 33. LIQUID FLUORINE COMPATIBILITY TEST SETUP

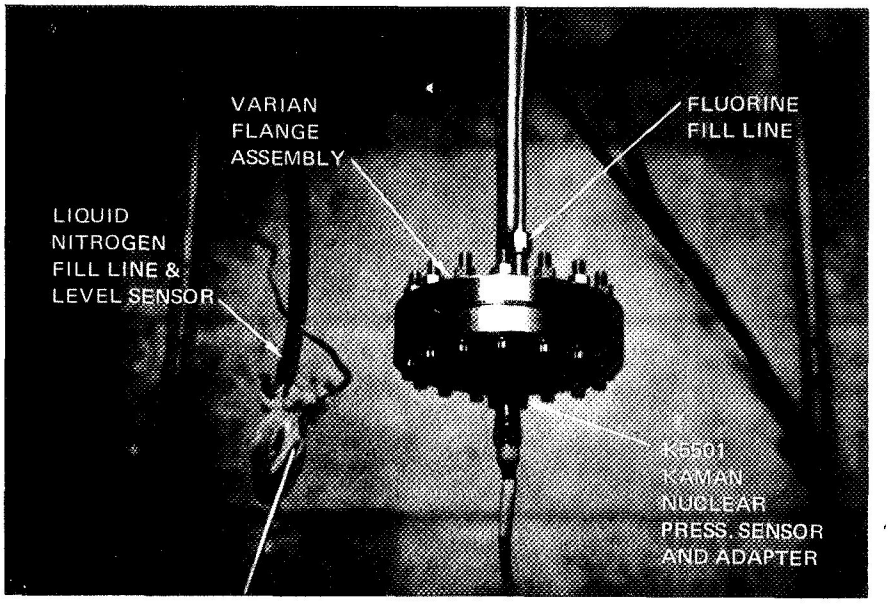

Figure 34 Test Apparatus – LF_2 Compatibility Test

The Kaman Nuclear sensor, model 1501-2, serial number 1305, with interconnecting cable and electronic package S/N Fluorine 1305 were selected for the test. After cleaning, the sensor and its adapter were reassembled and installed in the Varian flange. The sensor installation shown in Figure 30 was submerged in a liquid nitrogen dewar where the liquid level was maintained approximately 3 inches (7.62 cm) above the top of the Varian flange assembly. The assembly was then leak-checked and proofed at 300 psig (217 x 10^4 pascals). The pre-test calibrations were made using gaseous helium pressure while the sensor was submerged in liquid nitrogen. After temperature stabilization, the instrument's zero and sensitivity were adjusted to allow for an initial zero offset of -171 millivolts at -320°F (-196°C). Then pre-test pre-passivation calibrations were performed going up and down the scale at 0, 50, 100, 150, and 190 psig (10, 44.6, 79, 113, and 141 x 10^4 pascals) repeated three times and recorded.

The system was warmed to ambient temperature and then passivated by evacuating test sytem to 2 in. (5.07 cm) of mercury (Hg), and allowing gaseous ambient fluorine to enter the test system, sensor and adapter inlet. The GF_2 pressure was applied at a rate less than 25 psia per minute (17.2×10^4 pascals/min). The pressure was increased incrementally to 0, 75, 150, and 250 psig, (10, 61.8, 113, and 182×10^4 pascals) and was held for 10 minutes at each of these pressure levels.

Post-passivation calibration tests were then performed. The apparatus was again chilled down (submerged in LN_2), then evacuated, and gaseous fluorine allowed to enter the test apparatus where it condensed approximately 140 ml of liquid fluorine above the sensor and in the Varian flange. The calibration tests were again performed three times. After completion of these tests, the system was warmed to ambient temperature and nitrogen was used to remove all traces of fluorine. Following this purge, the system was evacuated to 2 in. (5.07 cm) Hg and purged once again.

After the completion of the cycle test and purge, the system was disassembled and carefully inspected for any deterioration of the sensor or adapter caused by the LF_2 exposure.

5.1.2 Results

The calibration results are presented in Table 6. The pretest and the postpassivation calibrations show a 30 to 40 millivolt difference. This shift is believed to have resulted from the thermal cycling. Shifts of this order are, however, normal within specifications and adjustable. The results before and during the fluorine exposure show the system measurements to be linear to +0.8% F.S. (best straight line) and repeatable to 0.16% F.S.

A thin fluoride film was deposited on the sensor diaphragm as expected.

The visual inspection of the sensor, adapter, and "O" ring after exposure to fluorine showed no deterioration or damage to any of the exposed parts.

Table 6

LIQUID FLUORINE COMPATIBILITY TEST DATA

		OUTPUT VOLTAGE					
		Increasing	Decreasing	Increasing	Decreasing	Increasing	Decreasing
Pre-test Calibration	Pressure (psig)/Pascals x 10^4						
	0/0	0.007	-0.004	-0.004	-0.005	-0.005	-0.005
	50/44.6	1.350	1.353	1.349	1.352	1.354	1.359
	100/79.0	2.684	2.687	2.687	2.686	2.689	2.681
	150/113	4.009	4.013	4.011	4.014	4.013	4.009
	190/141	5.035	5.035	5.040	5.040	5.045	5.045
Post Passivation Calibration	0/0	0.031	0.029	-	-	-	-
	50/44.6	1.390	1.393	-	-	-	-
	100/79.0	2.728	2.731	-	-	-	-
	190/141	5.074	5.074	-	-	-	-
Liquid Fluorine Calibration	0/0	0.028	0.028	0.028	0.030	0.030	0.029
	50/44.6	1.393	1.389	1.383	1.383	1.379	1.383
	100/79.0	2.730	2.730	2.727	2.728	2.729	2.730
	150/113	4.049	4.054	4.048	4.050	4.051	4.055
	190/141	5.085	5.085	5.091	5.091	5.085	5.085

5.2 Vibration and Shock Tests

Vibration and shock tests were performed on the two pressurization system controllers. Sinusoidal, random and shock were performed in that order and in one axis. These tests were performed at the Vibration and Shock Facility of the MDAC-W Environmental Test Laboratories, Santa Monica, California on June 19, 1970. The purposes of these tests were to demonstrate that the pressurization system controllers are structurally sound and that the sensors while at cryogenic temperature, have a stable output when subjected to the vibration environment. The tests were performed with the controller power on while the outputs from the four sensors were being recorded. Calibration and operational tests were also performed before and after the testing to determine if any failure, damage, or out of tolerance conditions resulted.

5.2.1 Test Setup

Figures 35 and 36 show the shaker, two pressurization system controllers S/N 1 and S/N 2 and the cryogenic environmental test fixture in which the sensors are mounted. They were all mounted rigidly on the model A249 shaker plate. Holes were drilled and tapped in this plate to accommodate the mounting flanges of the controllers and the environmental test fixture. An oil-film granite block table was used to support the shaker plate and the test specimens. The vibration and shock tests were performed in this horizontal slip axis. The accelerometer was mounted between the controllers shown in Figure 36 and was used simultaneously for both shaker control and data recording. The controller sensors were connected to their respective controller by 20 ft (6 m) of interconnecting cable and their output was connected to a Mincom 3M tape recorder. Six channels were used to record the four analog voltages from the sensors and the shaker vibration frequency. The sixth channel was voice used to identify the testing. A digital voltmeter, a counter and a selector were used to monitor individually the four sensor outputs and the vibration frequency during the testing. Liquid nitrogen was used to provide the cryogenic environment for the controller sensors. The test chamber was fiberglass insulated along with the flexible tubing that provided the cryogenic

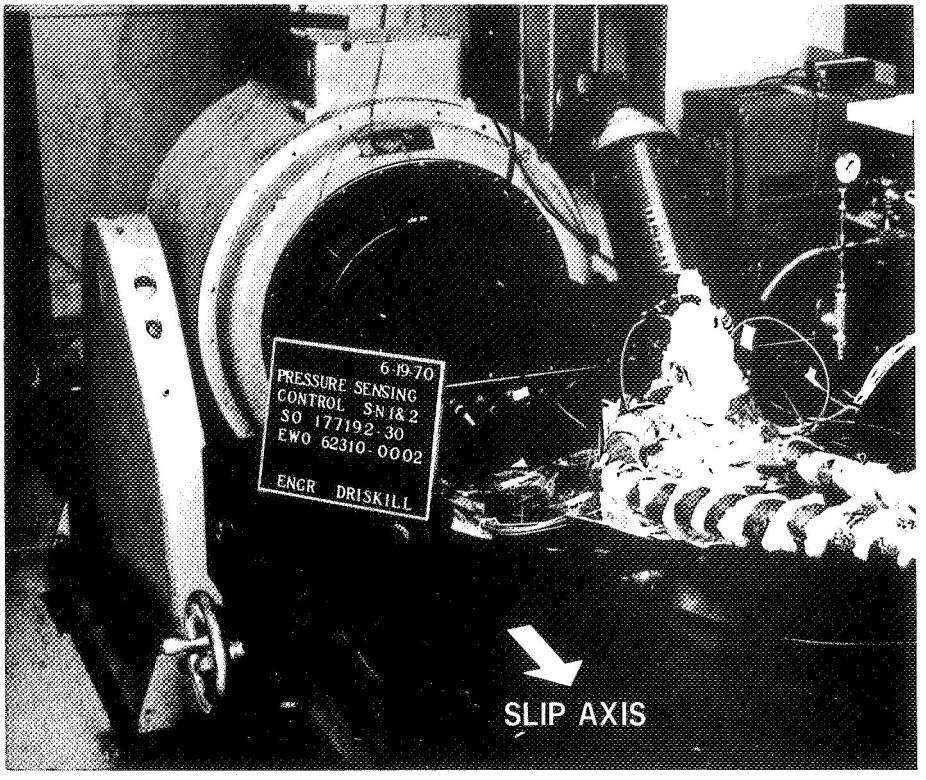

Figure 35 Vibration Test Setup — Slip Axis

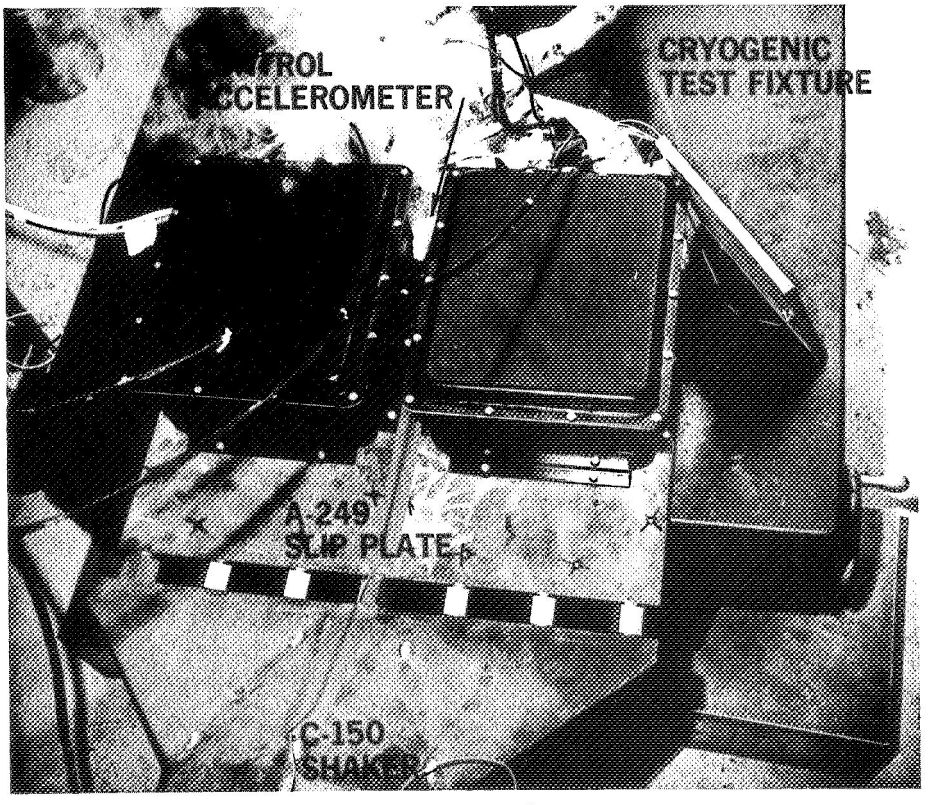

Figure 36 Vibration Test Setup — Control Accellerometer Location

fluid feed and vent. A liquid nitrogen trailer was used to supply the cryogenic fluid and the chamber temperature was controlled using the LN_2 trailer outlet valve and the test fixture fluid temperature (T1) measured by the CEC S/N T3754 probe and read out on a DVM. Gaseous helium was used to pressurize and calibrate the total pressure transducers. The schematic in Figure 37 shows the test setup used. Both systems including the test fixture and slip plate weighed 86 lbs (39.1 kg). The basic vibration systems consisted of the Model C150 MB-Electronics 15,000-lb force, (66,800 Newton) 1-inch (2.54cm) stroke shaker, and a 4700 MB Electronics power amplifier. The random excitation control was accomplished with the use of an ASDE-80 Ling Equalizer. A list of all the equipment used for the vibration tests is given in Table A-2 of Appendix A.

Figures 29 and 30 shows the test fixture cover, base plate and sensor installation.

5.2.2 Test Procedure

The sensors within the environmental test fixture were chilled down using cold nitrogen gas. The platinum resistance sensor (T_1) was monitored during the chilldown and the temperature stabilized at -316°F (-193°C).

The system was leak checked by locking up 200 psig (148×10^4 pascals) He during the stabilization time. The precision pressure Heise gas was also monitored during this period.

After temperature stabilization and leak checks, the 28 volt power was turned on and controller systems allowed to warm up. Using the test calibration unit shown in Figure 32, calibration and operational tests were performed. These tests were performed before and after the vibration and shock testing. They consist of the following measurements:

a. Binary and analog voltage outputs for pressure inputs of 0, 50%, and 100% F.S. with the total pressure sensor maintained at -316°F (-193°C) $\pm$ 4°F ($\pm$ 2°C).

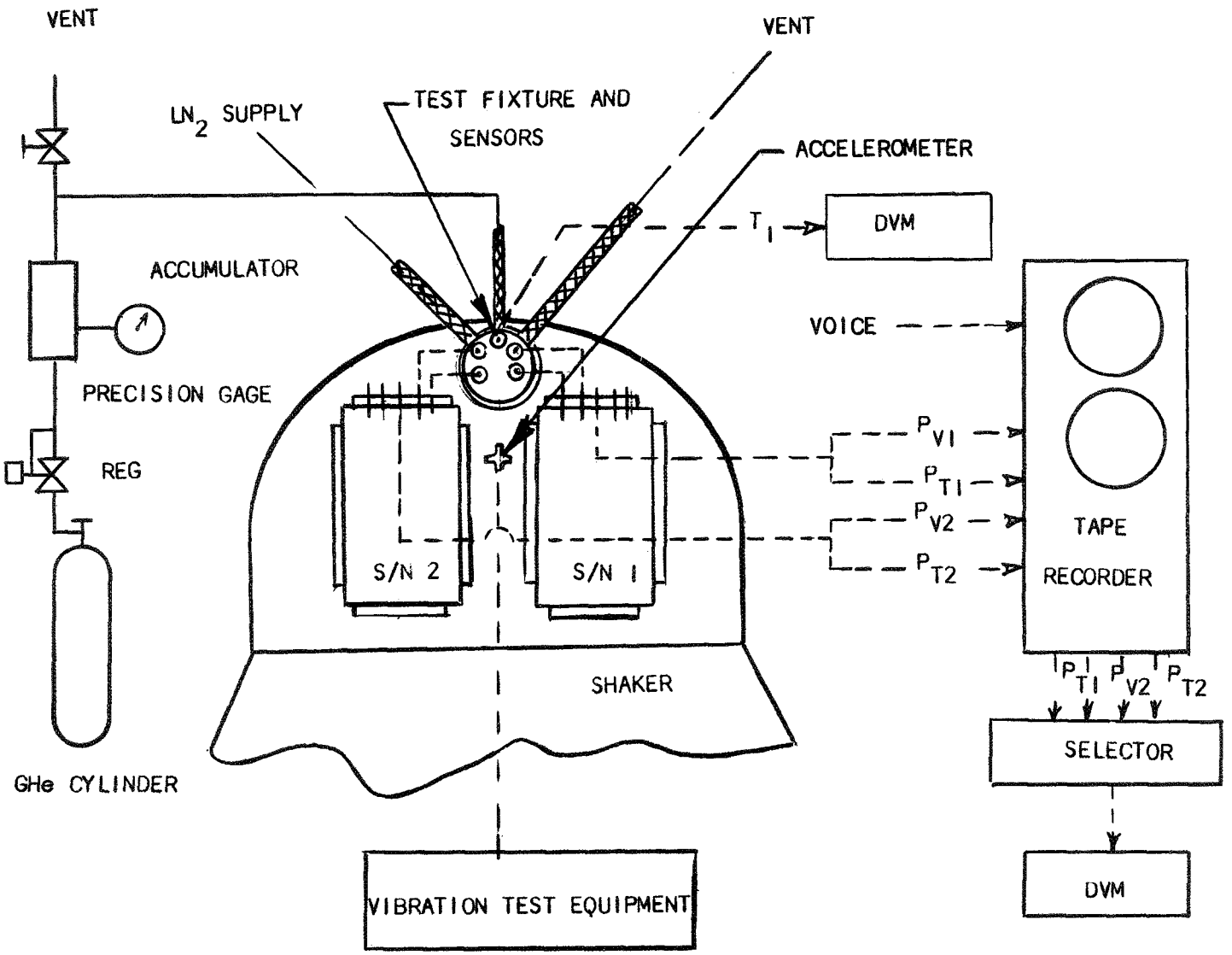

FIGURE 37 VIBRATION AND SHOCK TEST SETUP

b. Analog voltage outputs for the temperature sensors at -316°F ±4°F, (-193°C ±2°C) and for the 50% full scale electrical calibration for the vapor pressure sensing system.

c. Voltage output from the ±15 volt and +5 volt voltage regulators.

d. Voltage output from the 28 volt valve driver.

e. Logic level voltage.

f. Operational test consisting of various voltage inputs to simulate P_T and P_V in the firing and standby operations (see the operation checkout data sheet, Table 7).

While maintaining the sensors temperatures at -316°F, (-193°C) the total pressure sensors were pressurized to 50 ±0.5 psig (44.5 ±0.3 x 10^4 pascals) and the vibration tests were performed in the sequence that follows as discussed in the following paragraphs:

The sinusoidal sweeps were conducted logarithmically at the rate of one octave per minute from 5 to 2000 to 5 Hz. The specified input levels were as follows:

Sinusoidal Vibration

Frequency Range (Hz)	Level
5 - 13	0.25 inch (0.64 cm) single amplitude
13 - 600	3.15 g (rms)
600 - 2000	4.50 g (rms)

A tracking filter with 5, 20, and 50 Hz bandwidths was used on the control accelerometer. The filtered signal from the control accelerometer was used in the control circuit.

Accelerometer signals during the sinusoidal testing were recorded on oscillograph charts and FM magnetic tape.

Random Vibration

Random vibration tests were performed in the following steps:

1. The spectral density equalizer was set to 1/10th of the full-power specification, and the spectrum was checked visually by examination of the equalizer meters.

Table 7

OPERATIONAL CHECKOUT SHEET

	Pre-set values
S/N No.	P_4 =
Program	P_5 =
Date	ΔP_2 =
	ΔP_3 =

Firing Operation

_____1. Set $P_T = 0$

_____2. Position and pre-firing and firing switch on

_____3. Check if firing light is on

_____4. Increase P_V >_____>$(P_4-\Delta P_3)$

_____5. Check if vent light turns on and off

_____6. Increase P_T >_____>(P_5)

_____7. Check if vent light stays on

_____8. Set $P_T = 0$

_____9. Check if vent light turns on and off

_____10. Decrease P_V <_____<$(P_4-\Delta P_3)$

_____11. Check if pre-pres. valve light is on

_____12. Set $P_V \simeq$ 1/4 F.S. =

_____13. Check if pre-press. valve light is on

_____14. Increase P_T >_____>$(P_{V\ set} + \Delta P_2)$

_____15. Check if pre-press. complete light is on

_____16. Decrease P_T <_____<$(P_{V\ set} + \Delta P_2)$

_____17. Check if pressurization valve light is on

Standby Operation

_____1. Position firing switch off

_____2. Increase P_T >_____>(P_4)

_____3. Check if vent light is on

_____4. Decrease P_T <_____<(P_5)

_____5. Check if vent light is off

2. When the setting appeared satisfactory, a brief full-power run was made, during which time the signal response of the control accelerometer was recorded on a magnetic tape loop and subsequently analyzed and plotted by a continuous-sweep analysis system. The following filter bandwidths were used.

Frequency Range (Hz)	Bandwidth (Hz)
20 - 26	5
26 - 2000	20

3. When the tape loop analysis showed a satisfactory spectrum, the remainder of the full-power run was completed. Accelerometer response signals during the random testing were recorded on magnetic tape.
4. After completion of the test, the control signal recorded during the run was reduced as described in step 2.

Random vibration tests were performed for a total duration of 12 minutes. The input levels were as follows:

Frequency (Hz)	Level
20 - 600	6 dB/octave
600 - 1100	0.225 g^2/Hz
1100 - 2000	-12 dB/octave

Mechanical Shock

Before the mechanical shock tests were performed, system accuracy was checked as follows:

1. Horizontal scale accuracy (time) was verified by standard calibration procedures during the periodic calibration and certification of the storage scope.
2. Vertical input deflection was adjusted by inserting a calibration signal corresponding to a known acceleration level and adjusting the storage scope potentiometer until the trace coincided with the desired vertical scale divisions.
3. Shock pulses were shaped by a waveform synthesizer and a bandpass filter, displayed on a storage scope, and photographed by a scope camera. The input levels were as follows:

Number of shock pulses	3
Amplitude	60 g's peak
Input shape	Half sine wave
Duration	6 milliseconds

Upon completion of the sine, random and shock tests, the system calibration and operational test were again performed.

5.2.3 Results

The sinusoidal and random vibration tests were performed according to the input levels and specifications in Appendix D. The sinusoidal test data are presented as plots of acceleration versus frequency in Figure 38. The random vibration test data are presented as plots of Spectral Density versus Frequency in Figure 39. The shock test levels are given in Figure 40. The half sine shock pulses of 60 g's at 6 ms were achieved as planned. This shock level is less severe than that required for "High Intensity" (100 g's at 6 ms) testing for flight vehicle equipment but much more severe than that required for the Basic Design tests (15 g's at 11 ms) under MIL-STD-810B.

Following this testing, both controller units were found, in general, to be structurally sound and operational. The S/N 1 controller checked out completely following the vibration and shock tests and the visual inspection did not reveal any physical damage to any of its subsystems or components. The operational test data are given in Tables 8 and 9. Controller S/N 1 exhibited no deterioration in performance. However, controller S/N 2 did not check out operationally because of the vent valve driver failing to function. During the post-test visual inspection, two coupling capacitors were found broken off at the leads from the ICC cards, see Figure 41. The rework after testing included epoxing all the coupling capacitors to their respective circuit boards to insure the assembly's integrity. Further examination and testing revealed that the glass fuse associated with the vent valve driver had failed.

During the vibration testing, 50 psig (4.45×10^5 pascals) was applied to both the total pressure sensors (P_{T1} and P_{T2}). The signal levels for the vapor pressure sensors (P_{V1} and P_{V2}) and the total pressure sensors at -320°F (-196°C) were as follows:

P_{T1} = 0.630 volts
P_{T2} = 1.220 volts
P_{V1} = 5.759 volts
P_{V2} = -0.423 volts

SINUSOIDAL VIBRATION

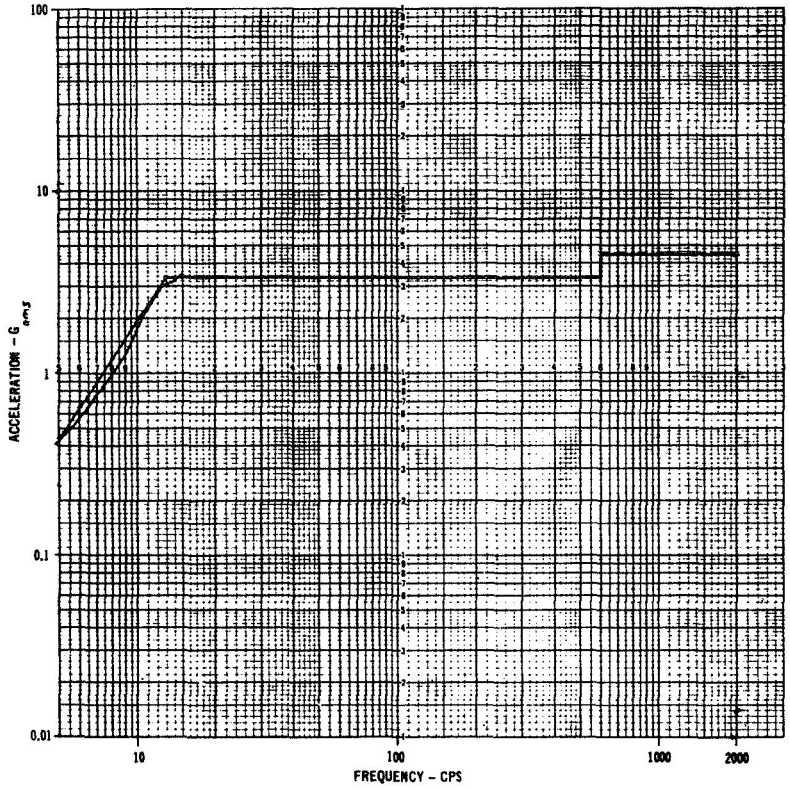

Figure 38 Vibration Data – Sinusoidal Upsweep

RANDOM VIBRATION

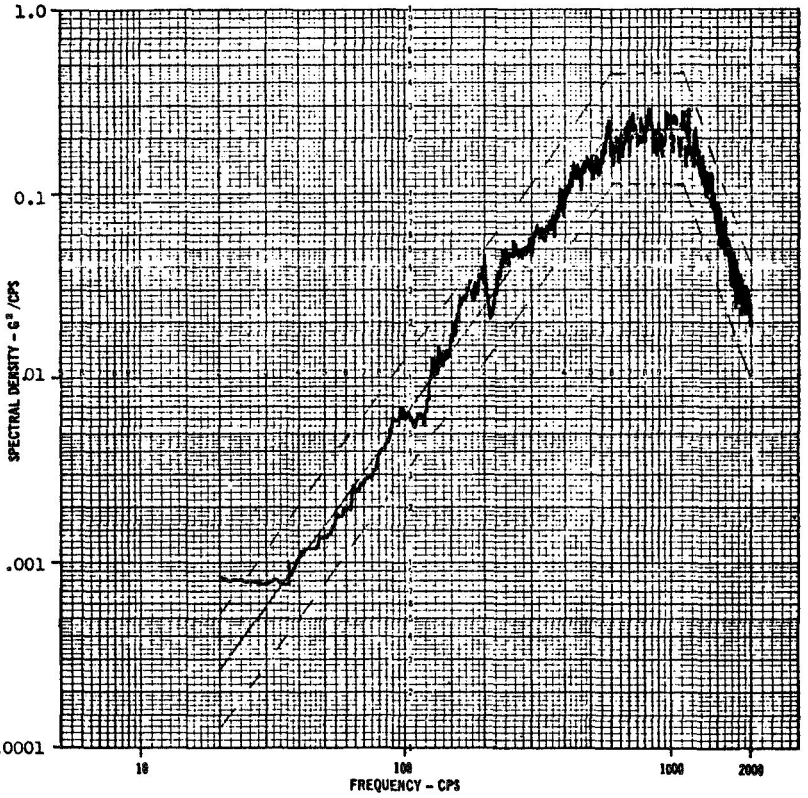

Figure 39 Vibration Data – Random

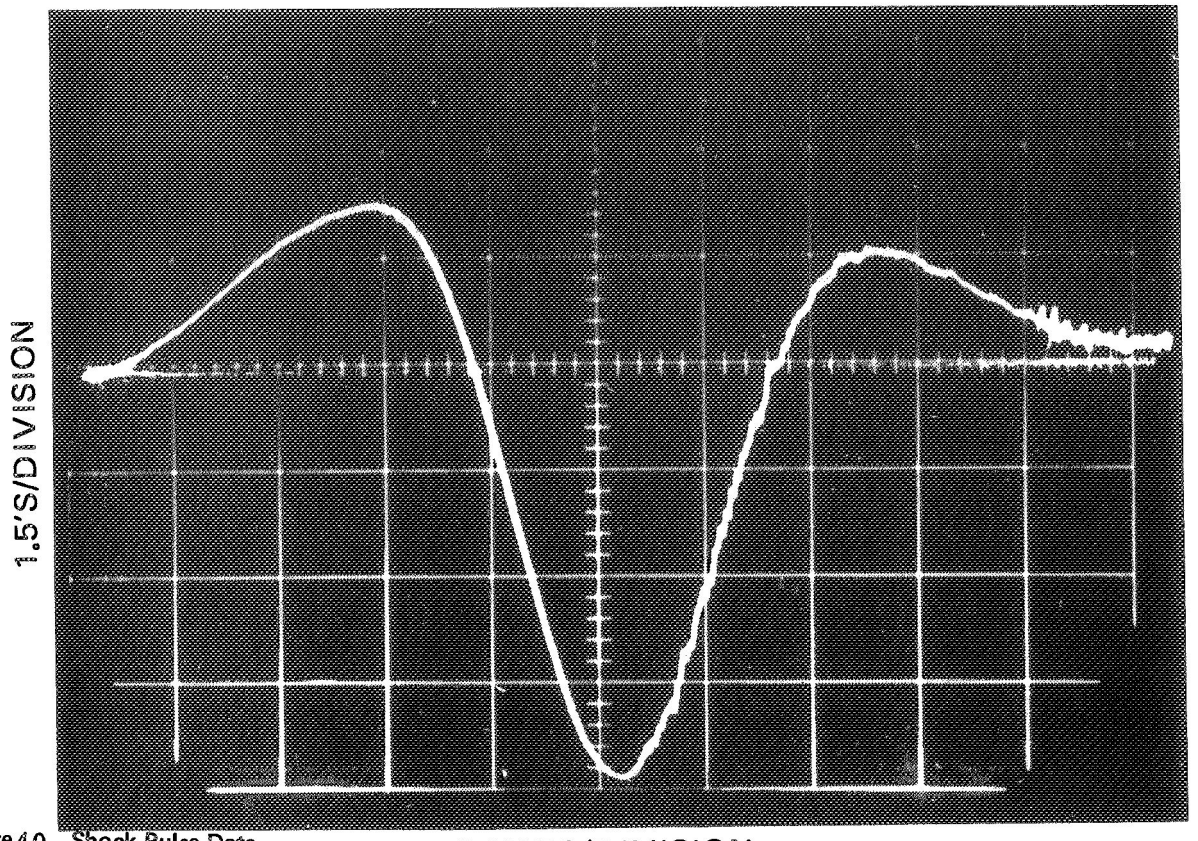

Figure 40 Shock Pulse Data

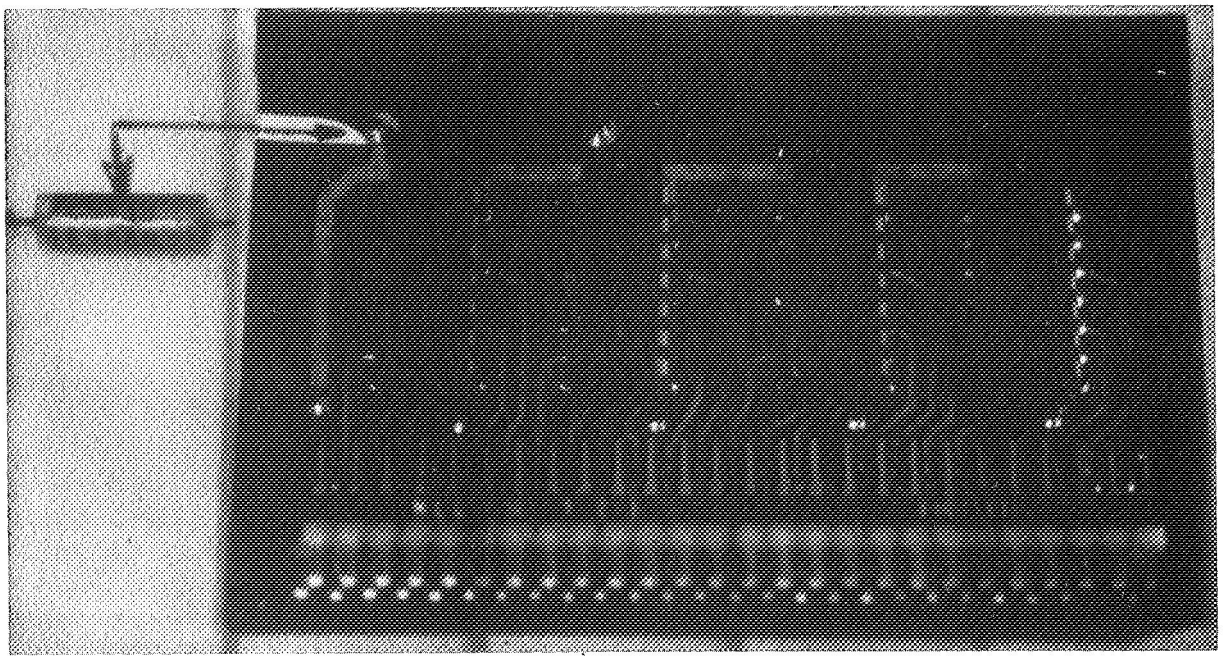

Figure 41 Broken Off Capactor After Vibration and Shock

Table 8

OPERATIONAL TEST

DATA SHEET

CONTROLLER: P/N 1T38533; S/N 1

TEST: Vibration & Shock

DATE: Pre-Test 6-19-70

Post-Test 6-22-70

NOTE: H, L, and H/L DENOTE THE LOGIC LEVELS:
$V_H \approx 3$ VOLTS
$V_L \approx 0$ VOLTS

TOTAL PRESSURE SIGNAL (P_T) CALIBRATIONS

	Applied Pressure % F.S.	Analog Voltage (Volts)	BINARY OUTPUT 1	2	3	4	5	6	7	8	O/R
PRE-TEST	0	-0.343				Under Range Not Applicable					
	50	1.841	H	H	H	H	H	L	H	L	H
	100	4.460	H/L	L	H	L	L	H	H	H	H
POST-TEST	0	-0.341				Under Range					
	50	1.804	H	L	H	H	H	L	H	L	H
	100	4.402	H	L	L	L	L	H	H	H	H

VAPOR PRESSURE SIGNAL (P_V) CALIBRATIONS

ELECTRICAL CALIBRATION	ANALOG VOLTAGE	
	PRE-TEST	POST-TEST
50% F.S. Check	2.502	2.501
-320°F (-196°C)	5.633	5.624

POWER AND VOLTAGE MEASUREMENTS

SUPPLY VOLTAGE	REGULATION	
	PRE-TEST	POST-TEST
V_H	3.413	3.450
5 Volts	5.012	5.020
28 Volts	28 Nominal	28 Nominal
-15 Volts	-14.998	-14.986
+15 Volts	+15.026	+15.020

Table 9

OPERATIONAL TEST

DATA SHEET

CONTROLLER: P/N 1T38533; S/N 2
TEST: Vibration & Shock
DATE: Pre-Test: 6-19-70
Post-Test: 6-22-70

NOTE: H, L, and H/L DENOTE THE LOGIC LEVELS:
$V_H \approx 3$ VOLTS
$V_L \approx 0$ VOLTS

TOTAL PRESSURE SIGNAL (P_T) CALIBRATIONS

	Applied Pressure % F.S.	Analog Voltage (Volts)	BINARY OUTPUT 1	2	3	4	5	6	7	8	O/R
PRE-TEST	0	+ .158	H	L	L	H	L	L	L	L	H
	50	2.740	H	L	H	H	L	L	L	H	H
	100	5.247	Over Range Not Applicable								L
POST-TEST	0	+ 126	H	H	H	L	L	L	L	L	H
	50	2.711	L	H	L	H	L	L	L	H	H
	100	5.220	Over Range Not Applicable								L

VAPOR PRESSURE SIGNAL (P_V) CALIBRATIONS

ELECTRICAL CALIBRATION	ANALOG VOLTAGE	
	PRE-TEST	POST-TEST
50% F.S. Check	2.448	2.442
-320°F (-196°C)	-0.456	-0.455

POWER AND VOLTAGE MEASUREMENTS

SUPPLY VOLTAGE	REGULATION	
	PRE-TEST	POST-TEST
V_H	3.440	3.434
5 Volts	5.018	5.005
28 Volts	28 Nominal	28 Nominal
-15 Volts	-14.970	-14.973
+15 Volts	+15.017	15.016

During the sinusoidal vibration all controller sensor outputs were stable. Two changes did occur however, but were not related to the vibration environment:

1. During the upsweep, at 6 minutes into the eight-minute run a step increase of approximately 2 psig (11.4×10^4 pascals) was recorded from P_{T1}. This increased level remained constant throughout the remaining tests indicating that perhaps the sensor body temperature was not in equilibrium, that is, the temperature was not uniform throughout the transducer at the beginning of the test.
2. During the downsweep, a 3°F (1.7°C) temperature excursion was recorded at 260 sec from the test fixture fluid temperature (T1) probe. This change affected the two total pressure sensor outputs. Their output dropped approximately 50 millivolts (1.5 psig) (11.63×10^4 pascals) for 1.5 seconds immediately following the recovery of the fixture fluid temperature.

This change indicates that the total pressure sensors are rather sensitive to transient changes at temperatures near the liquid nitrogen level. This temperature excursion was also seen in the P_{V2} output. The 261 mv change recorded, however, may not be used to compute the temperature change because the initial output (-0.423 volts) plus the change are in the non-linear range of the system.

During the random vibration, a low frequency oscillation (0.5 to 0.875 Hz) was recorded at five different periods of time during the 12 minute test. All four sensors experienced the same frequency oscillation. At 5.2 minutes into the test, P_{T1} and P_{T2} recorded a magnitude of approximately 50 millivolts for a duration of 32 sec, and the vapor pressure sensor P_{V1} recorded 270 millivolts for the same duration. P_{V2} magnitude was negligible. The remaining test showed no noise or instability. Because all four channels recorded the same frequencies at the same time, the disturbance must have been from a common source. A single 28 volt power supply was used to power both controllers and their P_T and P_V signal conditioners. The noise could possibly have been introduced by a loose connection at the power supply output terminals although there was no real evidence provided to establish this as fact.

5.3 Functional Cycle Test

The purpose of these tests was to demonstrate that both complete control systems S/N 1 and S/N 2 function in the manner for which they were designed. The demonstration was accomplished in a total of 8 test runs. A test run consisted of simulating the total tank pressure and the propellant vapor pressure while allowing the controller to function automatically according to the preset pressure values. Control valves were activated manually to simulate the pressure decay due to expulsion during the simulated engine burn and the pressure rise during standby to simulate overpressure in the emergency situation. In the test runs, the initial total tank pressure, P_6, and vapor pressure, P_1, were simulated in both the firing and standby conditions. Initial values of pressure were selected to allow the controller to execute its logic and control functions based on the preset pressure inputs P_4, P_5, ΔP_2, and ΔP_3 defined in Figures 1 and 2 along with the modes of operation. These test conditions were designed to exercise the controller within the design pressure range and to simulate all the possible conditions for which the controller must function.

A set of four runs for each controller was made with the initial values P_6 and P_1 (see Figure 2) chosen to set up the following conditions and to provide the following results:

Firing signal:

Conditions	Results
1. $P_3' < P_4$	No venting required prior to pre-pressurization.
$P_3' > P_T$	Pre-pressurization required.
2. $P_3' < P_4$	No venting required prior to pre-pressurization.
$P_3' < P_T$	No pre-pressurization required.

Firing Signal (Cont'd)

Conditions	Results
3. $P_3' \geq P_4$	Venting is required to condition tank.
	Pre-pressurization required after conditioning.
Standby	
$P_6 > P_4$	Emergency venting required.

NOTE: P_3' is the precalculated value of the run pressure (the pressure level at which pre-pressurization is complete). P_3' is also defined by:

$$P_3' = P_1 + \Delta P_3$$

The controllers were placed in a vacuum environment while the sensors were at ambient external pressure and at cryogenic temperature.

Pre-test and post-test calibrations and operational checks were performed on each of the two units tested.

5.3.1 Test Setup

Figure 42 schematically shows the test setup. The controller is shown mounted in a 24 inch (0.61 m) diameter by 14 inch (0.36 m) cylindrical vacuum chamber. Figure 43 is a photograph showing the controller placed inside the chamber. The controller rests on aluminum mounting blocks that are coated with thermally conductive paste to provide a good path for the conduction of heat. Attached to the controller base plate near the 5 volt power supply is a Cu-const. thermocouple (T/C3). With the controller cover removed, the bulkhead electrical connectors, J1 through J5 are unfastened from the controller and mated to the matching holes in the vacuum chamber cover. Figure 31 shows the lid and these holes along with the thermocouple feedthrough. The lid is sealed with "O" ring and then bolted to the chamber.

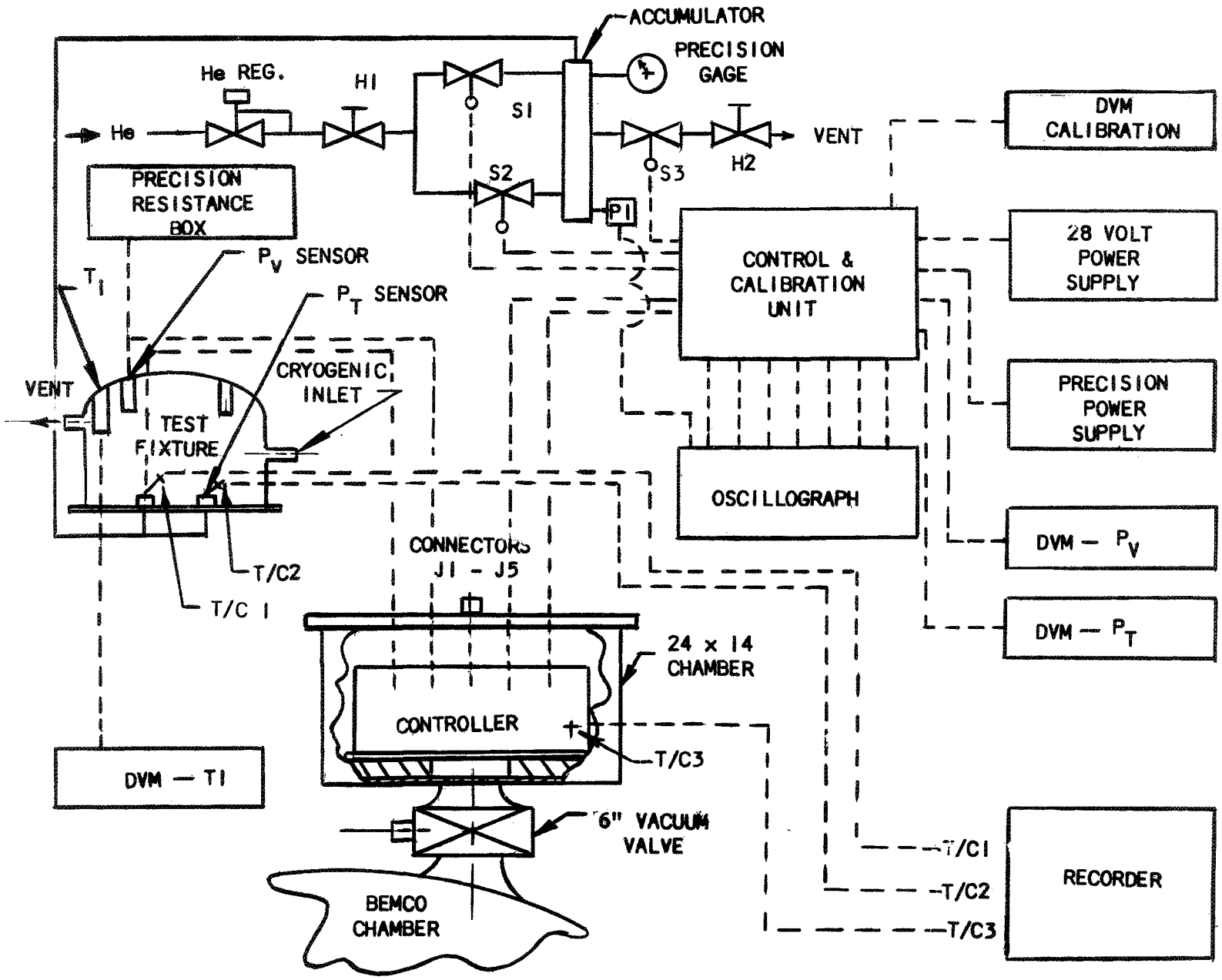

FIGURE 42 FUNCTIONAL/VACUUM TEST SETUP

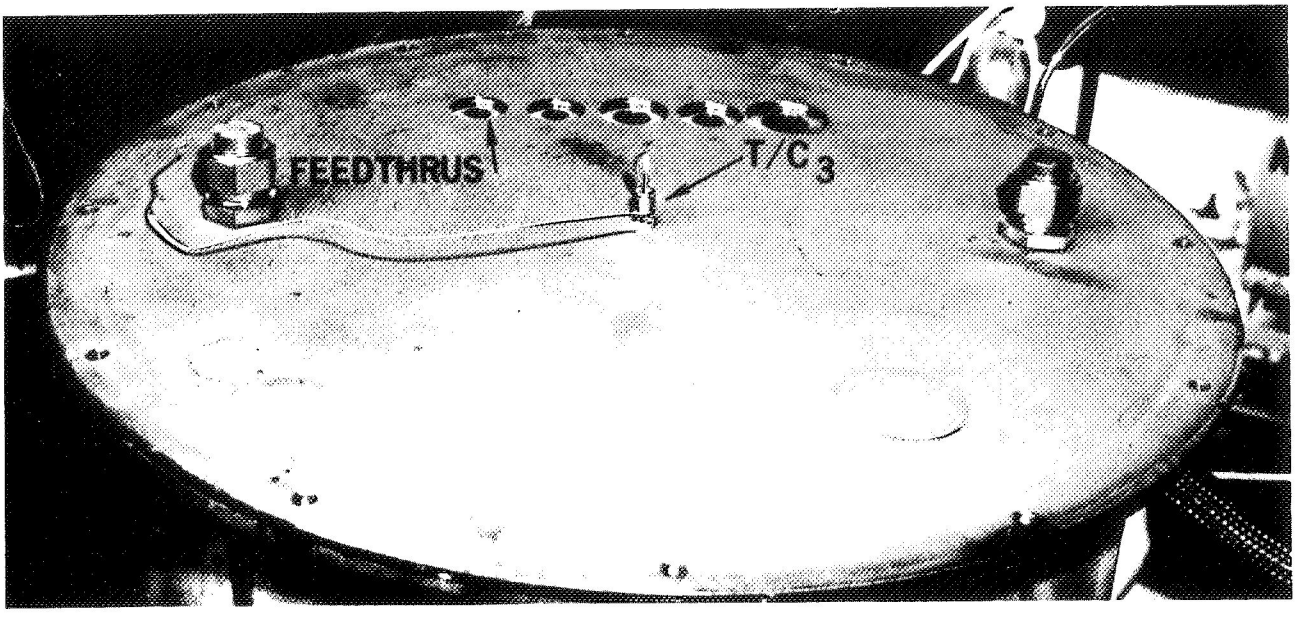

Figure 43a Vacuum Chamber (24 IN. X 14 IN.) – Lid and Feedthrus

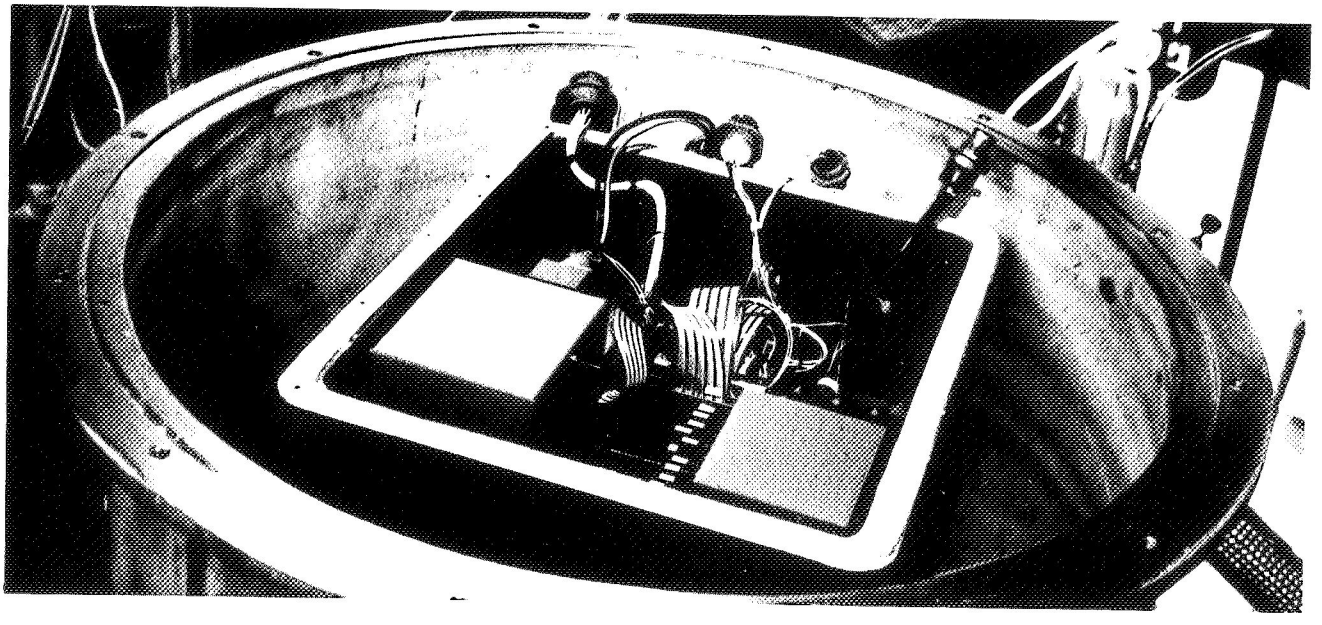

Figure 43b Vacuum Chamber (24 in. X 14 in.) – Controller Installed

A 6 inch (0.15 m) diameter vacuum valve separates the small chamber housing the controller from the main Bemco chamber system. This installation allows the main chamber to be evacuated while the smaller chamber is open for the controller checkout and installation. The diffusion pump and 5 x 7 (1.52 x 2.14 m) foot Bemco chamber is shown in Figure 44. Figure 45 shows the controller chamber mounted on the Bemco lid.

The cryogenic test fixture in Figure 29, was also used for the functional cycle tests in providing the cryogenic environment. All four sensors were mounted in the test fixture. Liquid hydrogen and gaseous hydrogen, supply lines and vent lines were connected to the test fixture. The test fixture fluid environmental temperature (T1) was monitored and controlled using the CEC platinum probe. Its output was monitored on a digital voltmeter while adjusting the liquid and gas supply valves. Two Cu-const. thermocouples were attached to the Kaman Nuclear sensor bodies. These temperatures were recorded on the L/N strip chart. The test fixture was insulated with fiberglass and located approximately 10 feet (3.05 m) from the controller. The pressure system, also shown in the schematic, was used to simulate the tank pressurization, expulsion and venting. This system is also used to calibrate the Kaman Nuclear total pressure measuring system. S1 was used to simulate the helium pressurization valve and S2 the vaporized propellant valve. S3 was used to simulate venting and expulsion. H2 regulated the rate of pressure decay and H1 was used to vary the pressurization rate. These valves are all mounted off the 2 1/2-inch (0.065 m) diameter by 36-inches (0.92 m) long accumulator and all the attached tubing is 1/4 inch stainless steel. A 300 psig (216 x 10^4 pascals) precision gage was used for calibrations.

The following parameters were recorded during the testing using an oscillograph.

a. Explosive vent valve open
b. Vent valve open (S3)
c. Helium valve open (S1)
d. Vaporized propellant valve open (S2)

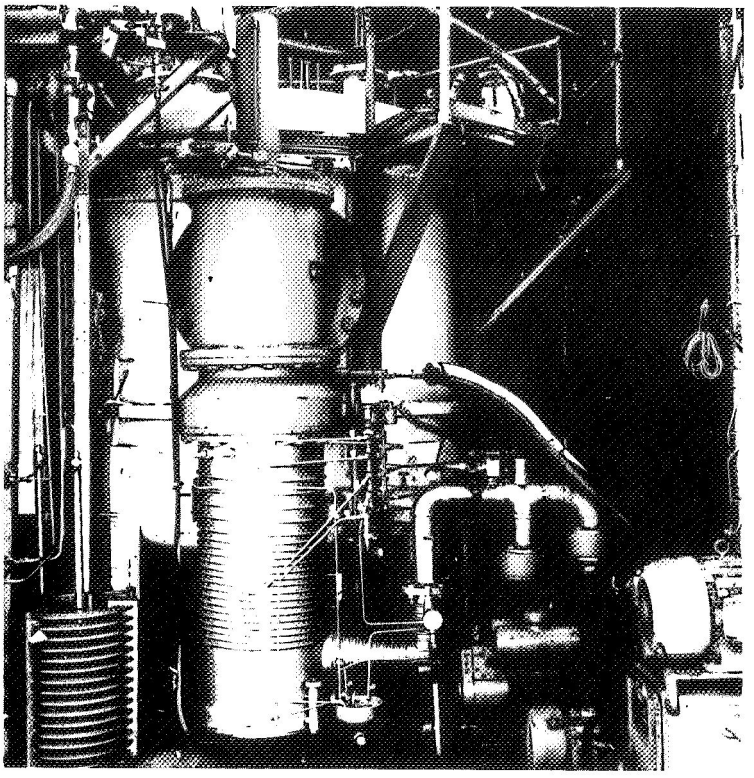

Figure 44 Bemco Chamber and Diffusion Pump

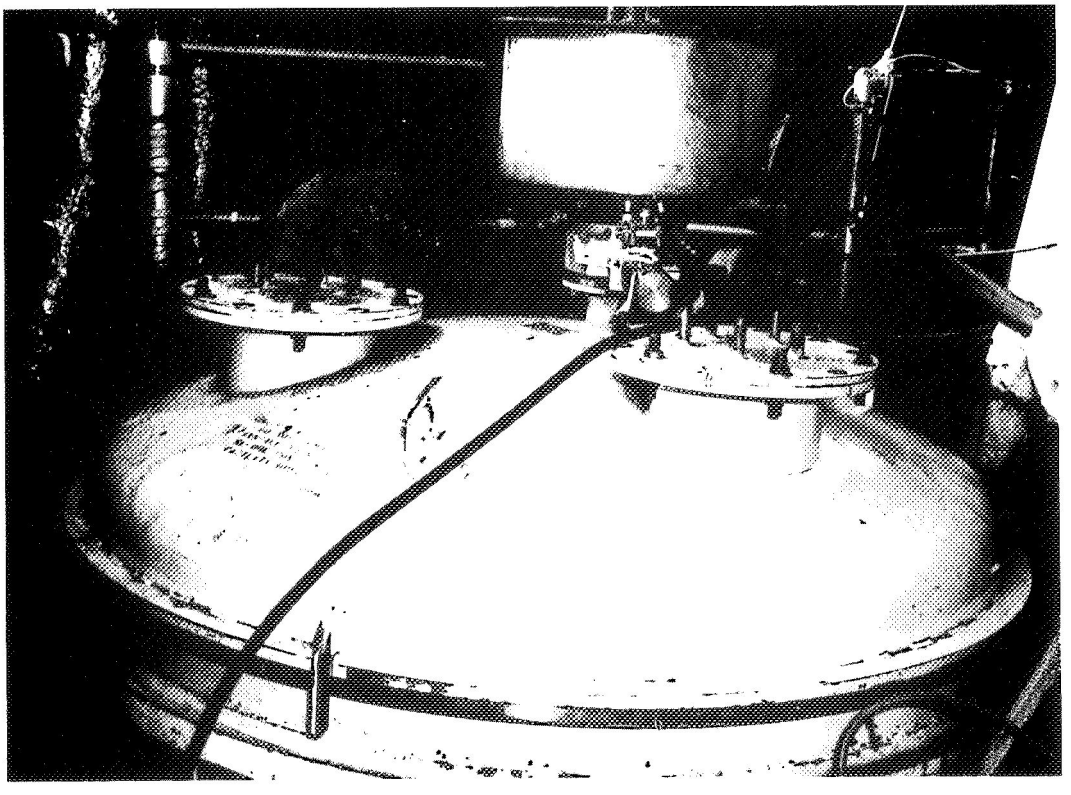

Figure 45 Bemco Chamber -- 24 In. X 14 In. Chamber and 6 In. Valve Installed

e. Pre-firing signal

f. Firing signal

g. Run pressure P

A 28 volt power supply was connected to the controller and calibration unit. The output voltages from the sensors, valve drivers, pre-press complete signal, 8-bit digital signals and the power regulators were measured using a digital voltmeter. Two precision power supplies were used to electrically input the P_T and P_V values for the checkout. P_T and P_V were measured in the block house on two additional voltmeters. Values of P_V were simulated using the precision resistance box. A list of all the equipment used is given in Appendix A, Table A-3.

The test schematic also shows the controller connectors J_1 through J_5 and their interconnections. The total pressure sensor P_T is connected to J_4. Similarly J_5 inputs the temperature sensor P_V to the controller. Connector J_1 is mated with either of three pre-wired mode selection connector containing appropriate jumper wires to select the operational modes I, II, or III.

Connector J_2 contains test and calibration outputs. Its mating "test and calibration" plug allows monitoring of the internal power converters and regulators which supply + 5 VDC and ± 15 VDC. In addition, a switch which is part of the test and calibration control unit allows inputing either electrically simulated or actual P_T and P_V analog 0-5V signals. Both analog 0-5V and 8-bit signals proportional to P_T and P_V are also accessible.

The test and calibration and control unit 1T36159 is shown in Figure 32. Positioning of the switch to normal position on the calibration and control unit allows the controller to function normally without the electrically simulated P_T and P_V inputs.

J_3 provides the following connections to the controller and calibration unit.

a. 28 VDC input to power the controller
b. Driver outputs (+ 28 VDC) to the four control valves
c. Pre-firing signal
d. Firing signal (+ 28 VDC) input
e. "Pre-press complete" signal (+ 3 VDC) output.
f. 28 VDC input to power valve drivers.

Two of the four I 905 modified ICC cards, programmed with the preset pressures were used for the testing.

The programs selected are identified in Tables 10 and 11. Program A was used with the hydrogen unit S/N-1 and program C was used with the fluorine unit S/N-2. The three mode selection connectors were also provided and were used in conjunction with these program cards.

5.3.2 Test Procedure

In the functional tests, the sensors within the test fixture were chilled down and maintained at -423°F (-253°C) using liquid hydrogen and at -320°F (-196°C) using liquid nitrogen as required by the units S/N 1 and S/N 2, respectively. The platinum resistance reference sensor T_1 and the thermocouples T/C 1 and T/C 2 were used in monitoring the chilldown. After these temperatures became stabilized, leak checks were made by locking up 200 psig (148 x 10^4 pascals) helium and monitoring the precision pressure gage.

The values of vapor pressure planned for in setting up the various test conditions were to be provided by controlling the test fixture fluid temperature. This was to be accomplished by mixing liquid and warm gas hydrogen. However, during the test setup checkout it was found impractical to control and maintain the stable temperatures necessary to simulate accurately the vapor pressures. The vapor pressure was, however, easily and precisely simulated by substituting the electrical resistance of the platinum sensor probe with an adjustable precision resistance decade box.

Table 10

PROGRAM A

	ΔP_2	ΔP_3	P_4	P_5
MATRIX CARD WIRING POSITION	2 & 3	4 & 2	4,5,6,& 7	5,6,& 7
COUNTS	6	10	120	112
PRE-SET (pascals) PRESSURE (psig)	13.07 4.45	15.11 7.42	71.2 89.06	67.2 83.13
VOLTAGE EQUIVALENT	0.117	0.195	2.344	2.188

PROGRAM B

	ΔP_2	ΔP_3	P_4	P_5
MATRIX CARD WIRING POSITION	4 & 5	3,4,& 5	5,6,& 8	2,5& 8
COUNTS	24	28	176	146
PRE-SET (pascals) PRESSURE (psig)	22.3 17.81	24.3 20.78	99.4 130.62	84.3 108.36
VOLTAGE EQUIVALENT	0.469	0.547	3.437	2.852

Table 11

PROGRAM C

	ΔP_2	ΔP_3	P_4	P_5
MATRIX CARD WIRING POSITION	3 & 4	5	7 & 2	2,5,& 6
COUNTS	12	16	68	50
PRE-SET (pascals) PRESSURE (psig)	16.13 8.906	18.16 11.875	47.8 50.47	35.6 37.11
VOLTAGE EQUIVALENT	0.234	0.312	1.298	0.977

PROGRAM D

	ΔP_2	ΔP_3	P_4	P_5
MATRIX CARD WIRING POSITION	4 & 6	5 & 6	2,4,5,6,7& 8	4,7,& 8
COUNTS	40	48	250	200
PRE-SET (pascals) PRESSURE (psig)	30.4 29.688	34.5 35.626	137. 185.55	112. 148.44
VOLTAGE EQUIVALENT	0.781	0.938	4.883	3.906

Calibration and operational tests were performed before and after the functional testing of each unit. These pre-test and post-test calibrations and operational tests were identical and consisted of the following measurements:

a. Pressure Sensor - Analog voltage outputs for nine point calibration going up and down scale in 25% F.S. increments. Gaseous helium was used as a pressurant while the fluorine sensor S/N 1306 was calibrated at -320°F (-196°C) and the hydrogen sensor S/N 1305 was calibrated at -423°F (-253°C).

b. Binary outputs for the above pressure inputs and conditions.

c. Voltage output from the ±15 volt and +5 volt power regulators.

d. 28 volt power supply input.

e. Logic level voltage (high voltage V_H)

f. Operational checkout (see the operational checkout data sheet Table 7).

g. Analog voltage output for the P_V sensors at -423°F (-253°F) and -320°F, (-196°C) as well as various outputs associated with certain equivalent ohm resistance inputs.

With the controller installed in the vacuum chamber, the chamber was evacuated to 10^{-5} torr (1.33×10^{-3} pascals or less). After achieving the vacuum and the temperature stabilization of the sensors, leak checks were completed. Then the system 28 volt power was turned on and the system allowed to warm up. Using the control and calibration unit, the pretest calibration and operational tests were performed. Then, after obtaining the stable test environment and the conditions the firing operation was simulated by the following control sequence:

a. All valve switches on the control unit are positioned in the normal position allowing the controller to operate automatically the solenoid valves S1, S2, and S3 as required by the preset pressure inputs.

b. Apply prefiring signal to controller. This allows the P_V signal conditioner to warm-up prior to initiating the firing signal.

c. After allowing the P_V signal conditioner to warm-up, the initial vapor pressure P_V is simulated by setting the required electrical resistance on the precision resistance box.

d. The firing signal is then applied. In tests 1, 2, 4 and 5, the vent valve S3 is opened manually (overriding the controller) just before applying the firing signal. S3 is opened to simulate the expulsion during the burn cycle. H1 and H2 are adjusted so that the pressurization rate will be slightly greater than the venting rate, allowing the controller to perform the pre-pressurization and pressurization functions. In run 3 and 6, the initial values of vapor pressure are set sufficiently large such that $P_3' > P_4$. The values are later changed during the run to simulate propellant tank conditioning due to venting.

The standby operation was simulated by setting the initial total pressure at a level below P_4, then adjusting H1 and H2 so that the venting rate is slightly less than the pressurization rate. The He pre-pressurization valve (S1) was opened by the override switch on the control unit to simulate the over-pressure. All the other valve switches were placed in the normal position, and the firing switch was positioned off for standby. Upon completion of the functional test, system calibrations and operational tests were again performed for each unit.

5.3.3 Test Results

5.3.3.1 (P_T) Sensor Calibration

The liquid hydrogen controller S/N 1 and its sensor were used during the test system checkout and were the first to be tested functionally. Before subjecting the controller to the vacuum environment, the Kaman Nuclear Sensor S/N 1306 with its electronic package S/N A1306 were proof tested at ambient temperature and 300 psig (216×10^4 pascals) helium, and then adjusted and calibrated at -423°F (-253°C). This calibration data taken on 6-30-70 and data taken during the vacuum functional testing are also presented in Table 12. The zero and span was adjusted without any difficulty and the initial calibrations were within the specifications. The maximum error was only 43 millivolts or 1.25 psig (11.26×10^{-4} pascals). However, during the testing that followed, the instrument's zero and full-scale values changed dramatically. The pretest calibrations made 7-6-70 were in error by as much as 15% F.S. which is completely out of

TABLE 12

S/N 1 KAMAN NUCLEAR SENSOR CALIBRATION

Calibration Date: As noted

Date	Sensor S/N 1306	Electronics S/N A-1306		Press	Voltage (Volts)	
	Temp.	Temp.	Press.	% FS	Increasing	Decreasing
6-30-70	-423°F (-253°C)	70°F (21°C)	Zero PSIG 10.013×10^4 Pascals	0	0.010	0.006
				25	1.272	1.270
				50	2.541	2.543
				75	3.792	3.794
				100	5.010	5.010
7-2-70	-423°F (-253°C)	70°F (21°C)	1×10^{-5} Torr 1.33×10^{-3} Pascals	0	-0.268	-0.267
				25	0.930	0.936
				50	2.340	2.344
				75	3.730	3.727
				100	5.081	5.081
7-6-70	-423°F (-253°C)	70°F (21°C)	Zero PSIG 10.013×10^4 Pascals	0	0.387	0.381
				25	1.375	1.366
				50	2.356	2.351
				75	3.320	3.323
				100	4.257	4.257
7-6-70	-423°F (-253°C)	70°F (21°C)	1.4×10^{-6} Torr 1.86×10^{-4} Pascals	0	0.716	0.684
				25	1.533	1.514
				50	2.352	2.350
				75	3.155	3.161
				100	3.910	3.910

tolerance. Functional tests, however, were continued because sufficient total pressure signals were still available for exercising the controller functions. Post-test calibrations were performed with the controller at 1.4×10^{-6} torr. These post-test measurements showed the instruments zero and full-scale values had changed even further (22% F.S. error). It was then concluded that a component failure must exist within the Kaman Nuclear system and not merely an adjustment or installation problem existed. The vacuum was removed from the chamber to determine its effect on the sensor output. There was no difference observed. At the end of the test program, the defective sensor system (sensor, interconnecting cable, and electronics) were sent to the vendor for examination and repair. Kaman Nuclear found the inactive coil, seen in Figure 19, loose. The ceramic cement that holds the platinum coil in place failed.

Although no extensive failure analysis was performed to determine the exact cause of failure, it was concluded that the bond strength between the ceramic insulator and coil was not sufficient. However, it is believed to be marginal in that the S/N 1305 sensor was also installed in the test fixture and was exposed to the same environmental and pressure loading conditions, but, did not fail. The defective sensor was repaired using Emerson and Cuming 2850 epoxy. Calibrations were then made at -320°F (-196°C). These final calibrations along with the originals performed by Kaman Nuclear for both S/N 1305 and S/N 1306 are presented in the Operation and Calibration Document 1T19806.

After the functional test for S/N 1 was completed, the liquid fluorine controller S/N 2 and its sensors were tested. Here the total pressure measuring system was adjusted, calibrated and tested at -320°F (-195.6°C). This system remained in calibration during the entire functional testing. The calibration data for this system is given in Table 13. Here the maximum error recorded was 72 millivolts (1.4% F.S.) with the electronics at approximately 75°F (24°C). At the end of testing the chassis plate was at approximately 104°F (40°C), where the maximum error was just 31 millivolts (0.62% F.S.).

TABLE 13

S/N 2 KAMAN NUCLEAR SENSOR CALIBRATION

Calibration Date 7-7-70

Sensor S/N 1305	Electronics S/N A-1305		Press.	Voltage (Volts)	
Temp.	Temp.	Press.	% FS	Increasing	Decreasing
-320°F -196°C	75°F 24°C	Zero Gage 10.13×10^4 Pascals	0	0.002	0.011
			25	1.275	1.282
			50	2.533	2.561
			75	3.818	3.822
			100	5.043	5.043
-320°F (-196°C)	75°F (24°C)	1 x 10-5 Torr 1.33×10^{-3} Pascals	0	+0.003	0.003
			25	1.275	1.275
			50	2.551	2.554
			75	3.814	3.814
			100	5.038	5.038
-320°F (-196°C)	104°F (40°C)	7.47×10^{-7} Torr 9.95×10^{-5} Pascals	0	-0.025	-0.028
			25	1.237	1.236
			50	2.512	2.513
			75	3.769	3.771
			100	4.993	4.993
-320°F (-196°C)	104°F (40°C)	Zero Gage 10.13×10^4 Pascals	0	-0.024	-0.031
			25	1.235	1.237
			50	2.513	2.517
			75	3.776	3.778
			100	5.002	5.002

5.3.3.2 (P_V) Sensor Calibration

Also, before conducting the functional tests, the vapor pressure systems were calibrated using the adjustable precision resistance decade box as a substitute for the vapor pressure probe. Tables 14 and 15 show data taken for the Rosemount probes and amplifier systems used in S/N 1 and S/N 2, respectively. These records compare the Rosemount data with that measured by MDAC using the precision resistance inputs. The maximum error (ideal vs MDAC measurements) are 1.16% for S/N 1 and 2.52% for S/N 2. These values are well within the design specifications. (1.5% F.S. and 3.0% F.S., respectively).

5.3.3.3 Functional Test Performance

The performance results of the functional testing are presented in Table 16a and 16b. For the firing operation, initial conditions for P_1 and P_6 are tabulated along with their various equivalent values. The tables also list the ideal and actual (measured) values of P_2, P_3, P_4 and P_5. Voltage values are compared with their equivalent pressure and the values of pressure measured from the Seegers gage and the oscillograph output. The data from all the firing operations (Table 16a) show excellent agreement between actual and ideal voltages for P_2 (the minimum NPSP). The maximum deviation was only 14 millivolts or 0.28 percent F.S. Comparing actual and ideal voltage is a measure of the controller accuracy independent of the transducer outputs for P_v or P_T. The actual pressures measured by the Seegers gage can be compared with the ideal values. For S/N 2, the maximum combined error was only 1 psig (0.5% F.S.) for P_2. The (P_2) combined errors for S/N 1 were larger and out of tolerance as would be expected because of the malfunctioning Kaman Nuclear sensor.

The voltage data measured for P_3 were all higher than ideal, by 20 to 67 millivolts, however, these values were high because of pressure overshoots resulting from the relatively slow A to D converter sampling rate

Table 14

(P_V) CALIBRATION DATA SHEET

S/N 1 Controller

Liquid Hydrogen Vapor Pressure Sensing System

Amplifier Model 510 BF26 Sensor Model 133CC24X

Amplifier S/N 58 Sensor S/N 1116

Supply Voltage 28VDC

Load Impedance 100 MegΩ

Lead Resistance 0.3Ω

Vapor Pressure		Temp.		Resistance OHMS	Output Voltage			Deviation
PSIG	Pascals X10^4	°F	°C		Rosemount	(1) MDAC	Ideal	(2) % F.S.
0.00	0	-423.21	-252.82	14.53	-0.027	-0.054	0	1.08
23.75	16.4	-416.49	-249.14	24.18	0.646	0.616	0.625	0.18
47.50	32.7	-412.33	-246.83	32.32	1.270	1.238	1.250	0.24
71.25	49.0	-409.19	-245.08	39.62	1.880	1.817	1.875	1.16
95.00	65.4	-406.64	-243.66	46.28	2.483	2.447	2.500	1.06
118.75	81.6	-404.42	-242.31	52.61	3.103	3.069	3.125	1.12
142.50	98.0	-402.47	-241.35	58.58	3.736	3.696	3.750	1.08
166.25	114.2	-400.77	-240.40	64.10	4.365	4.327	4.375	0.96
190.00	131.0	-399.20	-239.53	69.44	5.020	4.980	5.000	0.40

1) Amplifier at 1.4×10^{-6} torr

2) This deviation is based on Douglas measurements and the best straight line between 0 and 190 psig, 0-5 volts.

Table 15

(P_V) CALIBRATION DATA SHEET

S/N 2 Controller

Liquid Fluorine Vapor Pressure Sensing System

Amplifier Model 510 BF25 Sensor Model 176HY24X

Amplifier S/N 57 Sensor S/N 4851

Vapor Pressure		Temp.		Resistance OHMS	Output Voltage			(1) Deviation % F.S.
(PSIG)	pascals X10^4	°F	°C		Rosemount	(2) MDAC	Ideal	
0	0	-306.76	-188.18	304.20	+0.001	-0.020	0	0.40
23.75	16.4	-289.78	-178.75	360.64	0.739	0.715	.625	1.80
47.50	32.7	-279.67	-173.13	394.10	1.339	1.313	1.250	1.26
71.25	49.0	-272.16	-168.96	418.85	1.901	1.874	1.875	0.02
95.00	65.4	-265.20	-165.09	439.20	2.470	2.440	2.500	1.20
118.75	81.6	260.73	-162.61	456.39	3.050	3.018	3.125	2.14
142.50	98.0	-256.12	-160.05	471.47	3.658	3.624	3.750	2.52
166.25	114.2	-252.02	-157.77	484.89	4.303	4.264	4.375	2.22
190.00	131.0	-248.27	-155.69	497.11	4.995	4.953	5.000	0.94

1) These deviations are based on the MDAC measurement

2) Amplifier at 1.0×10^{-6} Torr

TABLE 16a

FUNCTIONAL TESTS RESULTS/FIRING OPERATION

TEST NO. / S/N	INITIAL CONDITIONS								TEST RESULTS											
	P_1 - VAPOR PRESSURE EQUIVALENTS				P_6 - TOTAL PRESSURE				P_2 - NPSP						P_3					
									IDEAL		ACTUAL				IDEAL		ACTUAL			
	OHMS SETTING	DVM (VOLTS)	(PSIG) / (Pascals) x 10^4	(°F) / (°C)	DVM (VOLTS)	EQUIV (PSIG) / (Pascals) x 10^4	SEEGERS GAGE (PSIG) / (Pascals) x 10^4	OSCILL-OGRAPH (PSIG) / (Pascals) x 10^4	(VOLTS)	EQUIV (PSIG) / (Pascals) x 10^4	DVM (VOLTS)	EQUIV (PSIG) / (Pascals) x 10^4	SEEGERS (PSIG) / (Pascals) x 10^4	OSCILL-OGRAPH (PSIG) / (Pascals) x 10^4	VOLTS	EQUIV (PSIG) / (Pascals) x 10^4	DVM (VOLTS)	EQUIV PSIG / (Pascals) x 10^4	SEEGERS GAGE (PSIG) / (Pascals) x 10^4	OSCILL-OGRAPH (PSIG) / (Pascals) x 10^4
1/1	24.180	0.625	23.8 / 36.5	-416 / -249	0.387	14.7 / 20.2	0 / 10.1	0 / 10.1	0.742	28.2 / 29.5	0.748	28.4 / 29.7	18.2 / 22.6	19.0 / 23.2	0.820	31.2 / 31.6	0.840	31.9 / 32.1	21.4 / 24.8	23.0 / 25.9
2/1	24.180	0.625	23.8 / 26.5	-416 / -249	- - - -	- - - -	90.0 / 72.1	- - - -	0.742	28.2 / 29.5	0.730	27.8 / 29.3	18.5 / 22.9	19.0 / 23.2	0.820	31.2 / 31.6	0.839	31.9 / 32.1	21.5 / 24.9	23.0 / 25.9
3/1	(1) 46.280 / 39.620	2.489 / 1.856	94.8 / 75.5 / 70.6	-407 / -244 / -409 / -245	2.700	103.0 / 81.1	- - - -	120.0 / 92.7	1.973	75.0 / 61.8	1.987	75.8 / 62.3	74.0 / 61.1	75.0 / 61.8	2.051	78.1 / 63.9	2.083	79.1 / 64.6	80.0 / 65.2	84.0 / 68.0
4/2	350.00	0.547	20.8 / 24.5	-292 / -180	0.505	20.0 / 23.9	20.6 / 24.3	20.0 / 23.9	0.781	29.7 / 30.6	0.785	29.9 / 30.7	30.1 / 30.9	32.0 / 32.2	0.859	32.7 / 32.7	0.926	35.2 / 34.3	35.4 / 34.5	35.0 / 34.2
5/2	350.00	0.547	20.8 / 24.5	-292 / -180	1.060	40.3 / 37.9	40.5 / 38.0	39.5 / 37.3	0.781	29.7 / 30.6	0.781	29.7 / 30.6	30.0 / 30.8	29.5 / 30.4	0.859	32.7 / 32.7	0.923	35.1 / 34.3	35.0 / 34.2	35.5 / 34.2
6/2	(1) 386.00 / 360.64	1.150 / 0.715	43.8 / 40.3 / 27.2 / 28.8	-281 / -174 / -286 / -177	1.626	61.8 / 52.7	61.5 / 52.5	62.5 / 53.2	0.949	36.1 / 35.0	0.948	36.1 / 35.0	36.5 / 35.3	36.5 / 35.3	1.027	39.1 / 37.1	1.110	42.3 / 39.3	42.2 / 39.3	43.0 / 39.7

TABLE 16b

FUNCTIONAL TEST RESULTS/STANDBY OPERATION

TEST NO. / S/N	TEST RESULTS															
	INITIAL				P_4						P_5					
	P_6 - TOTAL PRESSURE				IDEAL		ACTUAL				IDEAL		ACTUAL			
	(VOLTS)	EQUIV (PSIG) (Pascals) x 10^4	SEEGERS GAGE (PSIG) (Pascals) x 10^4	OSCILL-OGRAPH (PSIG) (Pascals) x 10^4	(VOLTS)	EQUIV (PSIG) (Pascals) x 10^4	DVM (VOLTS)	EQUIV (PSIG) (Pascals) x 10^4	SEEGERS GAGE (PSIG) (Pascals) x 10^4	OSCILL-OGRAPH (PSIG) Pascals x 10^4	(VOLTS)	EQUIV (PSIG) (Pascals) x 10^4	DVM (VOLTS)	EQUIV (PSIG) (Pascals) x 10^4	SEEGERS GAGE (PSIG) (Pascals) x 10^4	OSCILL-OGRAPH (PSIG) (Pascals) x 10^4
7/2	1.573	59.8/51.2	59.5/51.1	60.0/51.4	1.288	50.5/44.9	1.283	48.8/43.7	49.0/43.9	48.5/43.5	0.977	37.1/35.7	0.972	36.9/35.5	37.0/35.6	38.0/36.3
8/1	2.568	97.8/77.4	109.5/80.5	108.0/84.5	2.344	89.1/71.5	2.373	90.3/42.3	97.5/78.4	97.0/77.0	2.188	83.13/67.4	2.210	84.0/68.0	87.0/67.9	87.0/67.9

NOTE

(1) This is the resistance change for simulating the drop in P_v during venting.

(1.2 sec) and the rather rapid pressurization rates. A 1.7 to 2 psia/sec (0.8 to 1.4 x 10^4 pascals/sec) pressurization rate was recorded during test 4, 5, and 6 while during test 1, 2, and 3 the rate was smaller (0.3 to 1 psia/sec 0.2 to 0.7 x 10^4 pascals/sec). This rate difference accounts for the difference seen for the two sets of data. The ideal pressure and the actuals for P_3 were again quite different in test 1, 2, and 3 because of the overshoots and the defective total pressure sensor. In tests 4, 5, and 6 the ideal and actuals comparison revealed a 3 psig (12.1 x 10^4 pascals) error due to the pressure overshoot. Table 16b presents the performance results from the standby operations. The error for P_4 and P_5 are 0.5 psig (10.36 x 10^4 pascals) and 0.1 psig (10.072 x 10^4 pascals), respectively. A summary of the performance of both units is given below:

Max. Error	S/N 1				S/N 2			
	Firing		Standby		Firing		Standby	
	P_2	P_3	P_5	P_4	P_2	P_3	P_5	P_4
Analog Voltage (MV)	14	32	22	29	4	83(1)	5	5
Seegers Pressure % F.S.	(2) 5.27	(2) 5.15	(2) 2.05	(2) 4.42	0.21	(1) 1.42	0.53	0.33

NOTES: (1) Error due to pressure overshoot
(2) Error due to failed total pressure transducer

The above data does not truly establish the performance capability of the controller due to the slow A-to-D converter rates and failure of the total pressure transducer in S/N 1. The slow rate for the A to D converter was selected so that during checkout and testing, the functional operations could be more readily observed. The range of sampling rates at which the controller can function is .020 sec to 1.2 sec. Faster controller rates would most certainly improve the controller performance for these tests. For the procedure to change the sampling dates see the Operation and Calibration Procedures MDAC-W Drawing No. 1T19806.

The real measure of performance is seen in the separate calibrations for the sensors and controller. The total static worst case errors based on the post-test calibrations are estimated to be:

S/N 1 2.2% F.S.
S/N 2 3.5% F.S.

5.3.3.4 Functional Testing/Controller Operations

The results of the four test conditions were recorded on the oscillograph. These records were generated to show that the controllers function in the manner for which they were designed. The oscillograph records were reconstructed for clarity and are presented in Figures 46 through 49. They show typically the sequence of events performed by the controllers for the Mode I operation and the four test conditions outlined in Paragraph 5.3. During the checkout testing, it was discovered that Modes II and III were not yet operational due to a design error. The design error was later corrected by making the necessary wiring change. Both units were checked out for these two operating modes during the final calibration. The Mode I tests conducted, however, were sufficient for demonstrating the controller functions as well as in determining their vacuum capability. The Mode I test is the most significant in that this mode requires operation of both pressurization valve drivers. Test 1 and 4 are shown in Figure 46. Here the conditions $P_3' < P_4$ and $P_3' > P_T$ were established and the results are illustrated by the pressure history and sequence of events that follow the firing signal. Test 2 and 5 are shown in Figure 47, and satisfies the conditions $P_3' < P_4$ and $P_3' < P_T$ where no pre-pressurization is required. Here the helium pre-pressurization valve opened only momentarily immediately following the firing signal. It then closed allowing the simulated expulsion to continue until P_2 was reached, at which time the controller then cycled between P_2 and P_3. Tests 3 and 6, shown in Figure 48, satisfy the conditions for $P_3' > P_4$. Here venting is required, to condition the propellant tank and lower the vapor pressure, before the pressurization and engine burn cycle was demonstrated.

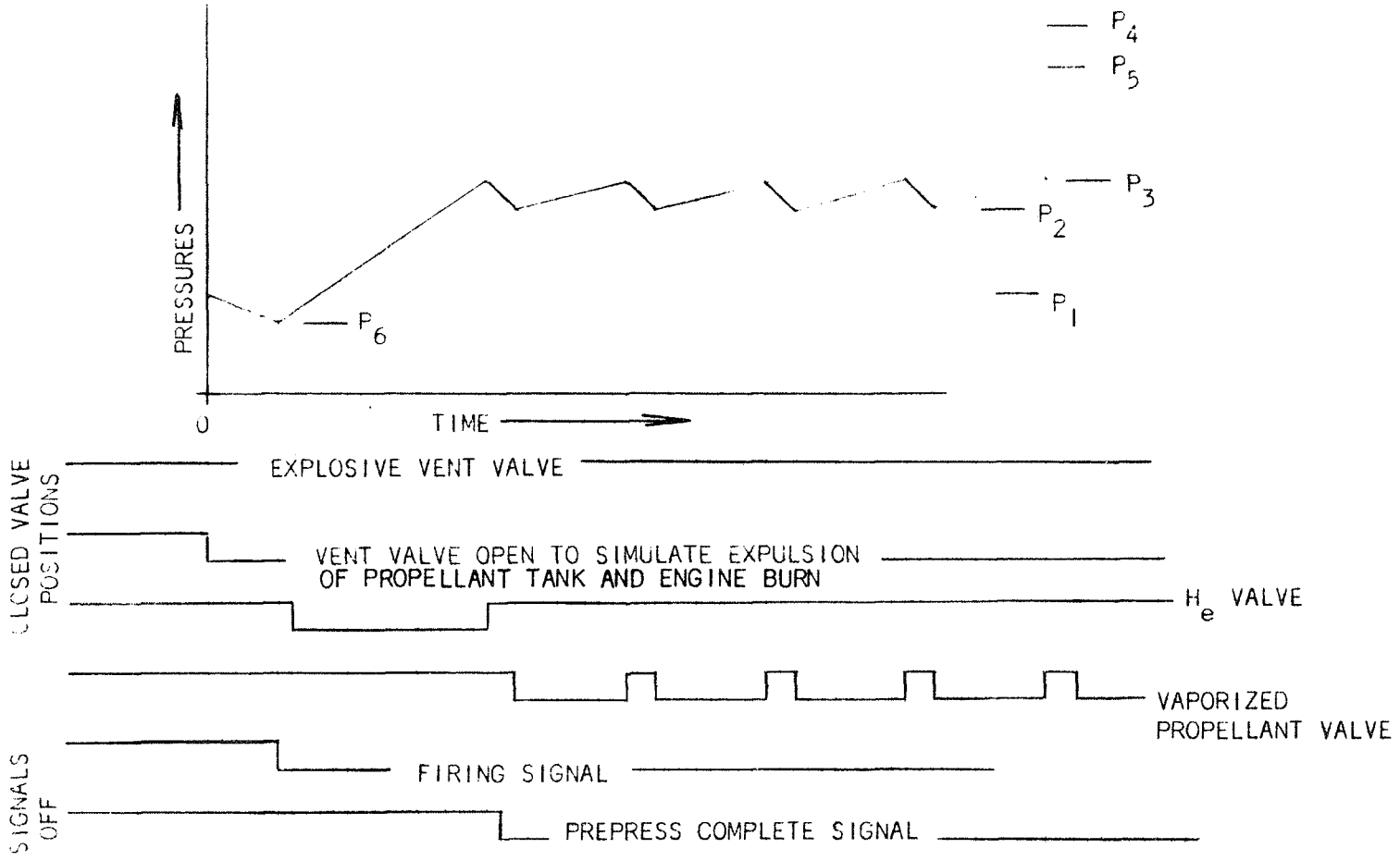

FIGURE 46 OSCILLOGRAPH RECORD - (TYPICAL OF TESTS 1 and 4)

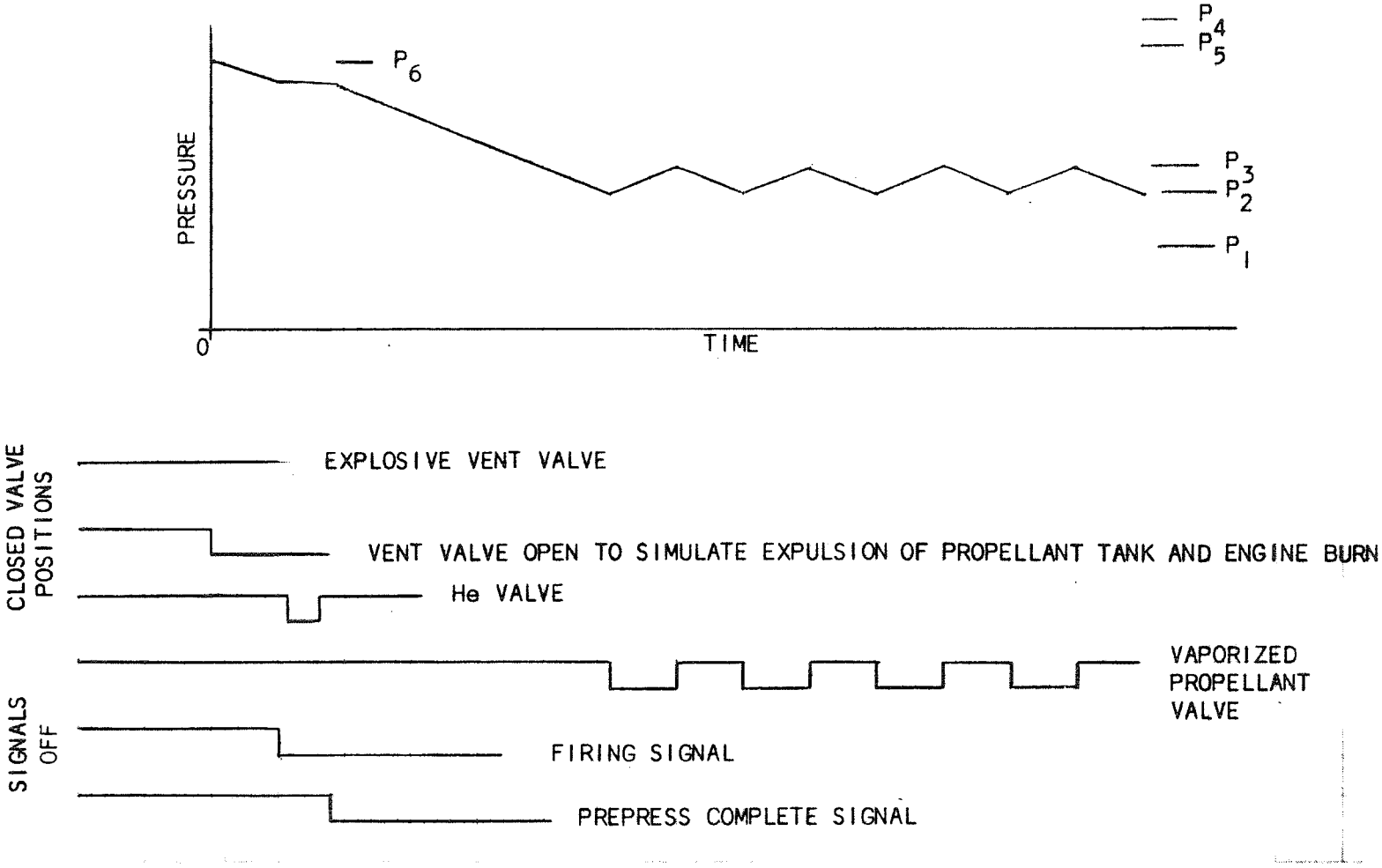

FIGURE 47 OSCILLOGRAPH RECORD - (TYPICAL FOR TESTS 2 & 5)

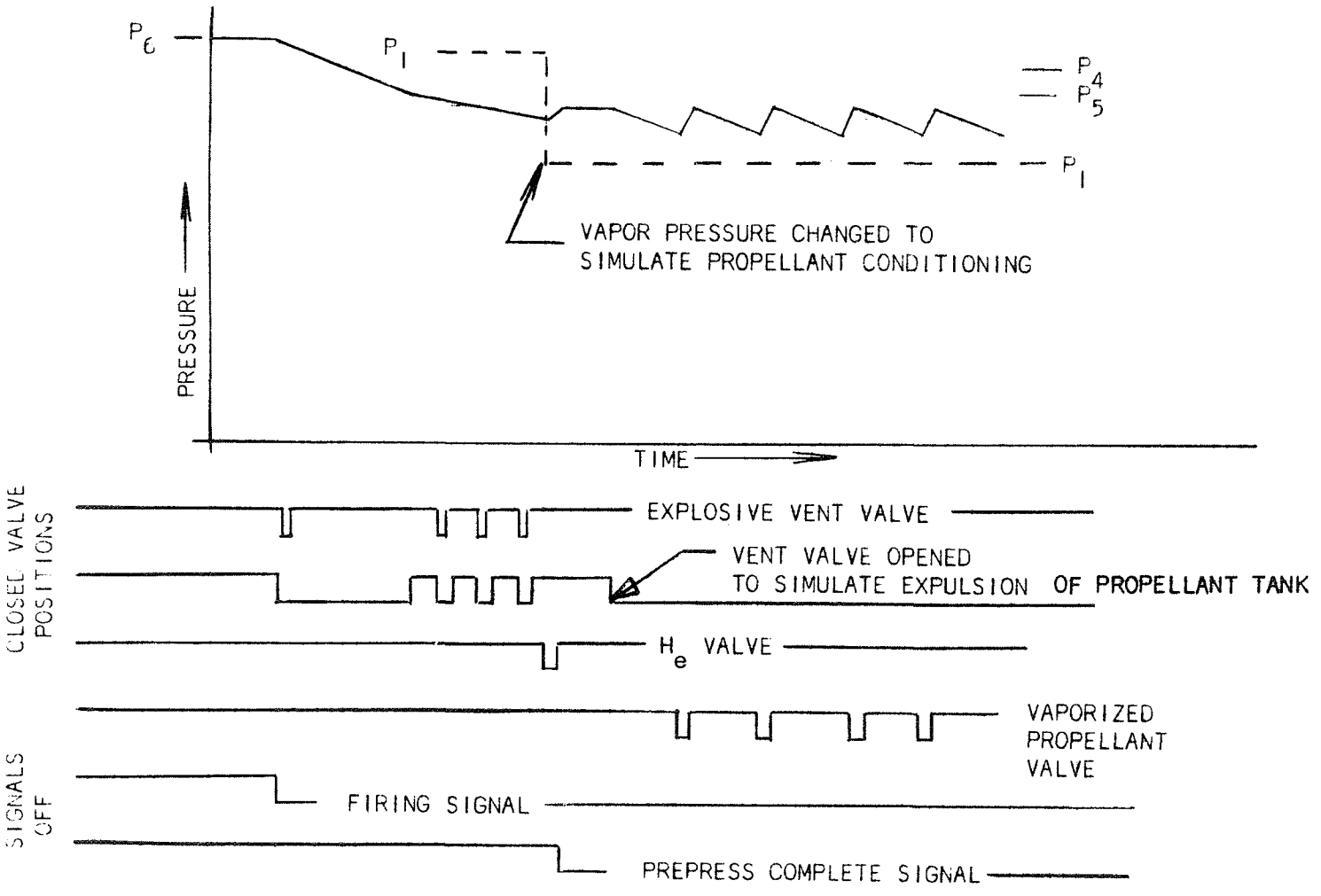

FIGURE 48 OSCILLOGRAPH RECORD - (TYPICAL FOR TESTS 3 & 6)

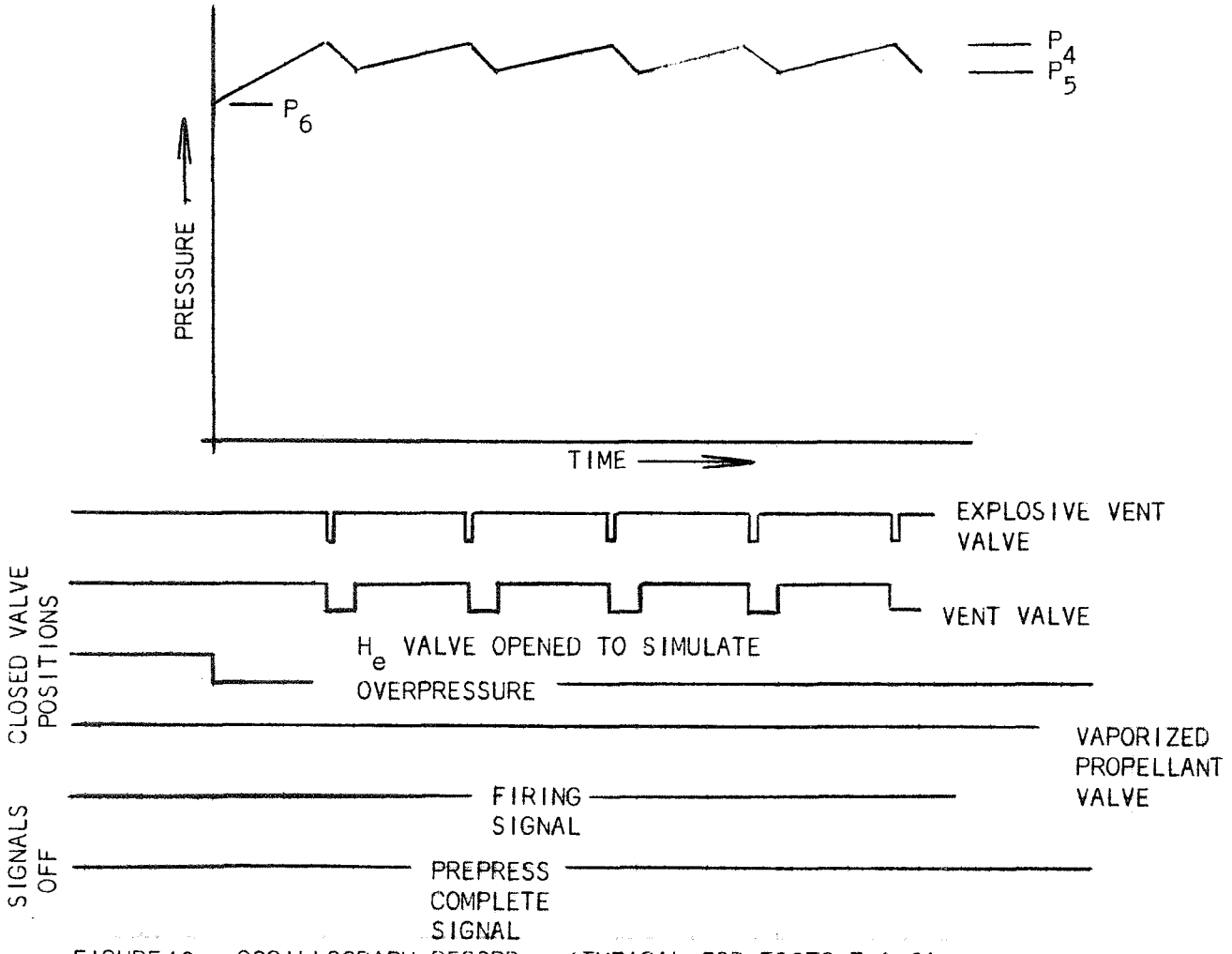

FIGURE 49 OSCILLOGRAPH RECORD - (TYPICAL FOR TESTS 7 & 8)

The controller continued to vent as designed until P_5 was reached, at which time the condition $P_3' > P_4$ was still existing. The explosive vent and vent valves cycled until the vapor pressure was manually changed to simulate the propellant conditioning that results from venting. At this time, the He pre-pressurization valve again opens momentarily and the pressurization cycle begins. Tests 7 and 8, Figure 49, simulate the emergency venting requirements in the standby operation; here both vent valves cycled between P_4 and P_5.

The results of these tests show both controllers to perform as designed with exception of the Mode selection, which was later corrected and proved operational. No performance degradation or failure resulted from the vacuum environment as can be seen from the test data presented in Tables 17 and 18. A summary of the pretest and post-test controller performance are for both vacuum and vibration tests shown in Tables 19 and 20. The maximum error is only 2 counts and 1 count for S/N 1 and S/N 2, respectively out of 256. The overrange and underrange condition is discussed in paragraph 3.4.

A record of the cycles and operating time accumulated by each controller is given in Tables 21 and 22.

5.4 Electrical Calibration Results

Tables 23 and 24 show the calibration results for controllers S/N 1 and S/N 2. The maximum error is 30 mv or 0.6% F.S. for electrically simulated P_V and P_T. The tables, in addition to presenting the calibration results, also show a convenient format for controller step-by-step calibration.

Table 17

OPERATION TEST

DATA SHEET

Controller: P/N 1T38533, S/N 1

Test: Functional Cycle Tests

Date: As Noted

NOTE: H,L, & H/L DENOTE THE LOGIC LEVELS:
$V_H \approx 3.5V$
$V_L \approx 0V$

TOTAL PRESSURE SIGNAL (P_T) CALIBRATIONS

Pre-Test
Pre-Vacuum
Date 6-30-70

Applied Pressure % F.S.	Analog Voltage (Volts)	BINARY OUTPUT (1)								
		1	2	3	4	5	6	7	8	$\overline{O/R}$
0	0.010	H	L	L	L	L	L	L	L	H
25	1.272	H/L	L	L	L	L	L	H	L	H
50	2.541	L	H/L	L	L	L	L	L	H/L	H
75	3.792	L	L/H	L	L	L	L	H/L	H/L	H
99.6	4.978	H	H/L	L/H	L/H	L/H	L/H	L/H	L/H	H

Post-Test
In-Vacuum
Date 7-2-70

0	-0.268			Under Range Not Applicable						
25	0.930	L	L	L	L	H	H	L	L	H
50	2.340	H	H	H	L	H	H	H	L	H
75	3.730	L	H	H	H	H	H	L	H	H
99.6	4.981	H	H	H	H	H	H	H	H	H

VAPOR PRESSURE SIGNAL (P_V) CALIBRATIONS

CALIBRATION	ANALOG VOLTAGE	
	PRE-TEST	POST-TEST
-423°F (-253°C)	0.006	-----
24.18 OHMS	0.616	0.625
46.28 OHMS	2.447	2.489
39.62 OHMS	1.817	1.856

Table 17 (Cont'd)

POWER AND VOLTAGE MEASUREMENTS

SUPPLY VOLTAGE	REGULATION		
	PRE-TEST	POST-TEST	
	DATE: 6-29-70	DATE: 7-2-70	DATE: 7-6-70
V_H	3.440	3.532	3.531
5 Volts	5.016	5.023	5.022
28 Volts	27.53	27.72	27.84
-15 Volts	-14.999	-14.996	-14.996
-15 Volts	+15.025	+15.024	+15.020

Table 18

OPERATIONAL TEST

DATA SHEET

Controller: P/N 1T38533, S/N 2

TEST: Functional Cycle Tests (Vacuum)

DATE: 7-7-70 and as Noted

NOTE: H,L, & H/L DENOTE THE LOGIC LEVELS
$V_H \approx 3.5V$
$V_L \approx 0V$

TOTAL PRESSURE SIGNAL (P_T) CALIBRATIONS

	Applied Pressure % F.S.	Analog Voltage (Volts)	BINARY OUTPUT								
			1	2	3	4	5	6	7	8	$\overline{O/R}$
Pre-Test Pre-Vacuum	0	0.002	H	L	L	L	L	L	L	L	H
	25	1.275	L	H	L	L	L	L	H	L	H
	50	2.553	H	H	L	L	L	L	L	H	H
	75	3.818	L	L	H	L	L	L	H	H	H
	99.6	4.980	H	H	H	H	H	H	H	H	H
Post-Test In Vacuum	0	-0.025	L	L	L	L	L	L	L	L	H
	25	1.237	L	L	L	L	L	L	H	L	H
	50	2.512	H	L	L	L	L	L	L	H	H
	75	3.769	H	L	L	L	L	L	H	H	H
	99.6	4.983	H	H	H	H	H	H	H	H	H

VAPOR PRESSURE SIGNAL (P_V) CALIBRATION

CALIBRATION	ANALOG VOLTAGE	
	PRE-TEST	POST-TEST
-320°F (-196°C)	5.624	---
350 OHMS	0.547	---
386 OHMS	1.146	1.150

Table 18 (Cont'd)

POWER AND VOLTAGES MEASUREMENTS

SUPPLY VOLTAGE	REGULATION	
	PRE-TEST DATE 7-6-70	POST-TEST DATE 7-7-70
V_H	3.499	3.566
5 Volts	5.024	4.970
28 Volts	28.01	27.73
-15 Volts	-14.98	-14.99
+15 Volts	+14.96	+14.90

Table 19

PRETEST/POST TEST
PERFORMANCE SUMMARY - S/N 1

	% FS PRESSURE	PRE-TEST DATA			POST-TEST DATA		
		ANALOG	BINARY OUTPUT		ANALOG	BINARY OUTPUT	
		VOLTS	IDEAL	ACTUAL	VOLTS	IDEAL (1)	ACTUAL
Vibration Tests	0	-0.343	Under Range		-0.341	Under Range	
	50	1.841	94	96	1.804	92	94
	100	4.460	228	230	4.402	225	226
Vacuum Functional Cycle Test	0	0.010	0	1	-0.268		
	25	1.272	65	64/65	0.930	48	48
	50	2.541	130	128/129	2.340	120	120
	75	3.792	194	192/194	3.730	191	191
	99.6	4.978	255	256	4.981	255	256

(1) These values are based on the analog input voltage to the A-to-D converter

Table 20

PRETEST/POST TEST PERFORMANCE SUMMARY - S/N 2

		PRE-TEST DATA			POST-TEST DATA		
		ANALOG	BINARY OUTPUT COUNTS		ANALOG	BINARY OUTPUT COUNTS	
	% F.S. PRESSURE	(VOLTS)	IDEAL(1)	ACTUAL	(VOLTS)	IDEAL(1)	ACTUAL
VIBRATION TEST	0	0.158	8	9	0.126	6	7
	50	2.740	140	141	2.711	138	138
	100	5.247	OVER RANGE		5.220	OVER RANGE	
VACUUM FUNCTIONAL CYCLE TEST	0	+0.002	0	1	0.010	0	1
	25	1.275	65	66	1.272	65	66
	50	2.553	130	131	2.541	130	131
	75	3.818	195	196	3.792	195	196
	99.6	4.980	255	256	4.978	255	256

(1) These values are based on the analog input voltage to the A-TO-D converter

TABLE 21

NO. OF CYCLES/OPERATING TIME
LIQUID HYDROGEN UNIT
S/N 1

Date	Time On	Time Off	Elapsed Time (Hrs)	No. Cycles	
				Standby	Firing
Vibration and Shock Tests					
6-18-70	10:45 PM	11:30 PM	0.75	2	12
6-19-70	10:30 AM	11:30 AM	1.00	-	-
6-19-70	1:30 PM	3:30 PM	2.00	-	-
6-22-70	9:30 AM	10:00 AM	0.50	2	12
SUB TOTALS			4.25	4	24
Functional Vacuum Tests					
6-30-70	1:00 PM	2:00 PM	1.3	2	12
6-29-70	11:00 PM	12:00 PM	1.0	2	12
6-29-70	1:00 PM	2:00 PM	1.0	-	-
7-1-70	11:00 AM	12:00 PM	1.0	-	4
7-1-70	1:00 PM	4:00 PM	3.0		12
7-2-70	10:00 AM	12:00 PM	2.0	-	14
7-2-70	1:00 PM	3:00 PM	2.0	7	4
7-6-70	11:00 AM	11:30 PM	0.5	-	20
7-6-70	1:00 PM	1:30 PM	0.5	10	10
7-6-70	1:30 PM	2:30 PM	1.0	2	12
SUB TOTALS			13.3	23	100
PRE AND POS ENVIRONMENTAL TESTS			100.00	16	84
TOTALS			117.55	43	208

TABLE 22

NO. OF CYCLES/OPERATING TIME
LIQUID FLUORINE UNIT
S/N 2

Date	Time On	Time Off	Elapsed Time (Hrs)	No. Cycles	
				Standby	Firing
Vibration and Shock Tests					
6-18-70	10:00 PM	10:45 PM	0.75	2	12
6-19-70	9:30 AM	10:30 PM	1.00	-	-
6-19-70	2:00 PM	4:20 PM	2.33	2	12
6-22-70	9:00 AM	9:30 AM	0.50	-	-
SUB TOTALS			4.58	4	24
Functional Vacuum Tests					
7-6-70	3:30 PM	4:30 PM	1.00	2	24
7-7-70	8:30 PM	3:30 PM	7:00	6	36
SUB TOTALS			8.00	8	60
PRE AND POST ENVIRONMENTAL TESTS			100	16	84
TOTALS			112.6	28	168

TABLE 23
CONTROLLER S/N 1, PROG I-A
PRETEST AND FINAL CALIBRATIONS - EL SIMULATED P_V, P_T INPUTS

OPERATION	FUNCTION/SETTING	TEST (1) @ 25°C VALUE	NOMINAL VALUE	ERROR (1)	LIGHTS
FIRING	SET P_T = 0V, TOGGLE FIRING SWITCH	MEASURED WITH HP 2401 C DVM - NEG. RETURN TO GND - 0V			FIRING
FIR 1⇄2	$P'_3 = P_V + \Delta P'_3 \geq P_4$	INCR. $P_V \geq$ 2.144V (2.137)	2.149V = $P_4 - \Delta P_3$	-5mV (-12mV)	VENT ON/OFF
FIR 2	$P_T > P_5$	INCR. $P_T >$ 2.203V (2.194)	2.188V = P_5	+15mV (+6mV)	VENT STAYS ON
FIR 2⇄1	SET P_T = 0V				VENT ON/OFF
FIR 1→3	$P'_3 = P'_V + \Delta P_3 < P_4$	DECR. $P_V \leq$ 2.142V (2.131)	2.149V = $P_4 - \Delta P_3$	-7mV (-18mV)	PRE-PRESS
FIR 3⇄4	SET $P_V \cong$ 1.235V (BIT NO. 7 = H ONLY)	SET $P_V \cong$ 1.240V (1.240)	1.250V = 1/4 SCALE	-10mV (-10mV)	PRE-PRESS
FIR 4→5	$P_T \geq P_3 = P_V + \Delta P_3$	INCR. $P_T \geq$ 1.435V (1.450)	1.445V = $\underbrace{(P_V)\ \text{SET}}_{1.250\text{V}} + \underbrace{\Delta P_3}_{0.195}$	-10mV (+15mV)	PRE-PRESS COMPLETE
FIR 5⇄6	$P_T > P_2 = P_V + \Delta P_2$				PRE-PRESS COMPLETE
FIR 6→3	$P_T \leq P_2 = P_V + \Delta P_2$	DECR. $P_T \leq$ 1.375V (1.383)	1.367V = $\underbrace{(P_V)\ \text{SET}}_{1.250\text{V}} + \underbrace{\Delta P_2}_{0.117\text{V}}$	+8mV (+26mV)	VAPOR, PROPEL
FIR 3⇄4	$P_T < P_3 = P_V + \Delta P_3$				VAPOR, PROPEL
STANDBY	SETTING P_V INCONSEQUENTIAL				
STA 1→2	$P_T \geq P_4$	INCR. $P_T \geq$ 2.339V (2.328)	2.344V = P_4	-5mV (-6mV)	VENT ON
STA 2→1	$P_T \leq P_5$	DECR. $P_T \leq$ 2.201V (2.193)	2.188V = P_5	+13mV (+5mV)	VENT OFF
	PWR SUPP SETTING +.038/9V	P_T READING .000V			

(1) ALLOW. ERROR = ±1% = ±50mV
PRE-TEST CALIBRATION
VALUES ARE IN BRACKETS

(2) MISC. READINGS:
LINE: 28.00V @ 1.1A = 30.8W
1.1A EXCLUSIVE OF SIG COND'S & VALVES (ESSENTIALLY RESIST. LOAD)

(3) PWR. SUPP. @ 25°C:
-14.99V, + 5.00V
+15.03V, VH = +3.43V

TABLE 24
CONTROLLER S/N 2, PROG I-D
PRETEST AND FINAL CALIBRATION - EL SIMULATED P_V, P_T INPUTS

OPERATION	FUNCTION/SETTING	@ 25°C TEST VALUE	NOMINAL VALUE	ERROR (1)	LIGHTS
FIRING	SET P_T = 0V, TOGGLE FIRING SWITCH	MEASURED WITH HP2401C DVM UNGROUNDED - NEG. RETURN TO GND - 0V			FIRING
FIR 1⇄2	$P'_3 = P'_V + \Delta P_3 \geqq P_4$	INCR. $P_V \geqq$ 3.939V (3.947)	3.945V = $P_4 - \Delta P_3$	-6mV (±2mV)	VENT ON/OFF
FIR 2	$P_T > P_5$	INCR. $P_T >$ 3.916V (3.924)	3.906V = P_5	+10mV (+18mV)	VENT STAYS ON
FIR 2⇄1	SET P_T = 0V				VENT ON/OFF
FIR 1→3	$P'_3 - P'_V + \Delta P_3 < P_4$	DECR. $P_V \leqq$ 3.935V (3.943)	3.945V = $P_4 - \Delta P_3$	-10mV (±12mV)	PRE-PRESS
FIR 3⇄4	SET $P_V \cong$ 2.5V (BIT NO. 8 = H ONLY)	SET $P_V \cong$ 2.488/9 2.505/6 } 2.497V (2.503)	2.500V = 1/4 SCALE	-3mV (±3mV)	PRE-PRESS
FIR 4→5	$P_T \geqq P_3 = P_V + \Delta P_3$	INCR. $P_T \geqq$ 3.445V (3.452)	3.438V (3.441) = $\underbrace{(P_V)\ \text{SET}}_{2.5\text{V}} + \underbrace{\Delta P_3}_{0.938\text{V}}$	+7mV (±11mV)	PRE-PRESS COMPLETE
FIR 5⇄6	$P_T > P_2 = P_V + \Delta P_2$				PRE-PRESS COMPLETE
FIR 6→3	$P_T \leqq P_2 = P_V + \Delta P_2$	DECR. $P_T \leqq$ 3.306V (3.314)	3.281V (3.284) = $\underbrace{(P_V)\ \text{SET}}_{2.5\text{V}} + \underbrace{\Delta P_2}_{0.781\text{V}}$	+25mV +30mV	VAPOR. PROPEL
FIR 3⇄4	$P_T < P_3 = P_V + \Delta P_3$				VAPOR. PROPEL
STANDBY	SETTING P_V INCONSEQUENTIAL				
STA 1→2	$P_T \geqq P_4$	INCR. $P_T \geqq$ 4.876V (4.882)	4.883V = P_4	-7mV (-1mV)	VENT ON
STA 2→1	$P_T \leqq P_5$	DECR. $P_T \leqq$ 3.915V (3.920)	3.906V = P_5	+9mV (+14mV)	VENT OFF
	PWR SUPP SETTING +.038/9V	P_T READING .000V			

(1) ALLOW. ERROR = ±1% = 50mV
PRE-TEST CALIBRATION VALUES ARE IN BRACKETS

(2) MISC. READINGS:
LINE: 28.02V @ 1.1A = 30.8W
1.1A EXCLUSIVE OF SIG COND'S & VALVES (ESSENTIALLY RESIST. LOAD)

(3) PWR. SUPP. @ 25°C:
-14.97V
+15.02V V_H = +3.45V
+5.01V

5.5 Valve Driver Test Results

On-State

On-state tests consisted of voltage measurements at 3 temperatures (-60°C, +25°C, +90°C) with a 3 amp load. These results are shown in Figure 50. In addition, successful operation with an actual valve load was verified. The resistance of the valve was found to be 3.4 ohms after a cold soak in LN_2. Steady state current through the valve stabilized at 2 amps in approximately 3 seconds (R_L = 15 ohms) due to I^2R heating. Plots of various voltages with resistive 3 amp load are shown in Figure 50.

Off-State

In the off-state, the circuit voltages were measured as a function of a simulated Q_3 collector leakage current and the results are shown in Figure 51. In this test, transistor Q_3 was replaced by a variable resistor. The simulated leakage current at +90°C exceeds the maximum specified Q_3 leakage current by a considerable margin.

Overload Test

Figure 52 shows test data collected at various loads. This data shows a sufficiently low V_{CE} @ - 60°C for loads up to 7 amp.

5.6 Warm-Up Time, P_T Signal Conditioner/Warm-Up Tests

The warmup time of the P_T signal conditioner was measured and Figures 53 and 54 show the oscilloscope traces of the P_T signal conditioner full scale output immediately after the power has been applied to the unit and also simultaneously to the oscilloscope sweep trigger. The expanded amplitude trace indicates that an initial overshoot beyond the full scale output occurs within the first 50 milliseconds. Digital voltmeter readings showed that the full scale output during the first 2 minutes was below 5 volts. This output stabilized to 4.990 volts within this 2 minute period.

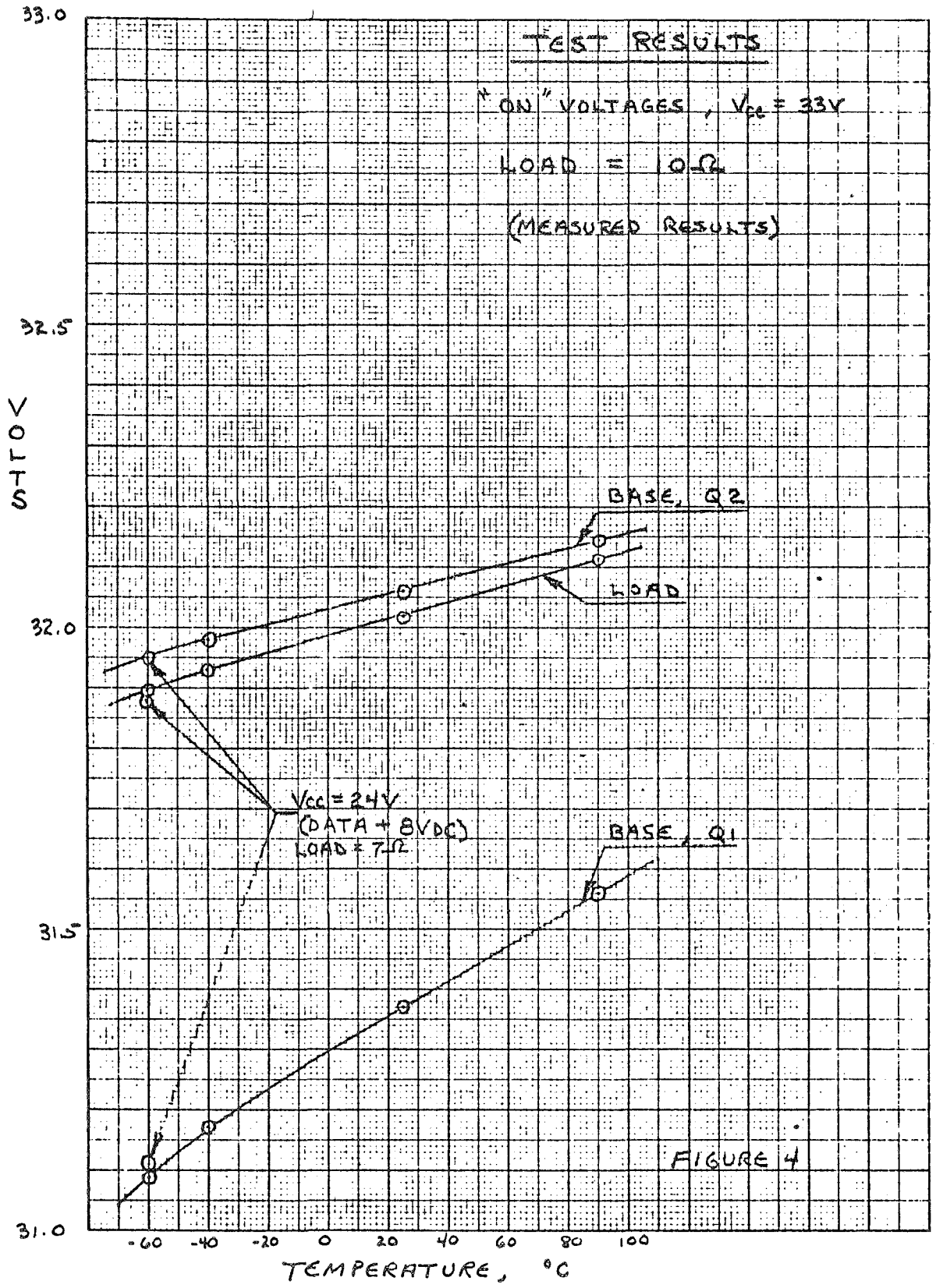

Figure 50. "On" Voltage Versus Temperature

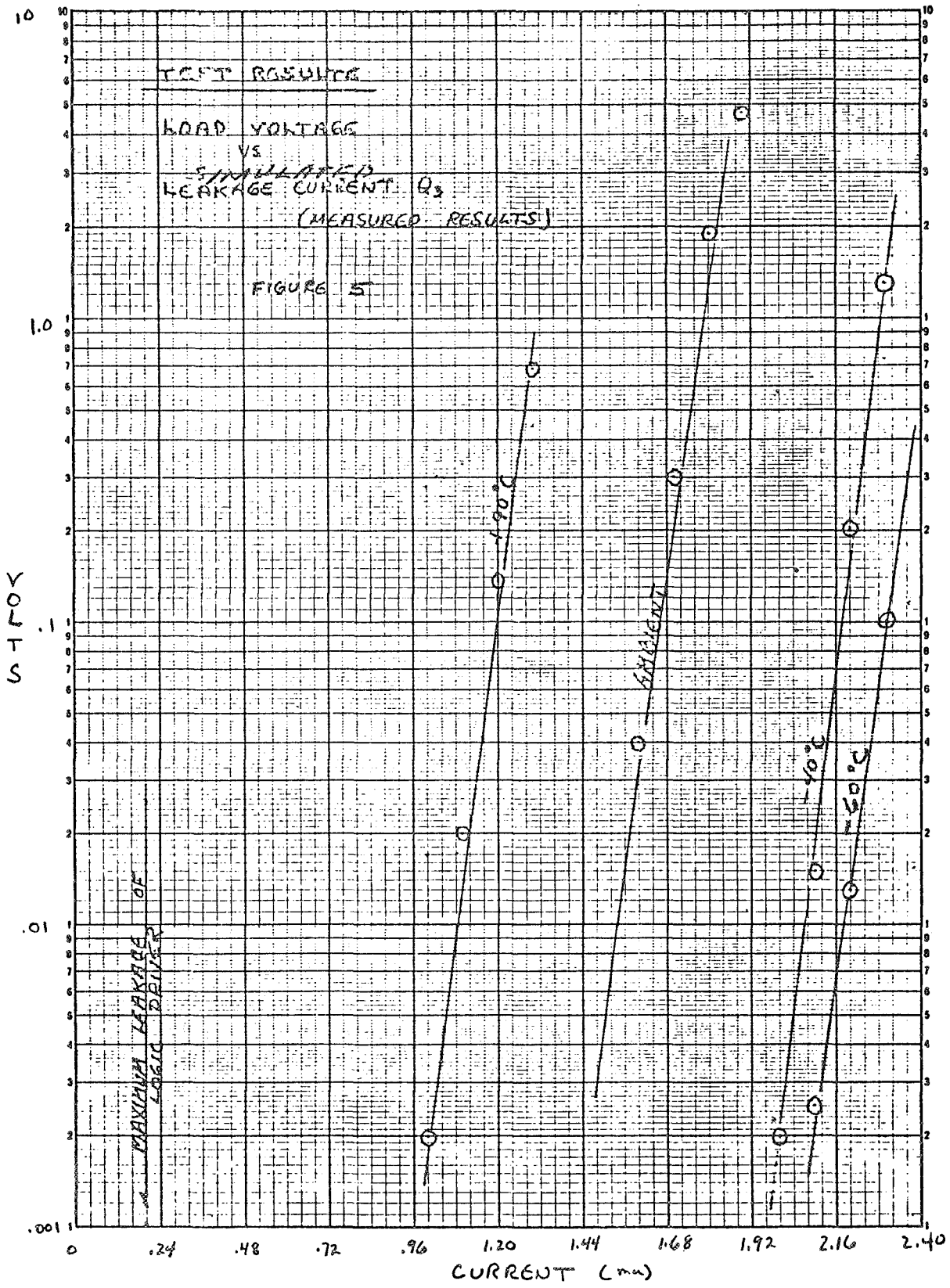

Figure 51. Load Voltage Versus Simulated Leakage Current Q_3

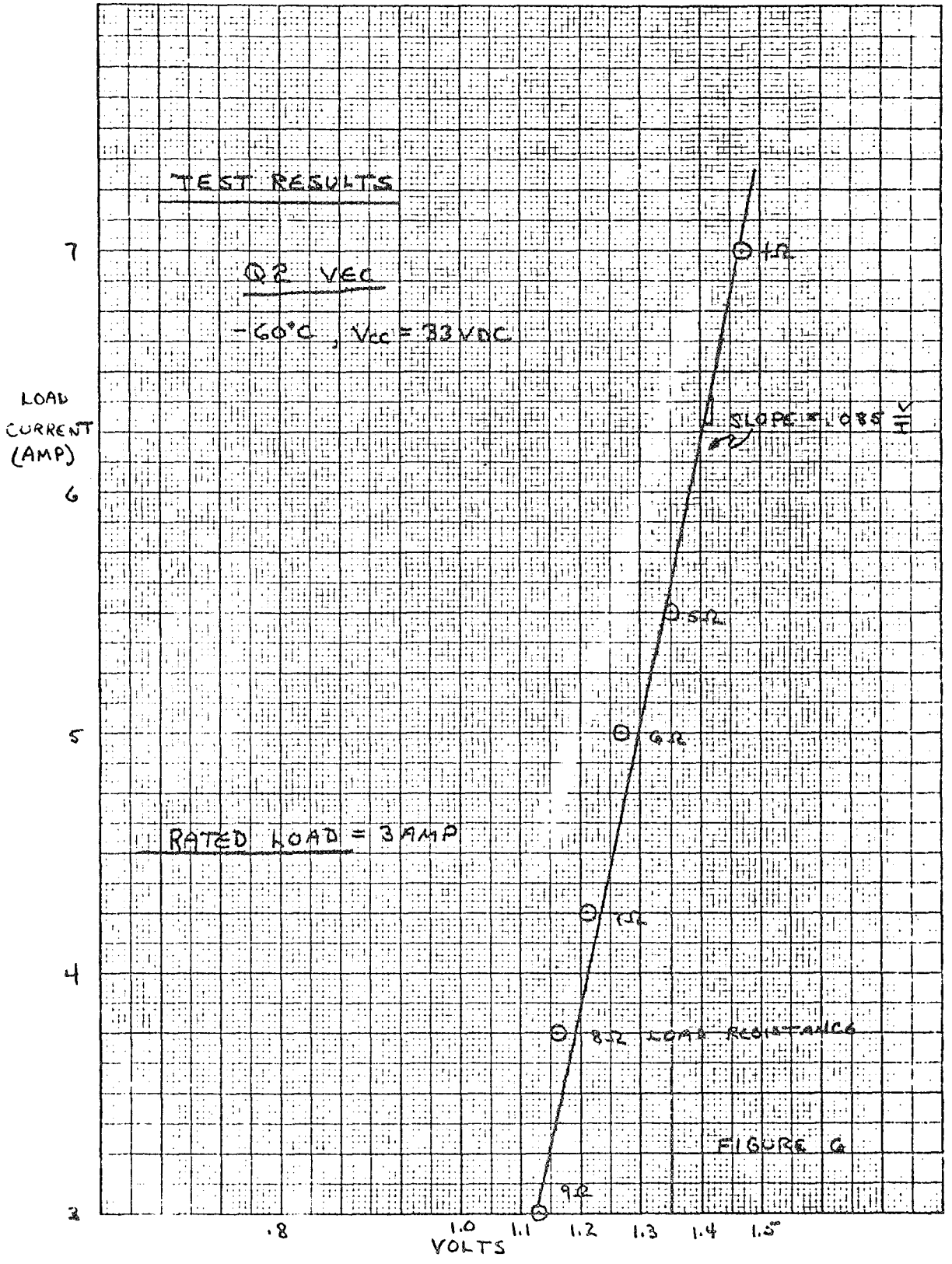

Figure 52. Load Current Versus Volts

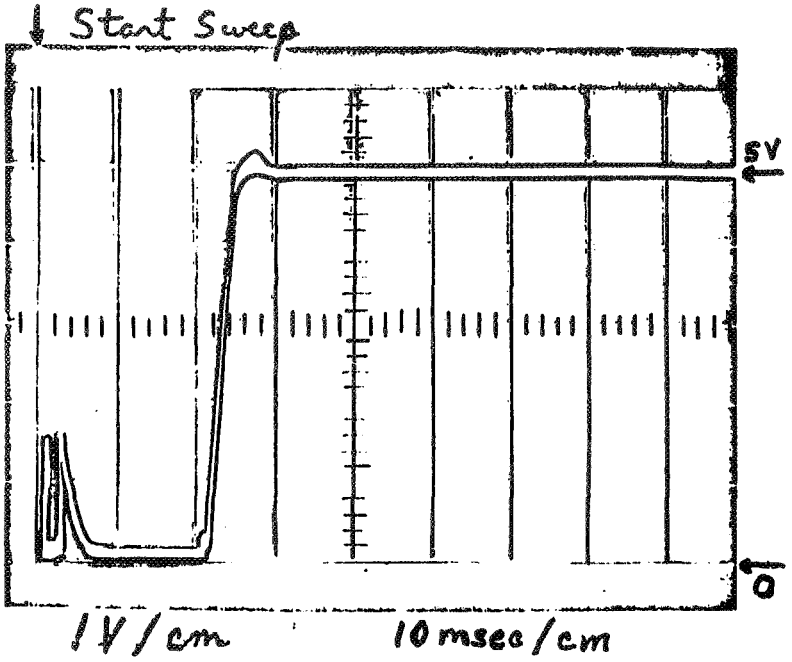

Figure 53. Kaman Nuclear Transducer System Full Scale Output Trace

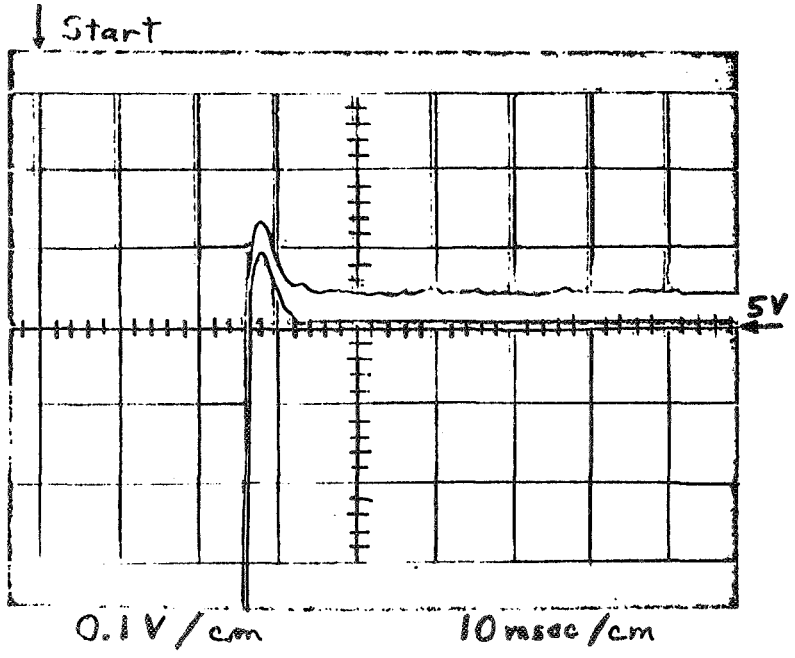

Figure 54. Kaman Nuclear Transducer System Expanded Amplitude Trace

5.7 Susceptibility Tests

The sketch below shows a block diagram of the test setup used to determine the susceptibility of the controller to power line noise. The pulse amplitude was increased until improper operation was noted. The pulse wave-form at this threshold is also shown below.

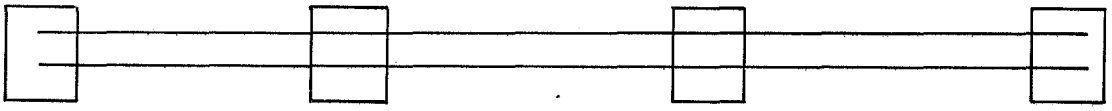

28 VDC POWER SUPPLY @ 1.1A	RFI TRANSIENT GENERATOR, SOLAR ELECTR. MODEL 6254-1	CONTROLLER S/N 1, STANDBY, MODE I	STORAGE OSCILLOSCOPE TEKTRONIX MODEL 564

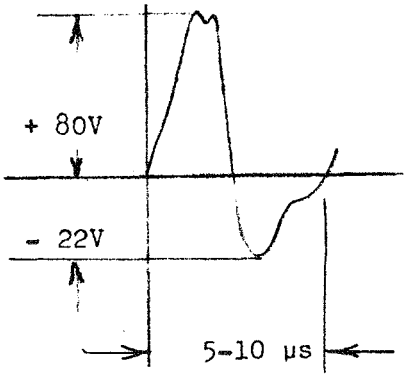

PULSE REPETITION RATE: 12 - 200 ms

SECTION 6
CONCLUSIONS AND RECOMMENDATIONS

This technology program was conducted to develop a long-life flight type cryogenic tank pressure sensing and control system. The program encompassed analysis, design, fabrication and testing of the sensors and the control logic system. Two flight type (prototype) pressure sensing and control systems were successfully developed for use with both a liquid hydrogen and a liquid fluorine feed system. These controllers provide both vent operation control, and "true" net positive suction pressure (NPSP) tank pressurization control. Both total pressure and vapor pressure are measured and used by the digital logic system of the controller which then provides the proper electrical signals to vent and pressurization valves. The total pressure is measured with a variable impedance flat diaphragm sensor and a platinum temperature sensor is used for the vapor pressure measurement. Both sensors are operated remotely from their signal conditioning electronic packages located within the controller. The two units fabricated were tailored for liquid fluorine and liquid hydrogen systems; however, they may be adapted to LO_2, FLOX, or CH_4 by providing the proper temperature probe and signal conditioning for the vapor pressure measurement. The system is also designed to be used with a pressurization system requiring: 1) helium for prepressurization and (autogeneous) vaporized propellant for expulsion pressurization, 2) helium for both prepressurization and expulsion pressurization, and 3) autogeneous propellants for both the prepressurization and expulsion.

In addition to driving two vent valves and two pressurant valves, the controller also outputs a prepressurization complete signal.

During the analysis phase of this program, two basic tank pressure control approaches were evaluated and compared for engine firing periods: (1) fixed differential total tank pressure control, where the minimum total tank pressure during engine operation is determined by having the control system add the preset NPSP to the measured total tank pressure prior to engine firing and (2) true NPSP control where the minimum total tank pressure during engine operation is determined by having the control system add the preset NPSP to the actual propellant vapor partial pressure. Listed below are some of the major conclusions that resulted from the limited feed system analysis that

assessed the benefits of true NPSP and established the accuracy requirements for the pressure sensors.

a. For systems that use helium pressurant, the true NPSP approach will minimize the amount of pressurant gas that must be added during the firing operation and it also maximizes the time that the feed system can be maintained in space until the tank vent pressure is reached.

b. For conditions where cold helium 37°R (20.6°K) is used for prepressurization and 300°R (167°K) heated helium is used for expulsion, the true NPSP approach resulted in a payload performance gain of 100 lbs (43.5 kg) out of 5,200 lb (2360 kg).

c. The effects of control system accuracy on the performance shows the fixed ΔP_T concept to be more sensitive to error (8 lbs of payload per psi)$^{-1}$ (5.38×10^4 kg/pascal) than the true NPSP (4 lbs/psi) (2.69 kg/pascal).

d. Pressurization systems that use helium for prepressurization and vaporized propellant for expulsion pressurization or helium for both, require that the hydrogen tank pressure measurement be more accurate than that of the fluorine system in order to provide a minimum pressurant weight for the overall system.

After the fabrication of the two controllers, a series of comprehensive functional and operation tests were conducted on both units to demonstrate their capability to perform according to the design specifications. The testing included: proof and leak tests of the pressure sensors, calibration tests of controller and sensors, vibration and shock tests, vacuum functional cycle tests, and fluorine compatibility tests. Listed below are some of the major conclusions that resulted from this testing:

a. Fluorine Compatibility Test

No deterioration or damage to the sensor resulted from the liquid fluorine exposure.

b. Vibration and Shock Test

Following the vibration and shock testing, both controllers were found in general to be structurally sound and operational. During the random and sinusoidal vibration all four sensor outputs were essentially stable except for an intermittent low frequency noise that was common on all the sensors during the random vibration.

c. Functional Cycle Test

Both controllers operated in the manner for which they were designed and no performance degradation or failure resulted from the vacuum environment. The maximum worst case errors for the two units with regard to the two operations are:

Standby Operation

S/N 1 and S/N2	1.2% full scale (F.S.)

Engine Operation

S/N 1 LH_2 System	2.2% F.S.
S/N 2 LF_2 System	3.5% F.S.

These errors are sufficiently small in that both the venting and engine operations can be adequately controlled.

Listed below are some important recommendations that should be applied to a future flight model in order to improve the system weight, accuracy, and reliability:

a. Non-Linear Sensor Conversions

The derivation of the propellant vapor pressure from a liquid propellant temperature measurement was chosen for the true NPSP control system. This derivation was made by linearizing the analog 0 to 5 volts signal. A recommended alternate method for providing greater accuracy would be to utilize a table-lookup technique with a read-only digital memory.

b. System Weight

Although the total weight of each of the flight type controllers is 29.5 lbs, a significant weight savings can result for the flight model. The power regulators, for example, weigh 35% of the total system weight. In a real flight system the power may be supplied from a single source battery or regulator that has similar requirements for other flight hardware. Reducing the specified input voltage range will also reduce the regulator weight and size. Packaging for flight would also result in a substantial weight saving. Here the subsystems could be integrated and the number of connectors reduced since all the flexibility required of the flight type would not be required for the flight model.

c. System Reliability

The use of Hi-Rel type parts for the flight controller would result in a system having reliabilities for 3 years of continuous operation of 0.896 at 77°F (25°C) and 0.811 at 170°F (77°C). If the total system were nonoperative except at monthly intervals during the mission, the controller reliability would be further increased. For a 3 year period, a reliability of .9948 can be realized using Hi-Rel parts at a 77°F (25°C) in this nearly nonoperative condition. It is therefore recommended that Hi-Rel parts be used in the flight model and that the system be operated only during given intervals in order to further increase the system reliability.

d. Fusing and Current Limiting

The fuses are provided for protection against shorts in the 28 volt lines. Since one of the fuses partially opened during vibration testing, it is recommended that high-reliability fuses and fuse holders be substituted instead of the presently employed units. The explosive vent valves squib may short or open after firing. It is therefore recommended that a current limiter be incorporated in its driver circuit.

e. Shielding and Packaging

Care has been taken to separate 28 volt wires carrying large currents from the rest of the system wiring. The card cage, for instance, was wired with green 28 volt wires on one side and white signal wires on the other side of the ground plane. The card cage ground plane is floating with respect to the main chassis plate and single-point grounded at the terminal block. To further improve the noise sensitivity of the controller, it is recommended that the 28 volt valve drivers be placed in a shielded enclosure adjacent to a separate valve connector. This will tend to isolate high current pulses from the rest of the power supply and signal lines.

f. Automatic Test

It is recommended for future developments that the test and calibration connector J2 be eliminated and the wire wrap plane be made accessible from the bottom of the enclosure instead. This can be accomplished by providing a RFI gasketed, hinged door at the bottom of the enclosure. When opening this door, the wire wrap plane would be exposed. Insulated templates may then be placed over the wire wrap plane. The templates will be marked to identify desired test points. These test points can be made accessible for manual testing by means of insulated test jacks which mate with the wire wrap pins. Similarly, automatic testing can be accomplished by mating the wire wrap plane with prepositioned contacts cabled to suitable automatic test equipment.

g. Total Pressure Sensors

One of the total pressure sensor models failed due to thermal shock or temperature cycling from ambient to -423°F (-253°C). The sensor coil cement and bonding technique used should be further investigated in order to establish the sensor structural integrity at cryogenic temperatures. It is also recommended that an all welded design be used for the flight model having both welded joints and weld seals at the pressure media.

h. Miniaturization

If it is required to miniaturize the total system for flight repackaging will be necessary. Repackaging of the A-to-D converter, the total pressure and vapor pressure signal conditioning units, terminal block, fuses, and valve drivers will contribute considerably to size reduction. For example, if these subsystems are repackaged by mounting their components on the standard ICC cards and incorporating them with a card cage configuration like that presently used for the logic components, the total package could be reduced to 1/4 the size

of the prototype model. Power regulators do not lend themselves readily to miniaturization as well as other electrical assemblies. This is because of the bulky transformers, filter chokes, capacitors and heat sinks which are the result of the power dissipation requirements. Employing low power logic integrated circuits and reducing the input voltage range will significantly reduce the power regulator size. If necessary, and if the cost is not prohibitive, further miniaturization can be obtained by using flat package integrated circuits and multilayer circuit boards. This technique could result in a package approximately 1/8 the size of the prototype model.

i. All-Digital System

A hybrid analog-digital system is presently employed for the controller. The analog portion consists of the total pressure and vapor pressure sensors and their signal conditioners. The signal conditioner outputs are input to the A-to-D converter which in turn yields a counting output. A similar counting output may be obtained from special sensors. Substitution of these sensors would eliminate the need for the A-to-D converter and would result in an all-digital system.

REFERENCES

1. G.W. Burge. System Effects on Propellant Storability and Vehicle Performance, Supplement Report. AFRPL-TR-68-227 (DAC-63061) December 1968.

2. P. Smerser. Pressure Measurements in Cryogenic Systems, Cryogenic Engineering Laboratory, National Bureau of Standards, Boulder, Colorado, Preprint Paper No. F-7 Prepared for Presentation at the 1962 Cryogenic Engineering Conference at University of California in Los Angeles, August 14 through August 16.

3. P.A. Kinzie et al. Temperature Response and Compensation for Pressure Transducers in Cryogenic Environments. NASA-CR-87152 Final Report (Rocketdyne), June 1967, pp 64.

4. G.W. Kamperman. ISA Transducer Compendium. 1963 (Copyright)

5. W.J. Barmore, Pace Wiancko. Pressure Measurements in Re-Entry Vehicles, Division of Whittaker Corp. from 22nd Annual ISA Conference and Exhibit, Preprint No. P8-5-PHYMMID-67.

6. William A. Holmgren. Shock Pressure Instruments for Severe Environment Applications. Kaman Corporation, Nuclear Division, From 22nd Annual ISA Conference and Exhibit, Preprint Number P19-4-PHYMMID-67, September 11, 1967.

Appendix A
TEST EQUIPMENT

Accuracy and repeatability of the following equipment was verified by standard calibration procedures during the periodic calibration and certification of this test equipment.

TABLE A-1

TEST EQUIPMENT USED IN

THE SENSOR EVALUATION

TESTING

	Test Equipment	Manufacturer	Model
1)	Platinum Resistance Thermometer	L&N	2240
2)	Bridge	L&N	Type G2
3)	DC Null Detector	L&N	Cat #9834
4)	Standard Cell	Eppley Laboratory Inc.	Cat #100
5)	Datran System	Datran Electronics	---
6)	Power Supply	Universal Electronics	Model TQ35-2
7)	Power Supply	Power Designs Inc.	Model 2240
8)	VOM	Simpson	Model 260
9)	Integrated Digital Voltmeter	Dymec	Model 2401A
10)	Electronic Counter	H.P.	Model 524C
11)	Oscilloscope	Tektronix	Type 535
12)	Cryogenic Chamber	Missimer	--
13)	Pressure Gage .1% 0-300 psia	Heise	---

TABLE A-2

TEST EQUIPMENT USED IN

THE VIBRATION AND SHOCK TESTS

Test Equipment

	Item	Manufacturer	Model	Serial/ Tag No.
1	Shaker	MB	C150	682218
2	Power Amplifier	MB	4700	682217-1
3	Equalizer	Ling	ASDE-80	9270
4	Automatic Acceleration Limiter	Ling	AAL-101	672508
5	No-Signal Detector	Ling	NSD-100	672514
6	Oscilloscope	Hewlett-Packard	130BR	22
7	Clipper-Mixer Amplifier	Ling	CMA-10	636074
8	Charge Amplifier	Unholtz-Dickie	D11	1832-1443
9	Voltmeters	B&K Ballatine	2416 320	1904 670356
10	Dynamic Analyzer	Spectral Dynamics	SD101B SD101A	690144 8414-15
11	X-Y Recorder	Varian Moseley	F80A 7005B	309927-5 682344-8
12	Electronic Counter	Hewlett-Packard	5512A	634956
13	Amplitude Servo/Monitor	MB	N753A	682344-3
14	Sweep Oscillators	Spectral Dynamics	SD104A-5	3009927-8 670436
15	Accelerometer	Endevco	2272	ND19
16	Tape Recorder	Ampex	CP100	611827
17	Multi-Filters	Spectral Dynamics	SD27	309927-18
18	Oscilloscope Camera	Hewlett-Packard	196A	332-02914
19	Log Converter	Technical Products	TP662	8414-17
20	Bandpass Filter	Krohn-Hite	330-M	1489-27
21	Waveform Synthesizer	Exact	200F	636059
22	Storage Oscilloscope	Hewlett-Packard	564	672701
23	A249 Slip Plate - drilled to accept two (2) specimens.			
24	Tape Recorder	Mincom 3-M	H	EL&S 51854

Table A-2 (Con't)

	Item	Manufacturer	Model	Serial/ Tag No.
25	Pressure Gage 0-300 psig 0.1% F.S. with O.Z. Subdivisions	Seegers Instrument Corp.	---	EL&S 46997
2	Platinum Resistance Probe	CEC	---	S/N T3754
27	Platinum Probe Control Panel	MDAC	---	1T24220-3
28	Digital Voltmeter	Trymetics Crop.	4243	DAC No. 681985
29	Resistance Box	Shallcross Mfg. Co.	8285	S/N 22360 U.S. Govern. No. 09721
30	PR Power Supply	Power Designs	2005	DACO 672309
31	PR Power Supply	Power Designs	2005	DACO 672310
32	Power Supply	Power Designs	2050	DACO 636171
33	Digital Voltmeter	Fairchild	7100	DACO 662446

Table A-3

TEST EQUIPMENT USED IN THE FUNCTIONAL VACUUM TESTING

	TEST EQUIPMENT	MANUFACTURER	MODEL
1)	5'X7' Vacuum Chamber	BEMCO (MDAC)	IT13576
2)	14"X24" Vacuum Chamber	MDAC	IT36226
3)	Pump	STOKES MICROVAC	S/N CA65444 DAC NO.662647-2
4)	Diffusion Pump 16"	NRC	---
5)	6" Vacuum Valve	SKINNER	V935 DX18
6)	Mini Mite (Potentiometer)	THERMO ELECTRIC	A0236
7)	0-300 psig Precision Pressure Gage	SEEGERS	---
8)	S1 Valve	MAROTTA	MV-74
9)	S2 Valve	MAROTTA	MV-74
10)	S3 Valve	MAROTTA	MV-74Z
11)	Hand Valves H1 & H2	CONTROL COMPONENTS	Model No. MV-1004T
12)	Oscillograph	HONEYWELL	Model 1508 DACO #670405
13)	Digital Volt Meter	TRYMETRICS CORP	Model 4243 DAC #681985
14)	Digital Volt Meter	HEWLETT PACKARD	Model 3443A NASA 9294-1 NAS 7-180
15)	Digital Volt Meter	HEWLETT PACKARD	Model 3443A DAC #636129
16)	Strip Chart Recorder	LEEDS & NORTHUP (L & N)	Cat No. 69953 S/N B62-751509-3-1 DAC #626249
17)	High Vacuum Ionization Gage	NRC	NRC-720 D DAC #662647-1
18)	Power Supply	POWER DESIGNS	Model 2005 DAC #672309
19)	Power Supply	POWER DESIGNS	Model 2005 DAC #672310

Table A-3 (Con't)

	TEST EQUIPMENT	MANUFACTURER	MODEL
20)	Digital Volt Meter	FAIRCHILD	Model 7100 DAC #662446
21)	Platinum Probe	CEC	S/N T3754
22)	0-200 psig Pressure Transducer	STATHAM	S/N 504
23)	Decade Resistance Box	GENERAL RADIO CO.	1432-W S/N 49328

APPENDIX B
MULTISTART PROPULSION SYSTEM SIZING PROGRAM, H-109

B.1 INTRODUCTION

The most difficult problem in sizing a multistart cryogenic upper stage is to assess the effects of propellant heating during the relatively lengthy coast phases. The effects of propellant heating may include propellant boiloff and tank pressure rise which, in turn, affect mixture ratio, propellant utilization, initial propellant load, tank weight, and the weight of the propellant pressurization and feed systems.

A closed form solution of the cryogenic stage-sizing problem which includes an accurate assessment of the heating effects is not possible. However, the multistart propulsion system sizing computer program developed under MDAC IRAD and designated H-109, enables rapid sizing of multistart cryogenic stages by means of an iterative procedure which considers the effects of heating the stage. The program can handle analyses of either pump or pressure fed stages that require as many as 20 engine starts.

In addition, the computer program is capable of determining the sensitivity of stage performance to changes in certain subsystem parameters. By using the results of a performance study conducted with the aid of H-109, the stage designer can select subsystems and combinations of system parameters which will result in maximum stage performance. In other words, program H-109 can be used for a stage optimization study even though it does not, by itself, select the optimum stage. The program provides for the measurement of stage performance in one of three ways:

1. For a given initial gross weight and stage velocity increment, performance is measured by the magnitude of the payload weight capability of the stage.
2. For a given payload weight and stage velocity increment, performance is measured by the magnitude of the initial gross weight of the stage.
3. For a given initial gross weight and payload weight, performance is measured by the magnitude of the stage velocity increment.

In addition to evaluating stage performance, the program also computes and prints out tank pressure history, venting requirements, and pressurant requirements for the overall mission as well as for each individual burn. The program has been used for this purpose for many contracted and in-house studies.

There are 1,500 input locations for the program. These include overall stage weights, engine geometry, engine mixture ratio, chamber pressure, tank pressures, initial propellant temperatures, propellant tankage stress and weight factors, stage and tankage geometry, tank insulation densities, sheet numbers and thermal performance factors, NPSH values, propellant and pressurant gas properties, correction factors for pressurant requirements, vehicle equilibrium temperatures, reaction control system weight and performance factors, refrigeration system weight and performance factors, pressurant inlet gas temperatures for repressurization and expulsion, thermal heat short factors, mission and duty cycle parameters, pressurization and feed system factors, and others.

B.2 PROGRAM CONSIDERATIONS

Vehicle operations are analyzed by the program using the following sequence of events; coast, conditioning, repressurization, burn, and decay. In the event of multistart operation, this sequence is repeated, using the assigned inputs for coast and burn times for each restart.

B.2.1 Coast Routine

Coast is that phase of vehicle flight during which the engine is not operating. Coast times are specified by inputs. During the coast period, the vehicle is exposed to solar radiation which heats the propellants to an intensity that is controlled by the specification of vehicle wall temperature data and the insulation data.

The coast heating routine determines the thermodynamic conditions in the propellant tanks during the coast phase of the mission. The outputs of this routine include pressure histories of the propellant tanks, final tank conditions, and the weights of propellant vapors and foreign gases vented.

Initially, the heat flux into the tank raises the tank pressure and temperature by uniformly heating the liquid and ullage gases. Propellant is evaporated to maintain the partial pressure of the propellant vapor in the ullage in equilibrium with the propellant vapor pressure. If the vent pressure of the tank is reached before the end of the coast, the routine is automatically directed into the second phase of the calculation which is the venting phase. By specifying the appropriate inputs, the tank may be vented either continuously or intermittently.

B.2.2 Conditioning Routine for Pump Fed Systems

At the end of each coast phase, just prior to an engine start, a check is made by the program to determine whether the existing tank conditions will permit attainment of the required net positive suction pressure (NPSP).

Since the start pressure, pressure drop in the lines, and acceleration pressure are more or less fixed, the only means to increase NPSP is to reduce the vapor pressure of the propellant. This can be done by venting the tank; this will force the propellant to evaporate and cool. This is what the preconditioning routine simulates if the NPSP available is found to be too low prior to engine start. The output from this routine includes the final equilibrium tank conditions, and the weights of propellant vapor and pressurant gas vented.

B.2.3 Repressurization Routine

Before an engine can be restarted, the propellant tanks must be pressurized to the required start pressure. This requirement is referred to as "repressurization" and is a different requirement than pressurization for expulsion. No distinction is made in the program between pump-fed and pressure-fed expulsion systems. The essential difference is that pressurization requirements for pump-fed systems as outlined above must consider the NPSP required by the pump to prevent cavitation. Pressure-fed systems, on the other hand, operate at inherently higher total pressures in the tank and must supply a pressure that is greater than the

combustion chamber pressure to overcome all pressure losses in lines and injectors. In addition, repressurization must satisfy the preceding expulsion pressure requirements together with engine start requirements.

In general, there are several ways to effect repressurization. It may be accomplished by MTI or by stored gas. If the propellants are cryogens, the pressurizing gas may be stored in a high-pressure bottle immersed in the cryogen and heated before being introduced into the propellant tank ullage. The heating system in this application must operate under zero-g conditions. (The program does not design the heat exchanger or attempt to verify its performance: it simply accepts the inputs regarding inlet and outlet conditions and the fuel required.)

The repressurization routine calculates the weight of stored gas pressurant that is required for the repressurization function and determines the ullage conditions at the end of repressurization.

B.2.4 Burn Routine

The program can handle up to 20 burns (engine starts) with each one using arbitrary values of engine thrust, specific impulse, and nozzle and combustion efficiencies. In addition, the program can handle an arbitrary schedule of propellant weight burned. The computer burn routine is used to determine stage performance, burn time, and pressurant used during expulsion.

As mentioned in Subsection B.1, the program measures stage performance in one of three modes. In the first two modes, stage velocity increment (ΔV) is an input; in the third, the stage velocity increment is calculated. Delivered specific impulse (I_{spd}) is calculated for each burn by multiplying the theoretical specific impulse (I_{spt}), by both the nozzle and combustion efficiencies.

The velocity increment is a function of thrust to weight ratio in Modes 1 and 2, and is given by the following equation for Mode 3.

$$\Delta V = g\, I_{spd}\, \mathrm{Ln}\left(\frac{W_{Gross}}{W_{Gross} - W_{Burned}}\right)$$

where

W_{Gross} is the vehicle gross weight

W_{Burned} is the weight of propellant burned

The weight of propellant burned is calculated in Modes 1 and 2 by using the following equation:

$$W_{Burned} = W_{Gross}\left(1-e^{\frac{-\Delta V}{gI_{spd}}}\right)$$

Burn time (θ) is determined using the following equation, which relates the weight of propellant burned (W_{Burned}), the delivered specific impulse (I_{spd}), and the engine thrust (F),

$$\theta_{Burn} = \frac{W_{Burned}\ I_{spd}}{F}$$

B.2.5 Decay Routine

At engine cutoff, propellant expulsion is terminated and pressurant flow to the propellant tanks is discontinued. At that instant the gaseous constituents in the ullage are not in equilibrium. The decay routine examines the conditions in the tank at engine cutoff and establishes equilibrium by solving the general energy equation. The pressurant used for expulsion will nearly always be at a higher temperature than the liquid propellant. Consequently, equilibrium will result in a collapse of tank pressure.

Equilibrium is established in a series of steps as follows. The first step brings the corresponding species of ullage gases into thermal equilibrium. Values of specific heat at constant volume stored in the program (or constant value inputs) are used by the routine to establish the temperatures resulting from mixing the like species. At this point, the ullage gases have been reduced to one vapor phase and one foreign gas phase at different temperatures. In the second step, the vapor and foreign gas are allowed to mix and a new equilibrium temperature is determined which is uniform for the mixture. The third step completes

the heat transfer process by establishing thermal equilibrium between the ullage gas and the liquid propellant. The final step completes the equilibrium process by considering mass transfer across the liquid-vapor interface. If condensation occurs instead of evaporation, the mass transfer will be negative.

Appendix C
CIRCUITRY TO ELIMINATE PRE-FIRING SIGNAL

Figure C-1 shows the additional circuitry breadboarded and designed to allow for later construction of a delay generator eliminating the need for the pre-firing signal. If the additional delay circuitry is utilized, the firing rather than the pre-firing signal is used to intermittently power the vapor pressure (P_V) signal conditions during the firing operation. Warm-up and stabilization of the conditions occurs during the initial delay period.

After approximately 0.9 seconds a delayed firing signal appears at point E which switches the controller from standby to firing operation.

Fairchild IC's 9601 and 1/3 9003 are utilized in the construction of the delay generator. The integrator composed of the 47 ohms and 240 ohms resistors and 47 MFD capacitor insures that the re-triggerable one-shot 9601 can switch to its delay state before a high output appears at point E. It therefore eliminates the possibility of an output spike during the initial firing signal propagation delay time in the monostable multivibrator. Note that D only goes high after C goes high, thereby eliminating the possible spike at the output of the nand gate (point E).

The components connected to pins 11 and 13 of the monostable multivibrator determine its delay time. If a delay time other than the nominal 0.9 seconds is desired, capacitor or resistor values may be changed in accordance with the following relationship:

$$\text{Delay Time } T \cong 0.36\ RC_X\ [1 + \frac{0.7}{R}]$$

where: R is in K ohms and 5 K ohms < R < 12.5 K ohms

C_X is in pf

T is in ns

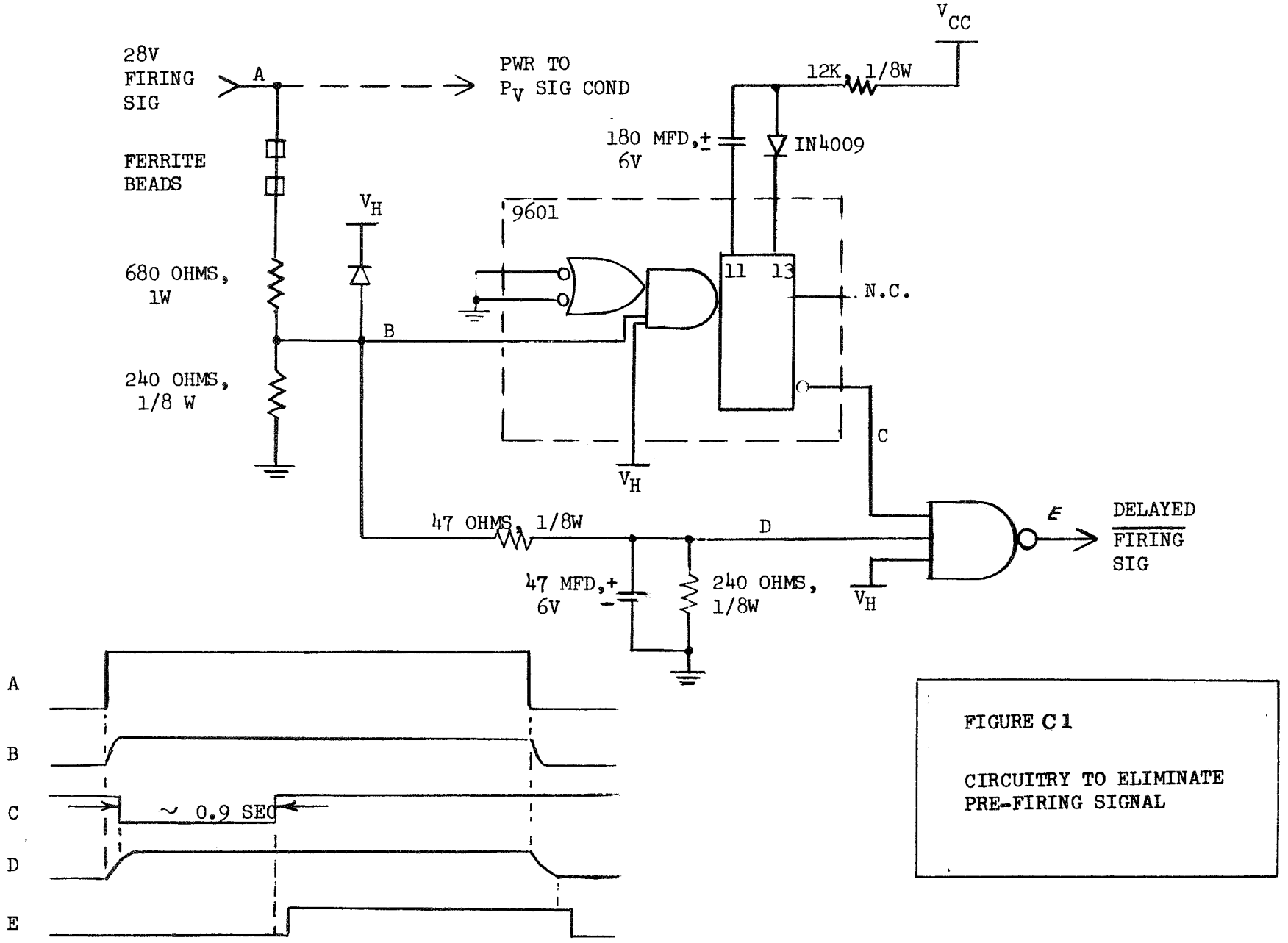

FIGURE C1

CIRCUITRY TO ELIMINATE PRE-FIRING SIGNAL

APPENDIX D

CONTROLLER/SENSOR DESIGN SPECIFICATIONS

1.	Internal Fluid Media Specifications	
	A. Pressure Sensing Passages -	Liquid Oxygen (MIL-O-25503) Liquid Fluorine (98.74 LF_2 Min.) (0.3% By Wt. Max. HF, CH_4) (1.0% By Wt. Max. O_2 N_2) (other inserts) Liquid FLOX (82.6% by Weight of Liquid Fluorine and 17.4% by Weight of LOX) Liquid Nitrogen (MIL-P-27401) Liquid Hydrogen (MIL-P-27201A) Liquid Methane (Commercial Grade)
	B. Leakage Test Media	Gaseous Helium (Grade A)
2.	Pressure Sensing Operating Range	Variable from 20 to 200 psia (5 to 185 psig) (13.8 to 138 x 10^4 pascals)
3.	Pressure Settings	
	A. Vent Pressure Adjustment Setting Range	Variable from 20 to 200 psia (13.8 to 138 x 10^4 pascals)
	B. NPSP Setting Range	Variable from 0 to 30 psi (0 to 20.9 x 10^4 pascals) above propellant saturation pressure
4.	Proof Pressure	300 psia (207 x 10^4 pascals)
5.	Burst Pressure	400 psia (276 x 10^4 pascals)
6.	External Leakage	1 x 10^{-9} Scc/Sec GH_e @ ambient temperature and proof pressure
7.	Operating Temperature	
	A. Pressure Sensor	
	(1) Located in propellant tank	-423°F to 170°F (-253°C to 77°C)
	(2) Located away from tank	-320°F to 170°F (-196°C to 77°C)
	B. Controller	-65°F to 170°F (-54°C to 77°C)

(All the controller components and subassemblies are designed for this temperature range except the Kaman Nuclear electronic package. The temperature range specified for this system is outlined in paragraph 3.5.1)

8. Size and weight - Design to a Minimum

9. Maintenance - there shall be no maintenance of components during the design life period.

10. Electrical power - All electrical components shall be designed and constructed for minimum power usage, and shall be signed to operate satisfactorily within a direct current supply voltage range of 24 to 32 volts (nominal voltage equals 28 volts and capable of carrying a minimum of 3.0 amperes load to operate external solenoid valve for one hour).

11. Service Life - 10,000 complete cycles.

12. Environmental Conditions

A. Combined sinusoidal and random vibration along any axis as follows:

(1) Sinusoidal portion

5 to 13 cps at 0.25 inch single amplitude
13 to 600 cps at 3.15g (rms) vibratory acceleration
600 to 2,000 cps at 4.50g (rms) vibratory acceleration

(2) Random portion

Increasing at the rate of 6 dB per octave to 0.225 g^2/cps at 600 cps.
0.225 g^2/cps from 600 cps to 1,110 cps.
Decreasing from 0.225 g^2/cps at 1,110 cps, at the rate of 12 dB per octave, to 2,000 cps.

B. Acceleration Loads — 12 g's parallel
12 g's perpendicular

C. Acoustics — 150 dB (re. 0.0002 microbars), 5 to 2000 cps

D. Vacuum - The controller shall be capable of operating within all performance requirements when exposed to an external vacuum environment of 1×10^{-7} mm of mercury pressure at operating temperature as specified in paragraph 7.B and when the vaccum is applied rapidly during simulated launch conditions.

E. Sea Level - The controller shall be capable of operating within all performance requirements in an external air environment at pressures ranging from 12 psia to 15 psia, (8.25 to 10.3×10^4 pascals) and air temperatures ranging from 460°R to 580°R at relative humidities up to 100 percent.

13. Explosive Atmosphere - the control shall be capable of operating within all performance requirements in an explosive hydrogen and oxygen atmosphere without causing ignition of that atmosphere.

14. Pressure Sensing - Port size shall be of the male type MS 33656, Size 4 7/16-20UNF3A for 1/4 O.D. tube or for an AND10050-4 boss.

15. Mounting provisions shall be made on each component for mounting by means of bolts or screws.

16. Dissimilar Metals - Dissimilar metals which may cause electrolytic corrosion shall not be used unless they are insulated from one another by a dielectric substance as defined by MS 33586.

17. Construction and Materials - Construction techniques and material selection shall conform to accepted standards for good practice by the Aerospace Industry. Air Force-Navy (AN) and Military Standards (MS) parts shall be provided instead of commercial parts when a choice is available. For fluorine use, construction techniques and materials shall conform to NASA procedures.

18. Workmanship - All components, including all parts and accessories, shall be constructed and finished in a thoroughly workmanlike manner. Particular attention shall be given to the neatness and thoroughness of soldering, wiring, the marking of parts, welding, plating, painting, riveting, machining and machine screw assemblies where applicable. All parts shall be free of burrs and sharp edges.

19. Pressure Calibration - The controller shall be capable of being checked out, calibrated, and adjusted on the ground, prior to launch. The calibration stage, adjustment devices, and checkout points shall be integral with the controller.

20. Additional Environmental Condition Shock - The controller shall withstand shock pulses that have a sinusoidal shape for one-half wave length during which the shock amplitude shall be 500g for a duration of 0.0004 seconds. Shock shall be applied, along any axis, at the controller mounts.

DISTRIBUTION LIST FOR FINAL REPORT

McDonnell Douglas Astronautics NAS3-13310
CR72748

Instructions:

Final reports are to be sent directly to the "Recipient" and the "Designee" per the quantities specified in the respective columns, R and D. When no copies are specified in Column D, a carbon copy of the letter of transmittal should be sent to the person named as the "Designee". The letter of transmittal should contain the contract number and complete title of the final report.

The distribution list, indicating all of the Recipients and Designees, should be included in the final report as an appendix.

REPORT COPIES R	D	RECIPIENT	DESIGNEE
		National Aeronautics & Space Administration Lewis Research Center 21000 Brookpark Road Cleveland, Ohio 44135	
1		Attn: Contracting Officer, MS 500-313	
5		Liquid Rocket Technology Branch, MS 500-209	
1		Technical Report Control Office, MS 5-5	
1		Technology Utilization Office, MS 3-16	
2		AFSC Liaison Office, 501-3	
2		Library	
1		Office of Reliability & Quality Assurance, MS 500-111	
1		D. L. Nored, Chief, LRTB, MS 500-209	
5		R. E. Grey, Project Manager, MS 500-209	
1		E. W. Contrad, MS 500-204	
1		R. H. Kemp, MS 49-1	
1		R. H. Knoll, MS 501-2	
1		J. W. Gregory, MS500-209	
1		W. R. Dunbar, MS 500-106	
1		A. J. Stofan, MS 500-103	
2		Chief, Liquid Experimental Engineering, RPX Office of Advanced Research & Technology NASA Headquarters Washington, D. C. 20546	

REPORT COPIES R	D	RECIPIENT	DESIGNEE
2		Chief, Liquid Propulsion Technology, RPL Office of Advanced Research & Technology NASA Headquarters Washington, D. C. 20546	
1		Director, Launch Vehicles & Propulsion, SV Office of Space Science & Applications NASA Headquarters Washington, D. C. 20546	
1		Chief, Environmental Factors & Aerodynamics Code RV-1 Office of Advanced Research & Technology NASA Headquarters Washington, D. C. 20546	
1		Chief, Space Vehicles Structures Office of Advanced Research & Technology NASA Headquarters Washington, D. C. 20546	
1		Director, Advanced Manned Mission, MT Office of Manned Space Flight NASA Headquarters Washington, D. C. 20546	
6		NASA Scientific & Technical Information Facility P. O. Box 33 College Park, Maryland 20740	
1		Director, Technology Utilization Division Office of Technology Utilization NASA Headquarters Washington, D. C. 20546	
1		National Aeronautics & Space Administration Ames Research Center Moffett Field, California 94035 Attn: Library	Hans M. Mark Mission Analysis Division
1		National Aeronautics & Space Administration Flight Research Center P. O. Box 273 Edwards, California 93523 Attn: Library	

REPORT COPIES R	D	RECIPIENT	DESIGNEE
1		National Aeronautics & Space Administration Goddard Space Flight Center Greenbelt, Maryland 20771 Attn: Library	Merland L. Moseson, Code 620
1		National Aeronautics & Space Administration John F. Kennedy Space Center Cocoa Beach, Florida 32931 Attn: Library	Dr. Kuit H. Debus
1		National Aeronautics & Space Administration Langley Research Center Langley Station Hampton, Virginia 23365 Attn: Library	E. Cortwright Director
1		National Aeronautics & Space Administration Manned Spacecraft Center Houston, Texas 77001 Attn: Library	J. G. Thiobodaux, Jr. Chief, Propulsion & Power Division
	1		Charles Yodzis, Code EP-2
	1		Henry Pohl, Code EP-4
1		National Aeronautics & Space Administration George C. Marshall Space Flight Center Huntsville, Alabama 35812 Attn: Library	Hans G. Paul Leon J. Hastings
	1	Jerry Thomson, PD-RV	James Thomas
	1	John McCarty, R-P&VE	Dale Burrows
	1	Charles Johnston, PD-RV-V	I. G. Yates Clyde Nevins J. Blumrich
1		Jet Propulsion Laboratory 4800 Oak Grove Drive Pasadena, California 91103 Attn: Library	Henry Burlage, Jr. Duane Dipprey

REPORT COPIES R	D	RECIPIENT	DESIGNEE
1		Defense Documentation Center Cameron Station Building 5 5010 Duke Street Alexandria, Virginia 22314 Attn: TISIA	
1		Office of the Director of Defense Research & Engineering Washington, D. C. 20301 Attn: Office of Asst. Dir. (Chem. Technology)	
1		RTD (RTNP) Bolling Air Force Base Washington, D. C. 20332	
1		Arnold Engineering Development Center Air Force Systems Command Tullahoma, Tennessee 37389 Attn: Library	Dr. H. K. Doetsch
1		Advanced Research Projects Agency Washington, D. C. 20525 Attn: Library	
1		Aeronautical Systems Division Air Force Systems Command Wright-Patterson Air Force Base, Dayton, Ohio Attn: Library	D. L. Schmidt Code ARSCNC-2
1		Air Force Missile Test Center Patrick Air Force Base, Florida Attn: Library	L. J. Ullian
1		Air Force Systems Command Andrews Air Force Base Washington, D. C. 20332 Attn: Library	Capt. S. W. Bowen SCLT
1	1	Air Force Rocket Propulsion Laboratory (RPR) Edwards, California 93523 Attn: Library	Tom Waddell, RPRPD Robert Wiswell W. W. Wells
1		Air Force Rocket Propulsion Laboratory (RPM) Edwards, California 93523 Attn: Library	
1		Air Force FTC (FTAT-2) Edwards Air Force Base, California 93523 Attn: Library	Donald Ross

REPORT COPIES R	D	RECIPIENT	DESIGNEE
1		Air Force Office of Scientific Research Washington, D. C. 20333 Attn: Library	SREP, Dr. J. F. Masi
1		Space & Missile Systems Organization Air Force Unit Post Office Los Angeles, California 90045 Attn: Technical Data Center	
1		Office of Research Analyses (OAR) Holloman Air Force Base, New Mexico 88330 Attn: Library RRRD	
1		U. S. Air Force Washington, D. C. Attn: Library	Col. C. K. Stambaugh, Code AFRST
1		Command Officer U. S. Army Research Office (Durham) Box CM, Duke Station Durham, North Carolina 27706 Attn: Library	
1		U. S. Army Missile Command Redstone Scientific Information Center Redstone Arsenal, Alabama 35808 Attn: Document Section	Dr. W. Wharton
1		Bureau of Naval Weapons Department of the Navy Washington, D. C. Attn: Library	J. Kay, Code RTMS-41
1		Commander U. S. Naval Missile Center Point Mugu, California 93041 Attn: Technical Library	
1		Commander U. S. Naval Weapons Center China Lake, California 93357 Attn: Library	
1		Commanding Officer Naval Research Branch Office 1030 E. Green Street Pasadena, California 90110 Attn: Library	

REPORT COPIES R	D	RECIPIENT	DESIGNEE
1		Director (Code 6180) U. S. Naval Research Laboratory Washington, D. C. 20390 Attn: Library	H. W. Carhart J. M. Kradll
1		Picatinny Arsenal Dover, New Jersey 07801 Attn: Library	I. Forsten
1		Air Forec Aero Propulsion Laboratory Research & Technology Division Air Force Systems Command United States Air Force Wright-Patterson AFB, Ohio 45433 Attn: APRP (Library)	R. Quigley C. M. Donaldson
1		Electronics Division Aerojet-General Corporation P. O. Box 296 Azusa, California 91703 Attn: Library	W. L. Rogers
1		Space Division Aerojet-General Corporation 9200 East Flair Drive El Monte, California 91734 Attn: Library	S. Machlawski
1		Aerojet Ordance and Manufacturing Aerojet-General Corporation 11711 South Woodruff Avenue Fullerton, California 90241 Attn: Library	
1		Aerojet Liquid Rocket Company P. O. Box 15847 Sacramento, California 95813 Attn: Technical Library 2484-2015A	R. Stiff C. W. Williams
1		Aeronutronic Division of Philco Ford Corp. Ford Road Newport Beach, California 92663 Attn: Technical Information Department	Dr. L. H. Linder

REPORT COPIES R	D	RECIPIENT	DESIGNEE
1		Aerospace Corporation 2400 E. El Segundo Blvd. Los Angeles, California 90045 Attn: Library-Documents	J. G. Wilder W. Wetmore
1		Arthur D. Little, Inc. 20 Acorn Park Cambridge, Massachusetts 02140 Attn: Library	A. C. Tobey
1		Astropower Laboratory McDonnell-Douglas Aircraft Company 2121 Paularino Newport Beach, California 92163 Attn: Library	
1		ARO, Incorporated Arnold Engineering Development Center Arnold AF Station, Tennessee 37389 Attn: Library	
1		Susquehanna Corporation Atlantic Research Division Shirley Highway & Edsall Road Alexandria, Virginia 22314 Attn: Library	
1		Beech Aircraft Corporation Boulder Facility Box 631 Boulder, Colorado Attn: Library	Douglas Pope
1		Bell Aerosystems, Inc. Box 1 Buffalo, New York 14240 Attn: Library	T. Reinhardt W. M. Smith J. R. Flanagin
1		Bendix Systems Division Bendix Corporation 3300 Plymouth Street Ann Arbor, Michigan Attn: Library	John M. Brueger

REPORT COPIES R	D	RECIPIENT	DESIGNEE
1		Bellcomm 955 L'Enfant Plaza, S. W. Washington, D. C. Attn: Library	H. S. London O. Bendersky
1		Boeing Company Space Division P. O. Box 868 Seattle, Washington 98124 Attn: Library	J. D. Alexander C. F. Tiffany
1		Boeing Company 1625 K Street, N. W. Washington, D. C. 20006	
1		Boeing Company P. O. Box 1680 Huntsville, Alabama 35801	Ted Snow
1		Chemical Propulsion Information Agency Applied Physics Laboratory 8621 Georgia Avenue Silver Spring, Maryland 20910	Tom Reedy
1		Chrysler Corporation Missile Division P. O. Box 2628 Detroit, Michigan Attn: Library	John Gates
1		Chrysler Corporation Space Division P. O. Box 29200 New Orleans, Louisiana 70129 Attn: Librarian	
1		Curtiss-Wright Corporation Wright Aeronautical Division Woodridge, New Jersey Attn: Library	G. Kelley
1		University of Denver Denver Research Institute P. O. Box 10127 Denver, Colorado 80210 Attn: Security Office	

REPORT COPIES R	D	RECIPIENT	DESIGNEE
1		Fairchild Stratos Corporation Aircraft Missiles Division Hagerstown, Maryland Attention: Library	
1		Research Center Fairchild Hiller Corporation Germantown, Maryland Attn: Library	Ralph Hall
1		Republic Aviation Fairchild Hiller Corporation Farmington, Long Island New York	
1		General Dynamics/Convair P. O. Box 1128 San Diego, California 92112 Attn: Library	Frank Dore R. NAU
1		Missiles and Space Systems Center General Electric Company Valley Forge Space Technology Center P. O. Box 8555 Philadelphia, Pa. 19101 Attn: Library	A. Cohen F. Schultz
1		General Electric Company Flight Propulsion Lab. Department Cincinnati, Ohio Attn: Library	D. Suichu Leroy Smith
1		Grumman Aircraft Engineering Corporation Bethpage, Long Island, New York Attn: Library	Joseph Gavin R. Grossman
1		Hercules Powder Company Allegheny Ballistics Laboratory P. O. Box 210 Cumberland, Maryland 21501 Attn: Library	

REPORT COPIES R	D	RECIPIENT	DESIGNEE
1		Honeywell Inc. Aerospace Division 2600 Ridgeway Road Minneapolis, Minnesota Attn: Library	
1		IIT Research Institute Technology Center Chicago, Illinois 60616 Attn: Library	C. K. Hersh
1		Kidde Aer-Space Division Walter Kidde & Company, Inc. 567 Main Street	R. J. Hanville
1		Ling-Temco-Vought Corporation P. O. Box 5907 Dallas, Texas 75222 Attn: Library	
1		Lockheed Missiles and Space Company P. O. Box 504 Sunnyvale, California 94087 Attn: Library	W. Sterbentz
1		Lockheed Propulsion Company P. O. Box 111 Redlands, California 92374 Attn: Library, Thackwell	H. L. Thackwell
1		Marquardt Corporation 16555 Saticoy Street Box 2013 – South Annex Van Nuys, California 91409	Irv Glasser T. Hudson
1		Martin-Marietta Corporation (Baltimore Division) Baltimore, Maryland 21203 Attn: Library	
1		Denver Division Martin-Marietta Corporation P. O. Box 179 Denver, Colorado 80201 Attn: Library	Dr. Morganthaler F. R. Schwartzberg J. McCown

REPORT COPIES R	D	RECIPIENT	DESIGNEE
1		Orlando Division Martin-Marietta Corporation Box 5827 Orlando, Florida Attn: Library	J. Fern
1		Western Division McDonnell Douglas Astronautics 5301 Bolsa Ave Huntington Beach, California 92647 Attention: Library	Dr. J. L. Waisman G. W. Burge P. Klevatt R. J. Gunkel Lambert Field
1		McDonnell Douglas Aircraft Corporation P. O. Box 516 Lamber Field, Missouri 63166 Attn: Library	R. A. Herzmark L. F. Kohrs
		Rocketdyne Division North American Rockwell Inc. 6633 Canoga Avenue Canoga Park, California 91304 Attn: Library, Department 596-306	Dr. R. J. Thompson S. F. Jacobellis S. Domokos
1		Space & Information Systems Division North American Rockwell 12214 Lakewood Blvd. Downey, California Attn: Library	Dr. L. A. Harris
1		Northrop Space Laboratories 3401 West Broadway Hawthorne, California Attn: Library	Dr. William Howard
1		Purdue University Lafayette, Indiana 47907 Attn: Library (Technical)	Dr. Bruce Reese

REPORT COPIES R	D	RECIPIENT	DESIGNEE
1		Radio Corporation of America Astro-Electronics Products Princeton, New Jersey Attn: Library	
1		Rocket Research Corporation Willow Road at 116th Street Redmond, Washington 98052 Attn: Library	F. McCullough, Jr.
1		Stanford Research Institute 333 Ravenswood Avenue Menlo Park, California 94025 Attn: Library	Dr. Gerald Marksman
1		Thiokol Chemical Corporation Redstone Division Huntsville, Alabama Attn: Library	John Goodloe
1		TRW Systems, Inc. 1 Space Park Redondo Beach, California 90278 Attn: Tech. Lib. Doc. Acquisition	D. H. Lee H. Burge
1		TRW TAPCO Division 23555 Euclid Avenue Cleveland, Ohio 44117	P. T. Angell
1		United Aircraft Corporation Corporation Library 400 Main Street East Hartford, Connecticut 06108 Attn: Library	Dr. David Rix Erle Martin Frank Owen Wm. E. Taylor
1		United Aircraft Corporation Pratt & Whitney Division Florida Research & Development Center P. O. Box 2691 West Palm Beach, Florida 33402 Attn: Library	R. J. Coar Dr. Schmitke Paul Nappi

REPORT COPIES R	D	RECIPIENT	DESIGNEE
1		United Aircraft Corporation United Technology Center P. O. Box 358 Sunnyvale, California 94038 Attn: Library	Dr. David Altman
1		Vickers Incorporated Box 302 Troy, Michigan	
1		Vought Astronautics Box 5907 Dallas, Texas Attn: Library	
	1	McDonnell-Douglas Astronautics, Co. Eastern Division P. O. Box 5941 Barkley, Missouri 63134	R. Quest J. B. Fleming
1		Garrett Corporation Airesearch Division Phoenix, Arizona 85036 Attn: Library	
1		Garrett Corporation Airesearch Division Los Angeles, California Attn: Library	